ISSN 0285-1989
NUP-A-2001-1

ANNUAL REPORT

2000

Atomic Energy Research Institute

of

Nihon University

This is a brief report of the research activities of Atomic Energy Research Institute of Nihon University for the academic year 2000. Main subjects of research are Nuclear Fusion and Plasma Physics, Superconductivity, Theoretical Physics – including Plasma, Astronomy and Statistical Physics, Particle and Nuclear Physics, and the History of Science – , the Application of Accelerators for Free Electron Laser and Quantum Optics. The report consists of abstract of individual works with introductory survey of each of the main subjects.

K. Kojima

Director

Contents

§1. Nuclear Fusion and Plasma Science

1A) Nuclear Fusion ..... 3 - 8

1B) Plasma Science ..... 9 - 14

§2. Superconductivity ..... 17 - 24

§3. Theoretical Physics

3A) Plasma, Astronomy and Statistical Physics ..... 27 - 40

3B) Particle and Nuclear Physics ..... 41 - 57

3C) History of Science ..... 58 - 60

§4. Accelerator Science ..... 63 - 74

§5. Quantum Optics ..... 77 - 82

§6. Other Researches ..... 85 - 96

§7. International Exchange Activities

7A) Visitors from Abroad ..... 99 - 99

7B) Visitors to Abroad and International Conferences ..... 100 - 104

§8. List of Publications

8A) Publications in Periodical Journals and Conference Reports ..... 107 - 115

8B) Nihon University Preprints ..... 116 - 118

8C) Books and Proceedings ..... 119 - 121

1. Nuclear Fusion

and

Plasma Science

1A) Nuclear Fusion

Personnel: Sigeo Hamada*, Shoichi Shiina, Kazuo Yokoyama*, Yasuyuki Nogi*, Shin Simamura*, Katunori Saito, Tutomu Takahashi*, Yukio Osanai†, Hirokazu Gesso†, Katuhiko Saito†, Hideki Nakamori**, Toshimichi Namba**, Yasuo Nagamine**, Kayoko Fujimoto**, Hiroyuki Shiinoki**, Kunihiko Nakajima**, Takahiko Akiyama**, Naoya Itoh**, Kaoru Iwata**, Mizuhiro Umino**, Katunori Ootuka**, Shinnichi Oomura**, Horoshi Gota**, Ryou Sasaki**, Nobuhiro Suzuki**

Introduction:

The following magnetic confinement systems have been investigated experimentally and theoretically; reversed field pinch (RFP), field reversal configuration (FRC), low aspect ratio tokamak and $L = 1$ torsatron. These investigations include objects associated with an approach to high beta and/or steady state confinement.

*concurrent member
†non-regular member
**graduate student

Magnetic Structure and Equilibrium of ATRAS-RFP Plasma

T. Namba, Y. Osanai*, S. Shiina and K. Saito

Details of confinement and relaxation process will be known from the structure of the internal magnetic field. We observed radial profile of the magnetic field on equatorial surface by using of a probe array inserted into plasma. This probe array is composed from sixty coils set on twenty points by 5mm to measure toroidal, Bz, poloidal, Bp, radial, Br, components of magnetic field at each points. Generally, the probe measurement inserted it in to plasma disturb the plasma seriously. Pratically, plasma current, toridal flux and duration of discharge decreases 20-30% when the probe is inserted, however pinch parameter Θ and reversal parameter F are not affect by the presence of probe. This means that the probe does not influence magnetic field configuration of ATRAS-RFP plasma (major radius of 50cm, minor radius of 10cm). Therefore, the magnetic field distribution observed by the probe is deeply reflecting one of the usual plasma without the probe array. The current density and plasma pressure profiles are calculated from the magnetic field approximated by a 6th-order polynomial by assuming the cylindrical symmetry of equilibrium configuration as follows,

$$\frac{dP}{dr}+\frac{B_z}{\mu_0}\frac{dB_z}{dr}+\frac{B_p}{\mu_0 r}\frac{d}{dr}rB_p=0, j_z=\frac{1}{\mu_0 r}\frac{\partial}{\partial r}rB_p, j_p=\frac{-1}{\mu_0}\frac{\partial}{\partial r}B_z.$$

Plasma pressure profile has the hollow shape oscillating with ~20KHz in the hollow and the maximum point is distance of ~6cm from the magnetic axis. Outside of the hollow, the profile is very stable during the discharge. This seems suggesting the existence of single helicity. By using these pressure and toroidal magnetic profile, the Grad-Shafranov equation was solved, numerically, and shown in fig 1. The contours of poloidal flux are elongated toward a port of discharge tube set up to insert the magnetic probe array. This probably means that local port effect extended all over the tours.

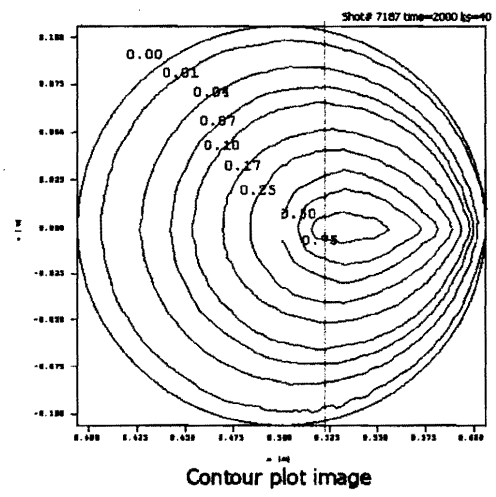

Fig. 1 The contour of magnetic surface obtained at 650 μ s after discharge.

DEVICE PARAMETER STUDIES OF LOW ASPECT RATIO REVERSED FIELD PINCH

Y.Nagamine, Y.Osanai, K.N.Saito, K.H.Saito, S.Shiina

It has been reported that approach to low aspect ratio improves the prospect for an economical, steady state reversed field pinch (RFP) reactor;
1) Significantly large bootstrap current ratio (F_{bs}) even at the moderate aspect ratio of 2~3 with less neutron wall loading, which reduces the requirements for external non-inductive current drive to generate a steady state RFPs, 2) Strong paramagnetism being nearly independent of aspect ratio in addition to small externally supplied magnetic field, which supports no need for superconducting toroidal coil; 3) The large magnetic shear at the lower aspect ratio, which enhances the stability beta limit (β_{st}). These results would make it possible to attain the compatibility of high stable beta, high enginnering reactor power gain and high mass power density, then lower cost of electricity (COE) for steady state RFP reactor. In order to minimize the COE, the device parameters determining MHD equilibrium are necessary to be optimized into high β_{st} and large F_{bs}. The low aspect ratio equilibrium is obtained by solving linear Grad-Shafranov equation with respect to flux function assuming partially relaxed state model (PRSM), $j_p=\lambda B_p/\mu_0$, and parabolic plasma pressure profile. Here is assumed the λ profile to be uniform since it is reasonably close to a stable minimum energy state at finite beta in the cylindrical approximation. The parameter dependence obtained suggests the existence of an optimum combination of device parameters over a certainly wide range of aspect ratio $A\leq 3.0$ to enhance further the ratio F_{bs} keeping a stability beta limit of volume average beta $<\beta>$ higher than 25%.

COMPARISON OF LOW ASPECT RATIO REVERSED FIELD PINCH AND TOKAMAK

Y.Nagamine, Y.Kondoh, S.Shiina

Tow types of magnetic confinement based on partially relaxed state model (PRSM), reversed field pinch (RFP) and tokamak, are compared through their MHD equilibria and stabilities. As for the PRSM-tokamaks, although the bootstrap current ratio is relatively large, the stability requirements for ballooning and internal and external kink modes lowers the stability beta limit, for instance, $\beta_{st}\sim$ 6.7% $<\beta>\sim$ 6.4% in the case of A=1.5, δ (triangularity)=0.4, κ (ellipticity)=1/4. The introduction of reversed magnetic shear, low aspect ratio and noncircular cross section to tokamak enhances the β_{st} value at a high current and reduces the growth rates of TAE (Toroidicity-induced Alfven Eigenmodes), neoclassical tearing, trapped particle and ITG (Ion Temperature Gradient) microinstabilities. As for the PRSM-RFPs, an important features different from the PRSM-tokamaks would make it possible to attain the compatibility of high stability beta limit, high Q (engineering reactor power gain) and high MPD (Mass Power Density) even at the moderate aspect ratio of 2~3 with less neutron wall loading, then lower cost of electricity for steady state RFP reactor.

BEHABIORS OF LONGITUDINAL ADIABATIC INVARIANT AND TRANSPORT IMPROVEMENTS IN L=1 HELICAL MAGNETIC AXIS SYSTEM

M.Aizawa and S.Shiina

We proposed a new approach to transport improvement in helical magnetic axis stellarator by reducing the effective toroidal curvature term ε_T, which is introduced as the sum of usual toroidal curvature term and one of the nearest satellite of L=1 helical field. The reduced ε_T configuration is found to be near the omnigeneity where the magnetic surface is close to the contour of longitudinal adiabatic invariant J. Recently, the J value in L=1 helical system with reduced ε_T is larger in central region than in plasma periphery, showing $\nabla J<0$ or maximum J, then satisfying the stability condition $\nabla P \cdot \nabla J>0$ against collisionless trapped particle microinstability. In conclusion, there exists the compatibility of the reduced effective toroidal curvature, the omnigeneity and the maximum J in L=1 helical magnetic axis system, indicating a novel transport features. Next problem to be solved is the compatibility with high beta approach and low aspect ratio confinement.

Global Motions of Highly Elongated Low Aspect Ratio Tokamak

Y. Narushima, H. Gota, T. Takahashi and Y. Nogi

An extremely highly elongated (κ~10) low aspect ratio tokamak has been produced and confined in a negative-biased theta-pinch device. It is possible to induce a large plasma current I_p (=280kA) for a few microsecond by using a first bank. In spite of a small current ratio I_{tfc}/I_p=0.01 (I_{tfc}:toroidal coil current), the safety factor of the plasma becomes very high (q~30). However, the plasma is easy to move since the plasma is confined away from the vacuum vessel. MHD fluctuations of the plasma are observed by using a magnetic probe array. It is discussed that the plasma shows a vertical displacement, a shift and a tilt motion, and an elliptical deformation of a toroidal cross-section. A scale length of each MHD event is estimated by the aid of an analytic model.

Control of an n=1 Motion on Field-Reversed Configuration

K. Fujimoto, S Ohmura, T. Takahashi and Y. Nogi

An n=1 mode global motion on a field-reversed configuration (FRC) plasma is observed by using a newly developed optical system. It is found that the magnetic axis of the FRC moves around the geometrical axis of the theta-pinch coil during the discharge period. The deviation of FRC from the coil axis reaches 20-40% of the plasma radius. In order to push back the FRC to the equilibrium position a multipole field (quadrupole or hexapole field) is applied. It is shown that the n=1 motion can be easily cotrolled by the field and the critical field strength is less than 10% of the confinement field.

The critical field to the n=1 mode is theoretically obtained by using a simple model in which the FRC is treated as a perfect conducting cylinder in the multipole field. The theoritical estimation agrees well with the experimental results.

Cross Sectional Shape of a Spherical Tokamak by High Repetition Rate Injection

S. Shimamura, M.Umino, K.Ootsuka, T. Takahashi, Y. Nogi

Confining high-pressure plasmas using modest magnetic field in small-size device has been a goal of magnetic fusion energy research. Spherical tokamak (ST), a low aspect ratio tokamak, was introduced to contribute to this goal. Recently, researches on ST are growing active. In ST, current start up, current drive and sustainment are an important subject, because conventional current start up by induction can not be used.

. Current start up and sustainment of a main ST plasma (single or plural) have been investigated by means of a high repetition rate injection of a small ST. This method can start up and sustain the main S.T. plasma by itself because the injected small ST has all torus plasma components of the main ST.

In this experiment, the torus axis of small ST was aligned with the torus axis of main ST and the small ST was injected along this axis. In case of insufficient sustainment by single injection, ST injection of high repetition rate is required.

A magnetized coaxial gun has been used for the experiment on repetitive injection of ST. Using the repetitive current pulse generated by a transformer-coupled circuit, a series of ST plasmas were generated and injected. A repetitive merging of the ST took place in the confinement region.

A fast-gated image intensifier and a CCD video camera took cross sectional views of ST plasma. Frame rate of video is not enough. One frame of picture was available for each discharge shot. We set a freezer circuit on the CCD video camera circuit.

Helium gas was used as a working gas. Two band pass filters, 467 ± 5nm and 589 ± 5nm, were used to take images for helium lines of 468.6nm and 587.6nm each.

First ionized state of helium emits the 468.6nm line and the cross sectional image of this line is shown in Fig. 1. On the other hand, neutral helium atom emits the 587.6nm line and this image is shown in Fig. 2. Shutter times of two pictures are same and 47 μs from the start of the gun current. This time corresponds to the second injection phase of ST plasma.

Fig.1 Cross sectional shape of 468.6nm line

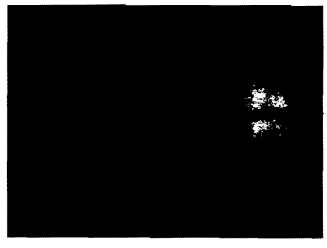

Fig.2 Cross sectional shape of 587.6nm line

1B) Plasma Science

Personnel: Tetsu Miyamoto, Keiichi Takasugi, Alexander Muravich†, Mehrdad Kashani**, Yoshitaka Mitamura**, Hisashi Akiyama**, Hajime Abe**, Hiroyuki Takenaka**, Ryusuke Muto**, Takashi Yoshida**, Satoru Narisawa**

Introduction

The plasma science group has investigated the physics and applications of hot, dense plasmas confined by self-magnetic field, that is, z-pinches and plasma foci. We have also studied in the diagnostics of the hot, dense plasmas and pulsed power technologies.

The following experimental and theoretical researches have been carried out :

1) X-ray spectroscopy of the SHOTGUN gas-puff z-pinch plasma (30 kV, 24 μF, 10.8 kJ) using a Johansson-type spectroscope
2) Interferometry of the z-pinch plasma using a pulsed YAG laser
3) Observation of Rayleigh-Taylor instability in the contraction phase of the gas-puff z-pinch plasma
4) Plasma focus and sheet z-pinch experiments using the 18 kJ capacitor bank (40 kV, 22.5 μF)
   (a) Effects of cathode electrode in plasma focus discharge
   (b) Production of dense sheet z-pinch
5) Theoretical study
   (a) Dynamics of dense sheet z-pinch
   (b) Steady state of dense sheet z-pinch with thermal conduction

At the same time several plasma diagnostic methods have been developed for these experiments.

---

†non-regular member
**graduate student

INTERFEROMETRY OF AN IMPLODING Z-PINCH

Ryusuke Muto, Keiichi Takasugi

The interferometric measurement of Ar gas-puff z-pinch plasma has been made by a Mach-Zehnder interferometer using pulsed Nd : YAG laser.

Figure. 1 shows observed the interferograms of the z-pinch plasma at different pinch phase, (1) early phase, (2) shrinking, (3) maximum pinch and (4) expansion. The shift of one fringe corresponds to line density of $4.2\times10^{21}\mathrm{m}^{-2}$. The fringe shift increased with implosion. In Fig. 1 (3) and (4) the fringe shift could not be observed well and the intergerogram became like the shadowgram.

The fringe shift of the interferogram Fig. 1 (2) was analyzed by a computer and plotted in Fig. 2. The plasma has a hollow density distribution, but the upper part has higher density than the lower part. This asymmetry indicates that Ar gas was not puffed symmetric from the gas nozzle on the anode. This symmetry of gas distribution was performed by improving the gas nozzle.

The observed fringe shift was 3-4 at maximum in this phase. Since the density of the shrinking phase is not so high, we cannot expect enough measurement at succeeding high density stages. The laser image looked like a shadowgram near the maximum pinch due to high line density and density gradient. Therefore, it seems better to use shadowgraphy for the observation of radial dynamics of the imploding z-pinch plasma.

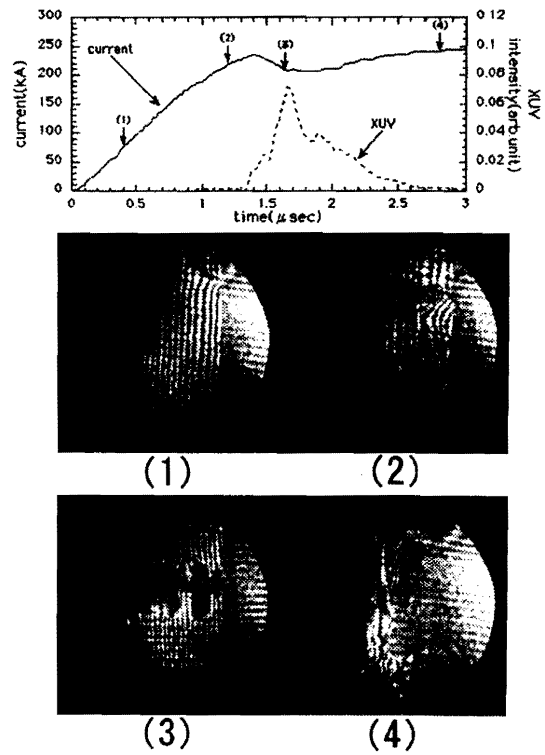

Figure 1: Interferograms of Ar z-pinch.

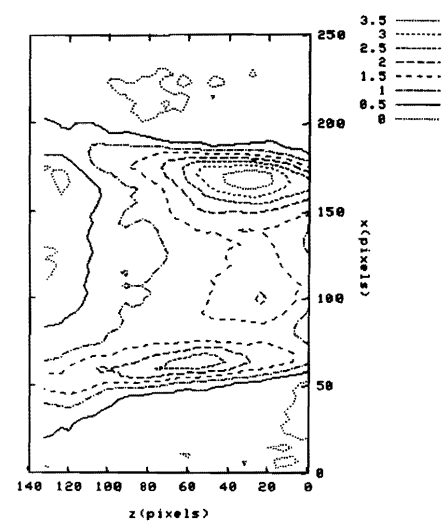

Figure 2: Contour plot of the fringe shift.

RAYLEIGH-TAYLOR INSTABILITY OF A Z-PINCH

Ryusuke Muto, Keiichi Takasugi

The development of Rayleigh-Taylor instability in the implosion process of Ar gas-puff z-pinch plasma was observed by a pulsed Nd : YAG laser shadowgraphy.

Figure. 1 shows the shadowgrams of the imploding z-pinch plasma. The Rayleigh-Taylor instability occured on the plasma surface at the early phase (1)-(3). The amplitude of the instability grew with implosion. The wavelength of the instability also increased with the growth. The envelope of the shadowgram was analyzed by using Fourier transform. The wave number and the wavelength of the instability were extracted and plotted in Fig. 2. It is clear that the wavelength increased with implosion.

The growth rate of the Rayleigh-Taylor instability with finite Larmor radius effect is expressed as

$$\gamma = \sqrt{gk - \frac{1}{4}\omega_{ci}^2 (k\rho_i)^4},$$

where ω_{ci} is the ion cyclotron frequency, ρ_i is the ion Larmor radius and g is the acceleration by implosion. The growth rate has the maximum at the wave numuber

$$k = (g\omega_{ci}^{-2}\rho_i^{-4})^{1/4},$$

and the instability grows at this wave number. As the acceleration g is considered to be proportional to B^2, the wave number $k \propto (B^4/T_i^2)^{1/3}$. The decrease of k with the time shows that the ion temperature T_i increased more than a square of a magnetic field B^2. This indicates that there is some mechanism of extra acceleration or heating of ion that accounts from preservation of magnetic moment.

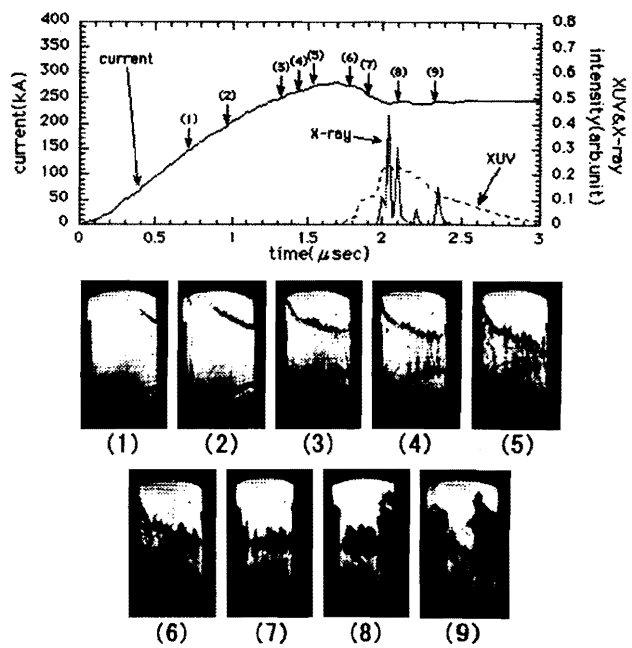

Figure 1: Shadowgram of Ar z-pinch plasma.

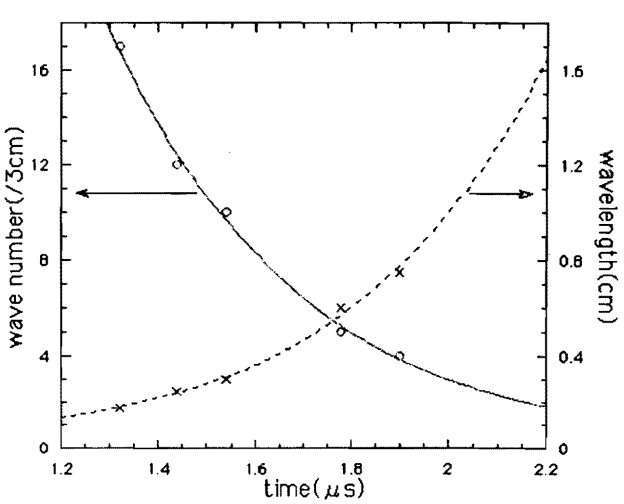

Figure 2: Wave number and wavelength of the instability vs time.

X-RAY SPECTROSCOPY WITH A CONVEX CRYSTAL

Satoru Narisawa, Keiichi Takasugi

A convex curved mica crystal ($2d$ = 19.884 Å) was used for x-ray spectroscopic measurement of Ar gas-puff z-pinch plasma[1]. Although a convex spectroscope has no focusing and is darker than a concave one, a wide range of wavelength domain can be provided. Figure 1 shows a photograph of the spectrooscope with a convex mica crystal. The curvature radius of the crystal is 19.5 mm.

The spectrogram and its densitogram are shown in Fig. 2. We can see an intense line emitted from He-like Ar ion (Ar XVII $1s^2$ - 1s2p, λ = 3.9488 Å). The line corresponds to the 3rd order ($n = 3$) of Bragg reflection,

$$2d \sin\theta = n\lambda.$$

As we look into the spectrogram carefully, we can see the 2nd ($n = 2$) and the 4th ($n = 4$) reflections of the same line. It is a characteristics of mica that odd order of reflectivities are higher than even ones.

We could not observe other spectral lines. This means that the populations of H-like and Li-like ions are small, and electron temperature of the plasma is 500 - 1000 eV assuming ionization equilibrium. The wavelength range below 2 Åcould not be seen due to direct exposure of incoming x-ray. We need to reduce this to get a clear spectra.

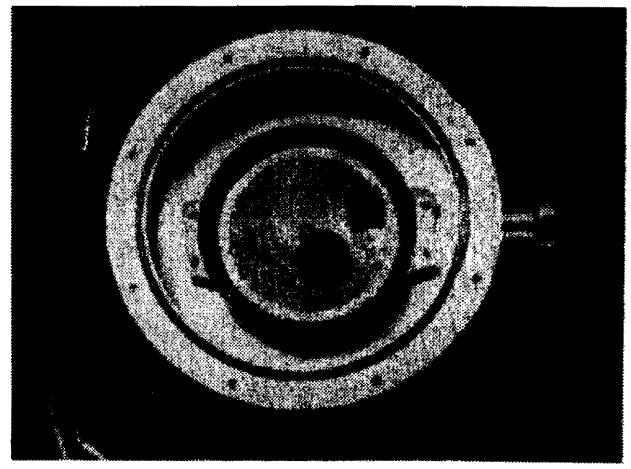

Figure 1: X-ray spectroscope with a convex curved crystal.

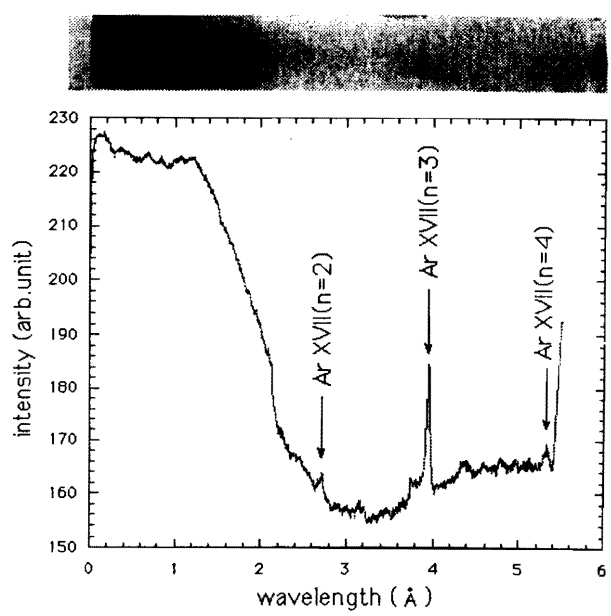

Figure 2: Spectrogram and its densitogram.

Reference

[1] E.O. Baronova, K. Takasugi : ANNUAL REPORT 1999, 13 (2000).

DYNAMICS OF DENSE SHEET Z-PINCH[1]

A. Muravich

The dense sheet z-pinches were proposed, and its steady state and transient processes were investigated for idealized cases[2] In this research, the dynamics of realstic sheet z-pinch with finite width was investigated using several models. First, the dynamics of thickness and width was investigated separately and analytically for a long enough sheet. It was pointed out that the viscosity is important and that the sheet does not contract continuously but splits when the initial sheet width is wide enough. Second, the dynamic was also studied using snowplow model. Finally, the general dynamical behaviors were numerically investigated. The contraction of sheet is classified into two types – slow and fast contraction. In the latter the uniformity of sheet is lost, and the current density is higher at the both ends.

1. A. Muravich, "Dynamics of Dense Sheet Z-Pinch", J. Phys. Soc. JPN, 69(6) (2000) pp.1692-1704.
2. T. Miyamoto, "Dense Sheet Z-Pinches", J. Phys. Soc. JPN, 68(4) (1999) pp.1238-1258.

STEADY STATE OF DENSE SHEET Z-PINCHES WITH THERMAL CONDUCTION[1]

A.Muravich, T.Miyamoto and V.Vikhrev[*]

The steady states and dynamical behavior of dense sheet z-pinches were investigated in the previous paper[2,3], in which thermal conduction effect was not considered. There are two types – compressional and stretched types – for generating the sheet z-pinches. In the compressional type, the conductor compressing the plasma must exist near the plasma. Hence, the thermal conduction effect will be important. In this study, the steady state of the sheet z-pinches was reexamined taking into account the thermal conduction. Then, the sheet z-pinches are classified into three types depending on the ratio of radiation loss to the thermal conduction loss (1) arc discharge and (2) z-pinch types that have only one peak in temperature, and (3) a type of the temperature profile with more than two peaks, that occurs as a result of poor thermal conduction.

(*) Russian Research Center, Kurchatov Institute (Russia)

1. A.Muravich, T.Miyamoto and V.Vikhrev, "Steady State of Dense Sheet Z-Pinches with Thermal Conduction", To be published in JJAP (2001).
2. T. Miyamoto, "Dense Sheet Z-Pinches", J. Phys. Soc. JPN, 68(4) (1999) pp.1238-1258.
3. A.Muravich, "Dynamics of Dense Sheet Z-Pinch", J. Phys. Soc. JPN, 69(6) (2000) pp.1692-1704.

CATHODE EFFECTS IN PLASMA FOCUS DISCHARGE[1,2]

A.M.Kashani, K.Sato, T.Miyamoto, A. Baba, A.Horiuchi, K.Takasugi, S.Sasak(*), M.Lu(**) and V.Vikhrev(***)

The plasma focus discharge was investigated using two types of cathode electrode -- sixteen copper-bars arranged along the envelope of cylinder and a conventional cylindrical tube. The neutron yield at the optimum pressure was three times lower in the latter in spite of low inductance that meant higher maximum current. The cause resulted from higher dissipation in the traveling phase preceding the plasma focus. In the latter the plasma was swept and compressed near the inner surface of the cylindrical cathode. This cold, dense plasma contacting with the cathode was cooled constantly. On the other hand, as in the bar cathode the considerable fraction of the plasma escapes through the separation between adjacent bars, the dissipation decreases. We conclude that the bars cathode is more excellent than the conventional cylindrical one, unless it spoils the uniformity of discharge.

(*) High Energy Accelerator Research Organization ; (**) Hebei University (China),
(***) Russian Research Center, Kurchatov Institute (Russia)

1. A.M.Kashani, K.Sato, T.Miyamoto, A. Baba, A.Horiuchi, K.Takasugi, S.Sasaki, M.Lu and V.Vikhrev, "Cathode Effects in Plasma Focus Discharge", "Int. Symp. on Pulsed Power and Plasma Applications", (Oct. 26-27, 2000, Korea), to be published in J of Korean Electric Soc..
2. M.A.M.Kashani, K.Sato, T.Miyamoto, A. Baba, A.Horiuchi, K.Takasugi, S.Sasaki, M.Lu and V.Vikhrev, "Effects of Cathode Electrode in Plasma Focus Discharges", Proc. of "The 8th. Asia Pacific Phys. Conf.", (Aug. 7-10, 2000, Taipei) pp.243-246.

OBSERVATION OF DENSE SHEET Z-PINCHES[1]

M.A.M.Kashani, A.Baba and T.Miyamoto

There are two types of dense sheet z-pinch plasmas – compressinal and stretched types[2]. Plasma focus electrode geometry is useful for producing both types. The former type requires the return current conductor adjacent to the plasma sheet and accompanys a little difficulty for observation. So first, we tried to produce the latter type of sheet z-pinch. The plasma is produced between two conducting bars attached at the top of the anode. The observation was carried out camera and Schlieren methods. The discharge are classified into three types depending on the filling pressure. The sheet z-pinch observed only for a moderate pressure region.

1. M.A.M.Kashani, A.Baba and T.Miyamoto, "Observations of Dense Sheet Z-Pinches", To be published in Proc. of 13th Int. Conf. on High-Power Particle Beams (June 25 - 30, 2000, Nagaoka).
2. T. Miyamoto, "Dense Sheet Z-Pinches", J. Phys. Soc. JPN, 68(4) (1999) pp.1238-1258.

2. Superconductivity

2) Superconductivity

Personnel: Kazuko Sekizawa*, Takeshi Ogasawara, Hisayasu Kobayashi, Yoji Kubota*, Kazuhiko Yasohama, Yoshiki Takano*, Koichi Takase*, G.Osabe**, T. Wuernisha**, M. Nakamura**, T. Tanifuji**, S. Nakazato**, H. Yumura**, A. Kikuchi**, J. Osakabe**, Y. Takahara**, N. Arai**, Y. Koyama**, S. Hara**, H. Hirose**, M. Ito**, K. Makihara**, K. izuno**, T . Tubaki**

Introduction:

The Superconductivity group has successively done works on the basic and applied superconductivity and magnetism including the related cryogenic technology. The main subjects are as follow :

i) Feasibility study on large - scale , high current density superconductor by dynamic stabilization.

ii) Electromagnetic properties of superconducting wires with fine filaments.

iii) Magnetic and superconducting properties of rare earth intermetallic compounds and high temperature superconductors.

iv) Magnetic and transport properties of low dimensional compounds containing transition - metal elements.

*concurrent member
**graduate student

ENERGY TRANSPORT THROGH THE LOW PRESSURE He II CHANNEL BY THERMAL ACOUSTIC EMISSION

Hisayasu Kobayashi

Intrinsically high thermal conductive He II must have more advantage to the low temperature equipments such as superconducting magnets if an additional heat transport mechanism is provided. In this study, we have observed that the temperature of He II in a channel is cooled down to the bath temperature at the pressure below the lambda point when the superfluidity is broken on the heated surface in spite of increase in the heat flux q. These phenomena look as if He II in the channel has super-thermal-conductive properties in the film boiling state. The acoustic emission in the film boiling state of heat transfer in the near saturated He II seems to be superimposed on the energy transport through the bulk He II in the quantized vortex state dominated by Gorter-Mellink thermal conductance.

The channel used in this experiment was made by the vacuum insulated stainless steel tube with the diameter of 6 mm in which the heated copper-surface is placed at the bottom. To observe preliminarily the signal of thermal oscillation, Rayleigh disk made of the plastic foil with the diameter of 6 mm was set at the exit of the channel. A small coil wound peripherally around the disk was attached on a ferromagnetic plate to detect the signal voltage induced across the coil. The direct observation of behaviors of the disk suggests that the acoustic emission accompanied with the turbulence of mixing of the liquid and the gas near the heated surface may transport forcedly the energy through the channel; the manner of energy transport in He II channels is switched from the heat conduction in the tangling quantized-vortex state to the acoustic energy transmission on the phase transition at the heated surface. In other words, at lower vapor pressure than the lambda pressure the temperature gradient across the channel length is disappeared at all, the heat conduction through the vortex state is entirely replaced by the acoustic transmission with high frequency of the sound. The apparent super-thermal-conductivity in the film boiling state can be stated as the entropy flow through the channel.

Large amount of the heat dissipated at a hot area is evacuated as the kinetic energy without thermally disturbing the surroundings. Besides, the evacuated energy may be released outside the channel where the pool of He II has essentially large thermal conductivity.

Hysteresis Loss and Critical Current Density of Multifilamentary $(NbW)_3Sn$ CompositeConductor for AC use

K. Yasohama, Y. Kubota, H. Kobayashi, T. Ogasawara,

H. Kasahara, S. Torii and S. Akita

Recently, the fabrication technology of Nb_3Sn conductor for AC use has been rapidly advanced Nb_3Sn conductors have the advantages of superior superconducting properties of critical temperature, critical current density and critical field compared with NbTi conductors. Thus, the development of Nb_3Sn conductors for AC use opens a new prospect of the application of superconductivity. While multifilamentary Nb_3Sn conductors have been made for AC use, they still have considerable AC losses. In field of 50 ~ 60 Hz for power frequency equipments, magnetic hysteresis loss accounts for the most of the loss. In order to decrease the loss and maintain high current density, the diameter and spacing of superconducting filaments must be reduced to submicron or less. This large reduction brings about serious problems which are a deformation of filament shape and a generation of superconducting links between filaments by the proximity effect or bridging. These deformation and links increase an effective diameter of a filament and induce excess hysteresis loss. It has reported that alloyed Nb filaments and alloyed matrix are effective for the suppression of the filament deformation and links in a Nb_3Sn conductor.

In this study, we fabricated a Nb_3Sn composite conductor employing Nb filaments alloyed W and Cu matrix alloyed Ni, and examined the effect of alloying on the effective filament diameter by measuring the critical current density and DC magnetization. For this conductor, several considerations are given to present the filament deformation and to reduce the electromagnetic coupling among filaments. One is that the stabilizer is composed of thirty-seven rods of Cu-10 wt%Ni clad copper, with which the coupling current through the stabilizer can be decreased by high resistance of Cu-Ni, and furthermore, the Cu-Ni cladding plays a role of tin-diffusion barrier for the stabilizer. Cu-10 wt%Ni is also used for the sheath of the conductor. We adopted alloyed Nb and alloyed Cu expecting that the increased hardness of Nb and Cu by alloying would suppress the filament deformation. Nb is alloyed with 1 at%W and Cu with 1 at%Ni. It is supposed that such a small addition of the elements does not make a harmful effect on tin diffusion in the matrix and superconducting properties of filaments. Samples of conductor were heat treated to form Nb_3Sn at 450 to 700°C for 24 to 740 hours. Superconducting critical currents of the short samples were measured at 4.2 K in transverse fields up to 5 T using the four point method. A criterion of 1 μV/cm was adopted to determine the critical current value. A SQUID magnetometer was used for the magnetization measurement at 4.2 K in transverse fields up to 5 T.

In this study, it was concluded that W to Nb filament and Ni to Cu matrix are found to be effective in reducing d_{eff} of Nb_3Sn filaments, in a field of 1.5T the d_{eff} is 3 ~ 5 μm. The overall critical current density is 4.9 GA / m^2 at 4.2 K in a transverse field of 1.5 T.

CRITICAL CURRENT DENSITY AND MAGNETIZATION OF PROXIMITY-EFFECT-INDUCED SUPERCONDUCTING Cu IN MULTIFILAMENTARY NbTi / Cu COMPOSITE CONDUCTORS

Y. Kubota, T. Moriya and K. Yasohama

Considerable progress in the manufacturing techniques for multifilamentary composite conductors has opened new prospects. Unfortunately, it was also found that ac losses in the conductor increased remarkably with decreasing filament spacing. This effect results from filament coupling due to the presence of a proximity-effect-induced superconducting matrix (PEISM) in the conductor. The amount of excess magnetization in the multifilamentary composite conductor is, therefore, much greater than that estimated from the Bean's critical state model.

Special sample conductors were used to measure the magnetization M_p of PEISC in multifilamentary NbTi/Cu composite conductors. They have the following specifications: filament diameter: 0.337 mm, width of the regular hexagonal filament: 7.60 μm, filament spacing: 1.38 μm, and filament number: 931. They have twist pitches of l_p: 6.9, 13, 20, 94 and 189 mm.

The magnetization M_p of PEISM in multifilamentary NbTi/Cu composite conductors has been measured in transverse fields B_e smaller than B_{c1} of the NbTi filament at 4.2 K. The conductors were designed specifically to subtract out the magnetization of the NbTi filaments from magnetization of the conductors. M_p was investigated as a function of the twist pitch l_p and the field amplitude B_m. The first penetration field B_{c1p} of the magnetic flux, the decoupling field B_{dp} of the filament coupling, and the width of the M_p at a given field are directly proportional to the twist pitch. M_p magnetization-loops intersect each other for $B_{c1p} \leq B_m \leq B_{dp}$ and decrease suddenly at B_{dp}. The critical current density J_{cp} of proximity-effect-induced superconducting Cu is proportional to B_e^{-2} and its value is 10 kA/m^2 at 7 mT.

Magnetism and Specific Heat of the Transition Metal Phosphorus Chalcogenides

Yoshiki Takano, Natsuki Arai, Kouichi Takase and Kazuko Sekizawa

The crystal structure of the transition metal phosphorus chalcogenides MPX_3 is closely related to the layered compound $CdCl_2$, where transition metal ions and phosphorus-phosphorus pairs occupy the cadmium positions and sulfur ions occupy the chloride positions. The transition metal ions form a honeycomb network structure and have localized magnetic moments. In the compound $M'^{I}_{0.5}M''^{III}_{0.5}PX_3$ where divalent M ions are substituted by equiamount of monovalent M'^{I} and trivalent M''^{III} ions, M'^{I} and M''^{III} ions order themselves. In $Ag_{0.5}V_{0.5}PS_3$ and $Ag_{0.5}Cr_{0.5}PS_3$, V and Cr ions are known to form quasi one dimensional antiferromagnetic zigzag spin chains. The former is a Heisenberg antiferromagnet with Haldane gap. The temperature dependence of the magnetic susceptibility χ of $MnPS_3$ shows a sharp kink at the Néel temperature T_N of 78 K. The braod hump which is characteristic to the low dimensional magnetic materials is observed. The magnetic anisotropy is scarecely observed above T_N. Anisotropy observed below T_N is explaind by spin flop mechanism. In $FePS_3$, the braod hump is observed and the Néel temperature T_N is not clearly identified. In such case, the Néel temperature T_N is defined by the temperature at which $d\chi/T$ shows a maximum. Anisotropy above T_N is explained by the crystalline electric field effect and spin-orbit interaction. The low temperature specific heat of $ZnPS_3$ obeys Debye T^3-law with the Debye temperature $\Theta_D = 225$K. The temperature dependence of the magnetic specific heat of $MnPS_3$ shows a large broad hump over rather wide temperature range and a small sharp peak at T_N. The temperature dependence of the specific heat of $FePS_3$ shows a large sharp peak at T_N. This sharp peak is considered to be the magnetic transition acompanied with first order transition due to the magnetostriction. Although the temperature dependence of the magnetic susceptibility of $Ag_{0.5}V_{0.5}PS_3$ is almost as same as the previous reports, the magnitude of the Haldane gap of 400 K is larger than that of the previous reports. The slope of the temperature dependence of the specific heat is smaller than that of $ZnPS_3$. The separation of the magnetic specific heat is not performed now.

Magnetic properties and specific heat of a ferromagnetic zigzag spin chain compound $LaCrOS_2$

Yoshiki Takano, Takamitsu Tsubaki, Kouichi Takase and Kazuko Sekizawa

Magnetic properties and the specific heat of $LaCrOS_2$, in which Cr ions form zigzag spin chains, has been investigated. While the temperature dependence of the magnetic susceptibility obeys Curie-Weiss law above 200 K. it shows a one dimensional character in the temperarture range between 200 K and Curie temperature, T_c of 32 K. The temperature dependence of the magnetic specific heat shows a broad hump which is characteristic to the one dimensional magnetic spin chain. The maximum occurrs at about 30 K. In addition to this broad hump, the small sharp peak due to the three dimensional order is observed at T_c. The one dimensional behavior observed in the magnetic susceptibility and the magnetic specific heat is well reproduced by an effective Ising chain with $S = 3/2$.

MAGNETIC AND TRANSPORT PROPERTIES OF $Nd(Ba_{1-x}Sr_x)_2Cu_3O_y$

T.Wuernisha, Y.Takano and K.Sekizawa

It was reported previously that the transport property of $Pr(Ba_{1-x}Sr_x)_2Cu3O_y$ changed drastically with x and it became almost metallic at x ~1. The origin of this substitution effect was attributed to the fact that due to the small ionic radius of Sr the distance between Pr ions and oxygen ions in the CuO_2 planes increased with x and the hybridization between Pr 4f and O 2p orbitals decreased.

We have studied transport properties of $Nd(Ba_{1-x}Sr_x)_2Cu_3O_y$ (x=0~0.5). Neodimiun is next to Pr in the periodic table and has an ionic radius next to that of Pr in the rare earth series.

The superconducting transition temperature T_c decreases with x, from 90 K for x=0 to 55 K for 0.5. This x dependence of T_c cannot be explained by the increase of the distance between Nd and oxygen ions and lead to the possibility of the site exchange of Nd and Sr ions on the Nd and the Ba site.

There is a possibility that a part of Sr ions occupies the Nd site and a part of Nd ions goes to the Ba site. This introduces the charge randomness on both the Nd plane and the Ba-O plane which causes the corrugation of the CuO_2-plane and results in the decrease of T_c.

To investigate the ion distribution on the Nd and the Ba site the intensity of the X-ray diffraction lines was calculated for various x and z of $Nd_{1-z}Sr_z(Ba_{1-x}Sr_{x-z/2}Nd_{z/2})_2Cu_3O_7$. The experimental result on the x dependence of the intensity of (001) line is well reproduced for z $\neq 0$, which shows that a part of Sr ions occupies the Nd site.

3. Theoretical Physics

3A) Plasma, Astronomy and Statistical Physics

Personnel: Ichiro Kawakami, Kimiaki Konno*, Setsuo Misawa*, Masatomo Sato*, Massamitsu Aizawa, Ippei Shimada, Chigaku Itoi*, Shiomi Kumagai*, Kiyomitsu Suzuki*, Akihoro Ishimori**, Koji Imai‡, Masato Sumihiro**, Daisuke Imai**, Kenji Nehashi**, Akio Fukuda**, Shin Honma**, Daisuke Yamakata**, Kenki Ushikoshi**, Katsunori Tanaka**, Shin Hirota**, Atsushi Iwasaki**, Kyouko Nogami**, Yoshito Maki**, Takumi Tamai**, Kazumasa Tsushima**, Michio Togo**, Kazuyoshi Watanabe**, Yoshinori Sakamoto**, Kazuo Hirano**, Kousei Iwabuchi**, Akiharu Kitoh**,

Introduction

The Theoretical Plasma and Statistical Physics groups in 1998 are grossly classified as follows:

i) computational plasma physics,
ii) nonlinear magnetohydrodynamics,
iii) theoretical study in nuclear fusion,
iv) Fermi liquid description itinerant-electron magnetism,
v) theory of strongly correlated electrons,
vi) theoretical study of nonlinear waves including chaos, turbulence and transport in plasmas,
vii) nonlinear dynamics, solitons in physical systems,
viii) dynamics of complex systems,
ix) astrophysics

*concurrent member
**graduate student
‡research fellow

Three Conditions for Optimization of Particle Confinement in L=1 Herical Systems

M. Aizawa, S. Shiina and I. Kawakami

We have pointed out three important notices for the helical magnetic axis system to consider the good particle confinement properties and the stability for magnetohydrodynamic instability.

1. Reduction of Effective Toroidal Curvature

The first is the role of the effective toroidal curvature term for localized trapped particles defined as the sum of the toroidal field and bumpy field. It determines the collisionless confinement conditions of helically trapped particles. We have reported that this small effective term leads to the good collisionless confinement of helically trapped particles [1,2]. The reduced effective term configuration can be seen in low aspect ratio stellarator/tokamak hybrid.

2. Suppression of Magnetic Island Formation

The formation of the largest magnetic islands at the lowest-order rational surfaces because they couple nonlinearly most readily to the non-resonant vacuum magnetic Fourier components, the helical magnetic axis field and toroidal field, which cause indirect resonant pressure driven currents at every rational surface and form the islands. This result requires the large periodic field number N.

3. Field Modifications for Magnetic Well Improvement

The smaller N system is easier for the magnetic well, on the other hand the larger N system is required the magnetic well improvement by some field modifications proposed; the negative pitch modulation in coil winding law and the superposition of relatively weak L=-1 field, multipole (dipole and quadrupole) and toroidal fields on standard L=1 systems.

Therefore, it is important to design the large N system with the reduced effective curvature term and the good magnetic well by its improvement for satisfying above three conditions.

[1] M.Aizawa and S. Shiina; Phys. Rev. Lett. **84**, 2638 (2000)

[2] M.Aizawa et.al.; *Proc. of the 27-th EPS Conf. on Controlled Fusion and Plasma physics* (Budapest, Hungary, 2000); 480 (2000)

Numerical Determination of the Magnetic Filed Line Hamiltonian in Helical Systems

K. Tsushima, M. Aizawa and I. Kawakami

The general magnetic field can be written in the canonical representation

$$\boldsymbol{B} = \nabla\psi \times \nabla\theta + \nabla\varphi \times \nabla\chi(\psi,\theta,\varphi),$$

where ψ is a toroidal flux, χ is a polidal flux function, θ and φ are a poloidal and a toroidal angle, respectively. When the magnetic field is integrable, χ is a function of ψ alone. The equations of magnetic filed line can be transformed to

$$\frac{d\psi}{d\varphi} = -\frac{\partial\chi}{\partial\theta}, \qquad \frac{d\theta}{d\varphi} = +\frac{\partial\chi}{\partial\psi} \ .$$

After identification of φ with time t, of χ with H, of θ with the coordinate q, and of ψ with the momentum p, above equations are Hamilton's equations of motion: $dp/dt = -\partial H/\partial q$ and $dq/dt = \partial H/\partial p$. The structure of a magnetic filed is determined by a one-degree-of-freedom, time-dependent Hamiltonian χ. This Hamiltonian is evaluated for a given field in a perturbed action-angle form [1]. The location and the size of magnetic islands in the given magnetic field are determined from Hamiltonian perturbation theory and from an ordinary Poiencaré plot of field line trajectries. We have tested by the straight helical field.

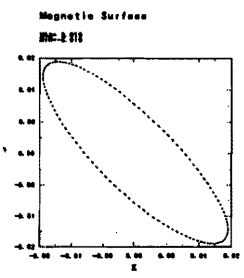

Fig.1(a)

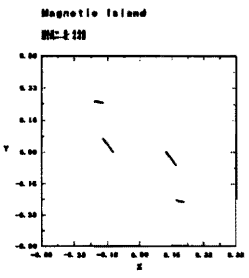

Fig.1(b)

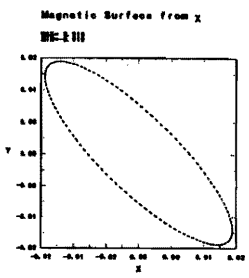

Fig.2(a)

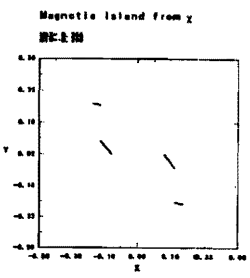

Fig.2(b)

Fig.1(a) is a magnetic surface and Fig.1(b) is a magnetic island. They are obtained by usual Poiencaré plot from filed line equations, while Fig.2(a) and Fig.2(b) are obtained by Poiencaré plot after evaluating magnetic field line Hamiltonian. It is shown that Fig.1 and Fig.2 are good agreement. We have attempted to obtain the magnetic field line Hamiltonian for the L=1 torsatron system, however, the strong numerical instabilities have occurred in integrating the coordinate transformation equations, and this subject remains for our future problem.

[1] G. Kuo-Petravic and A. H. Boozer; J. Comput. Phys. **73**, 107 (1987)

Bumpy Field Effect on Particle Confinement of L=1 Torsatron Systems

K. Watanabe, M. Aizawa, S. Shiina and I. Kawakami

We have reported the importance of the effective toroidal curvature term defined by the sum of a usual torus curvature term and a bumpy field term[1]. This term determines the confinement properties of localized trapped particle in helical system. The one of the methods for control of a bumpy field is a coil pitch modulation, another method is the addition of external field by circular loop coils.

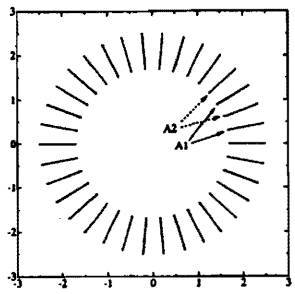

Fig.1(a)

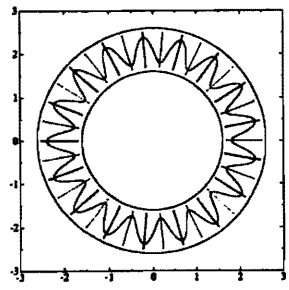

Fig.1(b)

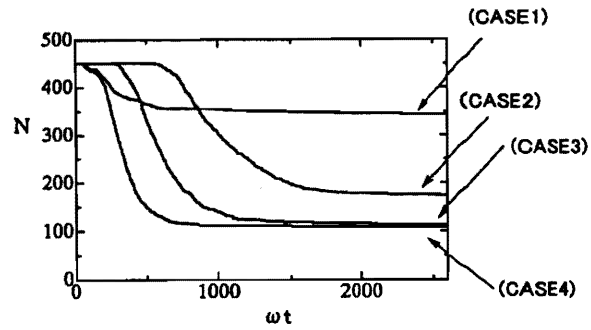

Fig.2

Fig.1(a) is a plan figure of circular coils for creating a bumpy field and Fig.1(b) is a plan figure of the base L=1 torstron field coil and circular coils which are shown in Fig.1(a). The mirror ratio M_r along the helical coil winding center line within one filed period is changed from $M_r = 1.07$ to $M_r = 1.18$ by controlling currents flowing the two types of loop coils A1 and A2(Fig.1(a)). The particle confinement properties are studied by loss-cone properties in the velocity space and the time dependence of the confinement particle number N.

Fig.2 shows that the four types of a confinement particle number N are plotted against the time normalized by the inverse of cyclotron frequency ω^{-1}. The Mirror ratio of Case1 is 1.07, of Case2 is 1.09, of Case3 is 1.13, of Case4 is 1.18. This result suggests that the particle confinement properties are good for Case1. The high mirror ratio prevents particle to flow along toroidal direction. The quantitative effect of bumpy field for the effective toroidal curvature term is not clear in these calculations, because the Fourie amplitude of bumpy field is not examined quantitatively.

[1] M.Aizawa and S. Shiina; Phys. Rev. Lett. **84**, 2638 (2000)

Application of Wavelet Analyses for Complicated Spectrum Identification on Magnetic coordinate Systems

K. Ushikoshi, M. Aizawa and I. Kawakami

When we establish the magnetic coordinates (ψ, θ, φ) from the three Cartesian components x, y and z in the real system, the Fourier spectrum mode identification is important process. In the near outer-most surface, these modes identification is very complicated process due to noisy signal data. We have examined to analyze these data precisely by applying the Wavelet Analyses and the Fourier Analyses at the same time.

High-Performance Computing by Personal Computer Based on Windows 2000 Operating Systems

N. Tanaka, M. Aizawa and I. Kawakami

It is paid attention that the parallel computing is setting new records for processing speed. But it has some technical problems for solving real physical systems. We have tried to apply parallel computing to the particle trajectory calculation problem. Usually, the PVM library [1], which is a software package that permits a collection of Unix computers hooked together by a network to be used as a single large parallel computer, is used. The main difference between PVM and parallel machine is the communication speed. We have tried to create the similar system in the dual processor machine based on the Windows 2000 operating system.

[1] A.Geist et al. : PVM3 User's Guid and Reference Manual (1996)

Symplectic Integration Study of Differential equations for Long Time Evaluation

S. Hirota, M. Aizawa and I. Kawakami

In the conservative system, the equations of motion satisfy the Hamilton's equations. When we analyze this system numerically, these differential equations are discretized to load computer process. Although the original differential equations satisfy the Hamilton's equations, the derived finite difference equations are not guaranteed to obey the Hamilton's equations. The numerical integration method which satisfies the canonical transformation is called 'symplectic integration method'. We have examined some symplectic methods to calculate the particle trajectory precisely in the herical system for very long time.

RECURSION FORMULA FOR INTEGRABLE EQUATIONS DERIVED FROM IKK SYSTEM WITH TWO HIERARCHIES

Kimiaki KONNO and Hiroshi KAKUHATA

We have proposed a system which has two hierarchies, each of which consists of an infinite member of integrable nonlinear equations. Given a symmetry group, we can derive the system through the inverse scheme. The scheme to derive nonlinear equations of the hierarchies is so constructive that relation between members among nonlinear equations of the hierarchies is systematically determined. In this report we present recursion formula by using the proposed system. We give the recursion formula of the localized induction hierarchy and the hierarchy with the dispersionless equation as a member and show that the formula give recursion formula for the famous nonlinear equations such as the modified Korteweg-de vries equation, the sine-Gordon equation and the nonlinear Schödinger equation.

THE PHENOMENON OF SURFACE TENSION MAXIMUM IN LIQUID ^{3}He

Setsuo Misawa

Recently the surface tension of liquid ^{3}He was measured by Matsumoto et al. at low temperatures; they found that the surface tension $\sigma(T)$ exhibits a small maximum at about 100mK. Existing theories are unable to explain this anomaly. On the basis of a local approximation for the entropy in which the Fermi liquid effect is included, we can evaluate the variation of $\sigma(T)$, $\Delta\sigma(T) = \sigma(T) - \sigma(0)$, as a function of T and of the number density (or the interaction strength). It is found that $\sigma(T)$ consists of two terms; a T^2 term and $T^4 \ln T$term. We predict that, for the density of real liquid ^{3}He, $\Delta\sigma$ exhibits a very tiny minimum and a small but relatively larger maximum. This prediction explains even qualitatively all salient features of the observed $\Delta\sigma$.

SUSCEPTIBILITY MAXIMUM OF NIOBIUM METAL

J.Xue[1], Q.Zhou[1], H. Suzuki[1] , and S. Misawa

At low temperatures the phenomenon of susceptibility maximum is universally observed in all paramagnetic 3d, 4d, and 5d metals except for niobium. We measured the temperature dependence of the magnetic susceptibility of niobium metal in various small magnetic fields very precisely by using a SQUID magnetometer. In niobium metal we have to consider the diamagnetic susceptibility due to superconducting fluctuations. We found that the susceptibility maximum was always observed when the applied field was lower than about 150 Oe. These results are consistent with Misawa's Fermi liquid theory.

[1] Department of physics, Faculty of Science, Kanazawa University, Kakuma, Kanazawa 920-1192, Japan

TEMPERATURE-SQUARED TERMS IN THE HEAT CAPACITIES OF ^{3}He FLUID FILMS

Masashi Morishita[1] and Setsuo Misawa

Recently the heat-capacity of a two-dimensional Fermi fluid is theoretically shown by Misawa to vary as $C(T) = \gamma_0 T - \gamma_2 T^2$ as a function of temperature T at low temperature, where γ_0 and γ_2 are constants. To check this prediction our measured heat-capacities of three different systems are reexamined, i.e., the first-layer and second-layer ^{3}He fluid films adsorbed on a bare graphite surface and monolayer ^{3}He films floated on a ^{4}He thin film adsorbed on graphite. The measured heat-capacities are reproduced well by the predicted formula. The areal-density dependence of γ_2 on each system also coincides with Misawa's prediction if the second order perturbation treatment by Fujimoto is adopted as the self-energy calculation.

[1] Institute of Phisics, University of Tsukuba, Tsukuba, Ibaraki 305-8571, Japan

MIND AT HEART

Ippei Shimada

Rene Descartes and William Harvey are the founders of modern mechanical view of human body. From after their new ideas, the place where our mind is being becomes not the heart but the brain. Neuro scientists reveal much functions of brain physiologically and anatomically recently. But, it seems to be not so hopeful to understand our mind as complex brain functions. Old picture of mind that is closely related to our heart gives us alternative tools to attack the problem of mind.

Neuro scientists' approach for this problem is curiously split into two ways. One is microscopic. They put a probe on a single neuron of rat's brain. Another is macroscopic. They observe the behaviors of rats, which resolve maze. "When we observe the voltage signals form a gate of CPU(Central Processing Unit), can we guess whether the computer is doing a word processing job or solving Newton's equations of motion for the system of planets?"[i] When rats resolve maze, we cannot say which parts of rats' neuron do that job. Miserable rats bearing probes on their brain and forced to resolve maze, their mind and behavior could not be understood forever.

Heartbeats are almost periodic. But when we analyze its rhythm more precisely, there are some fluctuations. Akselrod[ii] was pointed out that the power spectrum of heart beat fluctuations shows some peaks, which means that heartbeats is controlled by autonomic nerve system. Another type fluctuations are being interested recently among researchers[iii]. This new type fluctuation has long time correlation and selfsimiller structure of its diffusive character. When one falls into a deep sleep this type correlation of heart rate fluctuation disappears. Our heart rate reflects the activity of our central nerve system.

---

[i] Y. Sawada: speaking at annual meeting of Japan Physical Society.

[ii] S. Akselrod et al: Power spectrum analysis of heart rate fluctuation: a quantitative prove of beat-to-beat cardiovascular control. Science 213,220(1981).

[iii] M. Kobayasi ,T. Musha :1/f Fluctuation of heartbeat period. IEEE Transactions on Biomedical Engineering BME-29,456(1982).

Y.Yamamoto,et al: Sleep stage affected fractal nature of heart rate variability in humans. FASEB Journal. 10(3),A335(1996).

1. Random Matrix Theories and Metal-Insulator Transition

Hiroshi Hasegawa and Yoshinori Sakamoto

This article was published in *Progress of Theoretical Physics* Supplement **139**,2000, pp112-127, a contributed paper of Proceedings of International Workshop, *Let's Face Chaos through Nonlinear Dynamics* held at Maribor Slovenia, June 27-July 11, 1999.

It was based on an invited lecture by the first author at the workshop, but also in part on Master Thesis of Y. Sakamoto at *College of Science and Technology, Nihon University* which reviewed the recent development of the subject of metal-insulator transition(or, Anderson transition) as a second-order phase transition, in particular, one of the special topics *the compressibility of quantum levels at the mobility-edge* denoted by χ_c. The Anserson transition has been studied actively by a Japanese solid-state group(Y. Ono, T. Kawarabayashi, K. Slevin, and T. Ohtsuki [1]-[3]), establishing the critical exponent ν. The two quantities ν and χ_c have been regarded as the most important concepts of *universality* in the Anderson transition.

Sakamoto reviewed the paper by Chalker et al[4,5] who invented a formula

$$\chi_c = \frac{d - D_2}{2d} \quad d : \text{system dimension; } D_2 : \text{fractal dimension in } \left\langle \int d\mathbf{r} |\psi_n(\mathbf{r})|^4 \right\rangle \propto L^{-D_2}. \tag{1}$$

This was derived from Dyson's Brownian motion theory of level dynamics in conjunction with the knowledge of the critical eigenfunction to be shrinked as in the above formula. Our view on this result is that it should be deduced by means of the standard random matrix theory(RMT)i.e. by using the intermediate RMT joint N-level distribution(See **2**). Accordingly, we have proposed another formula

$$\chi_c = \frac{1 - e^{-\pi\beta g_c}}{\pi\beta g_c} \quad \beta = 1, 2, 4 : \text{(symmetry parameter) } g_c : \text{critical conductance.} \tag{2}$$

The validity of this formula is now being examined from several view points, and it has become clear to be modified as follows.

1. Coductance so far has been defined without including the spin multiplicity 2, and it should be taken into account so as to replace g_c by $2g_c$.

2. Conductance fluctuation should be adequatly taken into account so that g_c should be replaced by the average $\langle g_c \rangle$. (Identity of (1) and (2) is still not clear.)

References

1. T. Kawarabayashi et al, Phys. Rev. Lett.**77**,3593(1996).

2. K. Slevin and T. Ohtsuki, Phys. Rev. Lett. **78**,4083(1997).

3. K. Slevin and T. Ohtsuki, Phys. Rev. B**63**, 045108(2001).

4. J.T.Chalker, I.V.Lerner and R. Smith, Phys. Rev. Lett. **77**,554 (1996).

5. J.T.Chalker, V.E.Kravtsov and I.V.Lerner, JETP Lett.**64**,386(1996).

2. Statistical Mechanics of Random Matrices

Hiroshi Hasegawa

This paper was presented at International Conference on *Disordered and Complex Systems* held at King's College, London, July, 2000, to be published in Proceedings edited by P. Sollich(2001).

We begin with an axiomatic argument about Riemannian geometry of matrix space, and establish the most general form of Gaussian distributions on the ensemble of $N \times N$ hermitians which satisfy *representation covariance* and *translational invariance*, concluding that the resulting distribution of N eigenvalues of a sample hermitian, $P(x_1, x_2, .., x_N)$, must be of the form $\prod_{j<k} c(x_j - x_k)$ in terms of a single function $c(r)$ of the difference of a pair of eigenvalues, $x - y \equiv r$. It provides us with a view of level-statistics of quantum systems as a statistical mechanics of 1-dimensional gas (as first postulated by Dyson in early days) whose distribution function on $\{x_j\}$ may be represented as

$$P(x_1, x_2, .., x_N) = C_N \exp\left(-\beta \sum_{j<k} \phi(x_j - x_k)\right) \qquad \beta = 1,\ 2 \text{ and } 4. \tag{1}$$

The pair potential ϕ is given, on a further consideration of *level dynamics* and of complexifying the underlying Gaussian distribution, in the most general form as

$$\phi(r) = \frac{1}{4}\log\left(1 + 2\frac{a^2}{r^2}\cos 2\theta + \frac{a^4}{r^4}\right) \qquad a > 0; \quad 0 \le \theta \le \pi/2. \tag{2}$$

The angle parameter θ distinguishes three different possibilities for the nature of inter-level interactions: (a) repulsive $0 \le \theta < \pi/4$ everywhere as regards r, (b) attractive for $\pi/4 < \theta < \pi/2$, and (c) the attractive-repulsive boundary, $\theta = \pi/4$.

The special case $\theta = 0$, the simplest one of Case(a), is known as *Gaussian matrix ensemble model* proposed first by Yukawa[6] and later by Pichard and Shapiro[7]. A detailed study of this special case including the 2-point correlation function therefrom has been given by the present author[8], leading to a conclusion that there exists no phase transition. This constitutes the very motivation of the further study by enlarging the parameter range to $\theta > 0$ as above: $\theta = \pi/2$ provides the singular distribution of $P(\{x_j\})$. Who has given a prediction of the singularity of the level statistics for disordered $3d$-metal? Literature shows that in solid-state physics *finite size scaling method* is being developed to elucidate the phase-transition nature of the Anderson transition[9], where the concept of *critical disorder* is the answer. (Discussion of this subject in the present context will be presented elsewhere.)

References

6 T. Yukawa, Phys. Rev.Lett.**54**,1883(1985); Phys. Lett.A**245**,183(1998).

7 J.-L. Pichard and B. Shapiro,J.Phys.I(France)4,623(1994).

8 H. Hasegawa and J.-Z. Ma, J. Math. Phys.**39**,2564(1998).

9 See [1,2,3] and references therein.

Hard X-ray Study of SN 1987A in the Large Magellanic Cloud

Shiomi KUMAGAI

SN 1987A, the most recent supernova which can be seen by our naked eyes occured in the Large Magellanic Cloud on February 23th, 1987. This remarkable event told us the mechanisms and propagation of explosion, nucleosynthesis in the dying star.

One of the current interest of SN 1987A is the origin of its emission from the infrared to the X-ray band. At first, since its bolometric luminosity decreased by the decay time scale of a radioactive isotope ^{56}Co, which is a dHaughter nuclei of ^{56}Ni synthesized by rapid nucleosynthesis process, its origin was clearly attributed it to the decay seqence of $^{56}\mathrm{Ni} \longrightarrow {}^{56}\mathrm{Co} \longrightarrow {}^{56}\mathrm{Fe}$. Line γ-rays from ^{56}Co decays were also detected by the X-ray observation satellite such as Ginga and MIR, and the above theory was confirmed.

Nowadays, SN 1987A is observed by the Hubble Space Telescope and the bolometric luminosity is obtained. Synthesized ^{56}Ni and ^{56}Co at the explosion in SN 1987A have almost decayed and the resulted luminosity is much higher than that expected from ^{56}Ni decay. There are two possibilities to explain the recent observation; one is the decay of ratioactive isotope ^{44}Tim which has a half life of 65 years, and the other possibility is a young pulsar losing its rotation energy through particle acceleration.

INTEGRAL is planned to launch in 2002 and has good resolution in hard X-ray and γ-ray band. It is expected to observe both nuclear lines from ^{44}Ti and pulsed emission from young pulsar in SN 1987A.

^{44}Ti decays to^{44}Ca though ^{44}Sc by electron capture or beta decay emitting 67, 78 and 1158 keV γ-ray lines. The 10^6 sec observation by INTEGRAL allows us to search for the line down to 1.6×10^{-5}, 1.7×10^{-5}, and 6.3×10^{-6} photons/sec/cm^2 for the respective lines of energies. This intensity corresponds to the ^{44}Ti mass of 2.1×10^{-4} $M_\odot$ at the supernova explosion. This value is close to the expected mass of ^{44}Ti $1 \sim 2 \times 10^{-4}$ $M_\odot$ suggested by the current nucleosynthesis theory.

Considering the ambiguity of both the nucleosynthesis scenario and the sensitivity of INTEGRAL, there is still enough room to detect the γ-ray lines from SN 1987A. Even if note detected, we are able to set the tightest constraint on the amount of ^{44}Ti and also on the nucleosynthesis scenario.

As for the case of a young pulsar, INTEGRAL has capability to search for pulsation down to $\sim$ a few $\times 10^{-11}$ erg/sec/cm^2 around 100 keV band if searching is operated between 1 to 100 msec without considering the freedom of period derivative. The pulsation of newly-born pulsar has never been detected in the radio and the X-ray band, since these kind of pulsars are usually surrounded by the dense gas of supernova remnants. Hard X-ray and γ-ray emissions are transported in the gas without collision, therefore the observation of hard X-ray band is the only method to determine the period of young pulsar. It is expected that INTEGRAL will make clear of the theory of newly-born pulsar.

Analytic Solutions for Aspherical Supernova Light Curves

Koichi Iwamoto

Analytic solutions for light curves of aspherical supernova(SN) explosions are constructed in the framework of diffusion approximation. What is new in the solutions is that they allow for an aspherical distribution of ^{56}Ni, the radioactive element that power the SN light curve. The solutions are applied to Type Ia supernovae, for which turbulent burning-front propagation is likely to produce non-spherical ^{56}Ni distribution as has been suggested by recent 2D and 3D hydrodynamical simulations. Comparisons are made between theoretical and observed light curves in order to estimate a possible range of the degree of asphericity, which is attributed to the nature of explosion processes. Implications for the origin of the correlations among the light-curve properties of SN Ia are discussed. In particular, emphasis is placed on the interpretation of what is called the Phillips relation, i.e., the anti-correlation between brightness and decline rate of SNe Ia light curves.

Reference: Iwamoto, K. Astrophysical Journal, 2001, submitted

The Peculiar Type Ic Supernova 1997ef: Another Hypernova

Koichi Iwamoto, Takayoshi Nakamura[1], Ken'ichi Nomoto[1,2], Paolo A. Mazzali[2,3], I. John Danziger[3], Peter Garnanich[4], Robert Kirshner[4], Saurabh Jha[4], David Balam[5], and John Thorstensen[6]

[1] Department of Astronomy, School of Science, University of Tokyo, Bunkyo-ku, Tokyo 113-0033, Japan

[2] Research Center for the Early Universe, School of Science, University of Tokyo, Bunkyo-ku, Tokyo 113-0033, Japan

[3] Osservatorio Astronomico di Trieste, via G.B. Tiepolo 11, I-34131 Trieste, Italy

[4] Harvard-Smithsonian Center for Astrophysics, 60 Garden Street, Cambridge, MA 02138, USA

[5] University of Victoria, Victoria, BC, Canada

[6] Dartmouth College, Department of Physics and Astronomy, Hanover, NH 03755, USA

SN 1997ef has been recognized as a peculiar supernova from its light curve and spectral properties. The object was classified as a Type Ic supernova (SN Ic) because its spectra are dominated by broad absorption lines of oxygen and iron, lacking any clear signs of hydrogen or helium line features. The light curve is very different from that of previously known SNe Ic, showing a very broad peak and a slow tail. The strikingly broad line features in the spectra of SN 1997ef, which were also seen in the hypernova SN 1998bw, suggest the interesting possibility that SN 1997ef may also be a hypernova.

The light curve and spectra of SN 1997ef were modeled first with a standard SN Ic model assuming an ordinary kinetic energy of explosion $E_{\rm K} = 10^{51}$ erg. The explosion of a CO star of mass $M_{\rm CO} \approx 6M_\odot$ gives a reasonably good fit to the light curve but clearly fails to reproduce the broad spectral features. Then, models with larger masses and energies were explored. Both the light curve and the spectra of SN 1997ef are much better reproduced by a C+O star model with $E_{\rm K} = 8 \times 10^{51}$ erg and $M_{\rm CO} = 10M_\odot$. Therefore, we conclude that SN 1997ef is very likely a hypernova on the basis of its kinetic energy of explosion. Finally, implications for the deviation from spherical symmetry are discussed in an effort to improve the light curve and spectral fits.

Reference: Iwamoto, K., Nakamura, T., Nomoto, K., Mazzali, P., Danziger, I., Garnavich, P., Kirshner, R., Jha, S., Balam, D., Thorstensen, Astrophysical Journal, 534, 660-669, 2000

3B) High and Low Energy Physics

Personnel: Jun Otokozawa*, Shin Ishida, S. Y. Tsai, Shigefumi Naka*, Shinichi Deguchi, Eizou Umezawa*, Kenji Yamada*, Morishige Yoneda**, Ryuichi Oda**, Akiyoshi Morikawa**, Kenichi Aouda**, Toshihiko Komada**, Keiichi Abe**, Hiroyuki Iwata**, Yousuke Kokubo**, Haruki Toyoda**, Shinichirou Matsumoto**, Yoshiro Takeuchi**, Hisae Maiwa**, Hiroshi Tonooka**, Tomoyuki Suzuki**, Katsumi Matsuda**, Aiko Kimisima**, Kei Sato**, Tokuya Sato**, Daiki Ito**, Kaoru Kitsukawa**, Shigeki Tamura**, Yasumasa Matsuura**, Susumu Kamefuchi†, Sho Tanaka†, Tetsuo Sawada†, Naofusa Honzawa†, Motoo Sekiguchi†, Mitsuaki Obu, Takehisa Fujita*, Tomoko Asaga**, Kaori Itou**, Takuya Kobayashi**, Fumiko Okiharu**, Gyouichi Ohya**, Mitsuru Handa**, Kouichi Yazaki†

Introduction

Main interest of the high energy physics group is an attempt to formulate a unified description of quarks and leptons on the basis of extended and/or composite particle picture, which is the continuation of our previous work. Weak interactions, the problems related to exotic hadrons, anomalies in gauge theories, effective theory of QCD, string theories, supersymmetries, fundamental problems in quantum mechanics and cosmology are also the subjects of keen interest.

Activities of the low energy physics group include two-dimensional field theories, the problem of atomic electric dipole moment, hadron-hadron interaction interaction including NN and $\pi\pi$ Scatterings and numerical evaluation of path integrals.

*concurrent member
**graduate student
†non-regular member

Mass Spectra and Wave Functions of Meson Systems and the Covariant Oscillator Quark Model as an Expansion Basis

Ryuichi Oda, Kenji Yamada* , Shin Ishida,
Motoo Sekiguchi† and Hiroaki Wada

We examine mass spectra and wave functions of the $n\bar{n}$, $c\bar{c}$ and $b\bar{b}$ meson systems within the framework of the covariant oscillator quark model with the boosted LS-coupling scheme. We solve nonperturbatively an eigenvalue problem for the squared-mass operator, which incorporates the four-dimensional color-Coulomb-type interaction, by taking a set of covariant oscillator wave functions as an expansion basis. We obtain mass spectra of these meson systems, which reproduce quite well their experimental behavior. The resultant manifestly covariant wave functions, which are applicable to analyses of various reaction phenomena, are given. Our results seem to suggest that the present model may be considered effectively as a covariant version of the nonrelativistic linear-plus-Coulomb potential quark model.

Semi-Leptonic B Meson Decays to Excited D Mesons in the Covariant Oscillator Quark Model

Masuho Oda† , Kazunori Nishimura,
Muneyuki Ishida‡ and Shin Ishida

The spectra and branching ratios of the weak semi-leptonic B meson decays to the first excited D mesons are predicted, taking into account the confined effects of quarks using the covariant oscillator quark model (COQM). In the COQM the same relation between general weak transition form factors as that in HQET is derived, and the concrete form of the Isgur-Wise function is given with no free parameters. Our results are somewhat different from those of other models. The present experimental data are not sufficient for comparison.

* Department of Industrial Technology,Junior College Funabashi Campus Nihon University, Funabashi 274-8501, Japan
† Faculty of Engineering, Kokushikan University, Tokyo 154-8515, Japan
‡ Department of Physics, Tokyo Institute of Technology Tokyo 152-8551, Japan

Effect of Light σ Meson Production in $p\bar{p} \to 3\pi^0$ at Rest

Muneyuki ISHIDA* , Toshihiko KOMADA, Shin ISHIDA,
Taku ISHIDA† , Kunio TAKAMATSU‡ and Tsuneaki TSURU†

The $\pi^0\pi^0$ mass spectra and angular distributions around the $K\bar{K}$-threshold and at 1.5 GeV in $p\bar{p}$ (at rest) $\to 3\pi^0$ in the Crystal Barrel experiment are reanalyzed by applying a new method, which is consistent with the unitarity of the S-matrix and is expressed directly in terms of resonance parameters. The effects of light σ-meson production are clearly seen to improve the fit with σ in comparison with the fit without σ.

Covariant Quark Representation of Composite Meson Systems and Chiral Symmetry

Shin Ishida, Muneyuki Ishida* and Tomohito Maeda

Assuming spin-independence of the confining force, we give a covariant quark representation of general composite meson systems with definite Lorentz transformation properties. With this representation we are able to deduce automatically the transformation rules of composite mesons for general symmetry operations from those of constituent (exciton) quarks. Applying this, we investigate in particular physical implications of chiral symmetry for meson systems, and point out the possibility of the existence of new meson multiplets.

* Department of Physics, Tokyo Institute of Technology Tokyo 152-8551, Japan
† KEK, Oho, Tsukuba, Ibaraki 305-0801, Japan
‡ Miyazaki U., Gakuen-Kibanadai, Miyazaki 889-2155, Japan

Weak Radiative Decay Width $B^{\pm} \to K^{*\pm}\gamma$ in COQM Including Long-Range Contributions

Rukmani Mohanta* , Anjan K.Giri* , Mohinder P.Khanna* ,
Muneyuki Ishida† and Shin Ishida

The width of the weak radiative decay $B^{\pm} \to K^{*\pm}\gamma$ is calculated using the covariant oscillator quark model to estimate the quark confined effects. We improve our previous calculation, which includes only a short distance contribution, by adding a long distance contribution, and obtain the branching ratio as 4.595×10^{-5}. The magnitude of the direct CP asymmetric decay width is also estimated.

S-matrix Bases and Relation between $\pi\pi$-Scattering and Production Amplitudes

Shin ISHIDA and Muneyuki ISHIDA†

It is stated that the requirement of unitarity and of analyticity should be made on the S-matrix elements with right bases, and the "universality argument" made with the bases, which do not regard quark physical picture, is not right. Accordingly the result of the conventional analyses of the $\pi\pi$ production amplitudes following to this argument, leading to non-existence of the light σ-meson, is proved to lose its theoretical bases.

* Department of Physics, Panjab University, Chandigarh-160014, India
† Department of Physics, Tokyo Institute of Technology Tokyo 152-8551, Japan

Production of $3\pi^0$ and $\eta 2\pi^0$ from $\pi^- p$ Collision in GAMS Experiment

Masaaki KOBAYASHI* , T. TSURU* , K. TAKAMATSU* , S. ISHIDA, T. KOMADA, A. WAKABAYASHI and M. ISHIDA†

The data on the $\pi^- p \to M^0 n$, with $M^0 = \pi^0\pi^0\pi^0$ or $\pi^0\pi^0\eta$ obtained in the GAMS experiment may be useful to study the $\sigma(400 \sim 700)$ and $a_1^\chi(\sim 1000)$, which can be taken as chiral partners of π and ρ, respectively. A preliminary analysis for $3\pi^0$ invariant mass spectra gives a support for the assumed a_1^χ with a mass of $\sim 930 MeV$ and $\Gamma \sim 170 MeV$.

Light σ-Meson Production in Excited Υ Decay Processes I — Analyses —

Toshihiko KOMADA, Shin ISHIDA and Muneyuki ISHIDA†

We analyze the $\pi\pi$ production amplitudes in the excited Υ decay processes, $\Upsilon(2S) \to \Upsilon(1S)\pi^+\pi^-$, $\Upsilon(3S) \to \Upsilon(1S)\pi^+\pi^-$ and $\Upsilon(3S) \to \Upsilon(2S)\pi^+\pi^-$, and the $\pi\pi$ and $K\bar{K}$ production amplitudes in the charmonium decay processes, $\psi(2S) \to J/\psi\pi^+\pi^-$ and $J/\psi \to \phi\pi^+\pi^-$, ϕK^+K^-. The amplitudes are parametrized by the sum of Breit-Wigner amplitudes for the σ and the other relevant particles and of the direct 2π-production amplitude, following the VMW method. All the $\pi\pi$ (and $K\bar{K}$) invariant mass spectra are reproduced well with the σ Breit-Wigner amplitude by using the common parameters, $m_\sigma = 526^{+48}_{-37}$MeV and $\Gamma_\sigma = 301^{+145}_{-100}$MeV, which is almost consistent with the values obtained in our previous phase shift analyses. This strongly suggests the existence of light σ-meson.

* KEK, High Energy Accelerator Research Organization, Tsukuba, 305-0801, Japan
† Department of Physics, Tokyo Institute of Technology, Tokyo 152-8551, Japan

Light σ-Meson Production in Excited Υ Decay Processes II — Theoretical Investigation —

Muneyuki ISHIDA* , Shin ISHIDA and Toshihiko KOMADA

The results of analyses obtained in Part I are examined from the viewpoint of chiral symmetry. The mass spectra of $\pi\pi$ system are widely believed to be suppressed generally near the threshold, because of the derivative coupling property of Nambu-Goldstone π meson. However, this suppression does not hold in the processes with large energy release, and the steep increase from the $\pi\pi$ threshold observed in the transition $\Upsilon(3S \to 1S)$ is shown to be consistent with general constraints from chiral symmetry.

Covariant Level-Classification Scheme and Chiral Symmetry

Shin ISHIDA, Muneyuki ISHIDA* and Tomohito MAEDA

Starting from the bi-local Klein-Gordon Equation with spin-independent squared-mass operator, we give a covariant quark representation of general composite meson systems with definite Lorentz transformation properties. For benefit of this representation we are able to deduce automatically the transformation rules of composite mesons for general symmetry operations from those of constituent (exciton) quarks. Applying this we investigate especially physical implication of chiral symmetry for the meson systems, and present a covariant level-classification scheme, leading to a possible existence of new meson multiplets of "chiralons."

* Department of Physics, Tokyo Institute of Technology, Tokyo 152-8551, Japan

How to Understand the Lightest Scalars

Nils A. Törnqvist*

Based on previous papers I discuss how I understand the lightest scalars using a general coupled channel model. This model includes all light two-pseudoscalar thresholds, constraints from Adler zeroes, flavour symmetric couplings, unitarity and physically acceptable analyticity. One finds that with a large coupling there can appear two physical resonance poles on the second sheet although only one bare quark-antiquark state is put in. The $f_0(\approx 980)$ and $f_0(\approx 1370)$ resonance poles are thus in this model two manifestations of the same strange-antistrange quark state. On the other hand, the isoscalar state containing u and d quarks becomes (when unitarized and strongly distorted by hadronic mass shifts) a very broad resonance, with its pole at 470-i250 MeV. This is the sigma meson required by models for spontaneous breaking of chiral symmetry.

Summary Talk of the Conference on the Sigma Resonance

Nils A. Törnqvist*

This report summarizes the most important results presented at the recent conference held at the Yukawa Institute of Theoretical Physics in Kyoto, devoted to the recently confirmed light σ resonance. Remarkably, all speakers at this meeting took the light σ for granted and many mass and width estimations near 500 MeV were presented. We emphasize that if the light and broad σ is accepted as a true resonance it explains many basic problems of low energy hadronic physics in a simple way, especially if the linear sigma model (LσM) is used as an approximate effective low energy theory.

* Physics Department, POB 9, FIN–00014, University of Helsinki, Finland: Visiting Researcher of AERI

On the Role of Sigma-Particle and Other Resonances in Low-Energy Mesonic Processes

Evgeny Shabalin*

Using the principle of the most conformity of the QCD and real world objects we argue that σ-meson and other $\bar{q}q$ scalar mesons are the natural elements of the Chiral Theory. An existance of the light isoscalar σ-meson allows to understand many interesting features of K- decays. In $\pi\pi$ scattering, σ exchange gives the main contribution into phase shifts at energy near threshold and together with intermediate spin 1 and spin 2 resonances allows to obtain a good description of the phase shifts $\delta_0^0(s), \delta_0^2(s), \delta_1^1(s), \delta_2^0(s)$ and $\delta_2^2(s)$ for $\sqrt{s} \leq 1$ GeV.

Quark Level Linear σ Model (LσM) via Loop Graphs

Michael D. Scadron†

First, the LσM is nonperturbatively solved via loop-order gap equations. Then the Nambu-Goldstone theorem (NGT) is expressed in LσM language. Next, the Lee null tadpole sum for this SU(2) LσM theory is shown to require $N_c = 3$. Then LσM s-wave chiral cancellations are studied in tree-and in loop-order. Also, vector meson dominance (VMD) is shown to follow from this LσM. Next, the scalar nonet is studied in the infinite momentum frame (IMF). Finally, the LσM is suggested as the infrared limit of nonperturbative QCD.

* Institute of Theoretical and Experimental Physics, Moscow, Russia: Visiting Researcher of AERI
† Physics Department, University of Arizona, Tucson, AZ, 85721 USA: Visiting Researcher of AERI

On the Consistency Check of the Resonances of the π-π System

Tetsuo Sawada*

In order to examine the existence of the strong Van der Waals interaction acting between hadrons in addition to the ordinary forces arising from the exchanges of the mesons, the phase shift data of the pion-pion scattering are analysed. Large deviation of the P-wave amplitude from the predictions of Roy's equations indicates the extra long range force between pions. The parameters of such a long range force are determined from the P-wave data. It is also shown that the consistency of the curvatures of the S-wave amplitude of I=0 state in Roy's equations is recovered if we add the extra long range force with the strength fixed by the analysis of the P-wave.

* Associate Member

CP, T AND/OR CPT VIOLATIONS IN THE K^0-$\overline{K^0}$ SYSTEM – IMPLICATIONS OF THE KTeV, NA48 AND CPLEAR RESULTS –

Yutaka Kouchi, Yoshihiro Takeuchi and S. Y. Tsai

The possible violation of the CP, T and/or CPT symmetries in the K^0-$\overline{K^0}$ system is studied from a phenomenological point of view. With this aim, we first introduce parameters which represent the violation of these symmetries in the mixing parameters and decay amplitudes in a convenient and well-defined way and, treating these parameters as small, derive formulas which relate them to the experimentally measured quantities. We then perform numerical analyses, with the aid of the Bell-Steinberger relation, to derive constraints to these symmetry-violating parameters, firstly paying particular attention to the results reported by the KTeV Collaboration and the NA48 Collaboration, and then with the results reported by the CPLEAR Collaboration as well taken into account. A case study, in which either CPT symmetry or T symmetry is assumed, is also carried out. It is demonstrated that the CP and T symmetries are violated definitively at the level of 10^{-4} in 2π decays and presumably at the level of 10^{-3} in the $K^0 - \overline{K^0}$ mixing, and that the Bell-Steinberger relation helps us to establish that CP and T violations are definitively present in $K^0 - \overline{K^0}$ mixing and to test CPT symmetry to a level of $10^{-4} \sim 10^{-5}$.

HOW DO NEUTRINOS PROPAGATE? – WAVE-PACKET TREATMENT OF NEUTRINO OSCILLATION –

Yoshihiro Takeuchi, Yuichi Tazaki, S. Y. Tsai and Takashi Yamazaki

The wave-packet treatment of neutrino oscillation developed previously is extended to the case in which momentum distribution functions are taken to have a Gaussian form with both central values and dispersions depending on the mass eigenstates of the neutrinos. It is shown that the velocities of the neutrino wave packets do not in general agree with what one would expect classically but that relativistic neutrinos emitted from pions nevertheless do follow, to a good approximation, the classical trajectory. It is further pointed out that the conventional equal-energy (equal-momentum) prescription for neutrino oscillation seems appropriate to approximately describe oscillation experiments that involve something corresponding to time- (space-) integration or averaging.

Five Dimensional Spacetime with q-defomed Extra Space on Non-Commutative Geometry

Haruki TOYODA and Shigefumi NAKA

An attempt to get non-trivial hierarchy out of the Randall-Sundrum type of five dimensional spacetime with q-deformed extra dimension is discussed. In this model, we do not require any boundary condition for the fifth dimension, but the space time is assumed to be elastic in the fifth direction. The q-deformation is introduced so that spacetime coordinates become non-commutative between four dimensional coordinates and the fifth coordinate. As a result of this q-deformation, particles embeded in this spacetime acuire non-trivial mass heierachy; and one can show that some parameters introduced in the q-deformation naturally plays the role of ultraviolet cutoff parameters.

Geometric Symmetry Breaking in Supersymmetric Gluodynamics

Hiroyuki Iwata and Shigefumi NAKA

In the high energy physics, it is a very interesting problem to find the mechanism of supersymmetry breaking, since any super-partners of ordinary particles are not be found in the energy up to 1 Tev inspite of its theoretical importance. Recently, G. Dvali and M. Shifman (DS) propose a new mechanism for a supersymmetry breaking, which is caused by topological solutions involved in supersymmetric theories. In this work, we study the symmetry breaking of $N = 1$ supersymmetric gluodynamics according to DS's point of view. First, it is shown that the field equations allow topological solutions like 't Hooft-Polyakov monopoles, which yields non-conserve supercharge operators (NCSO). Secondly, we derive an effective field theory that produces the broken supersymmetry corresponding to the NCSCO. The field theory is realized as an infinite particle limit of the system of such 't Hooft-Polyakov-like monopoles.

Effective Abelian Gauge Theory of Massive Yang-Mills Theory

Shinichi Deguchi and Yousuke Kokubo

One of the most important subjects in particle physics is to understand the mechanism of quarks and gluons confinement on the basis of quantum chromodynamics (QCD). It has been argued that the (color-)magnetic monopole condensation leads to confinement phenomena of color charges through the dual Meissner effect, the dual version of Meissner effect in the superconductivity [1]; if the QCD vacuum is realized as a dual-superconductor described by the dual form of the Ginzburg-Landau (GL) theory, then color confinement of quarks and gluons is explained at least qualitatively by the dual-superconductor picture. To confirm this picture within the framework of QCD, it is necessary to find, at the first stage, magnetic monopoles in QCD and to clear the connection between QCD and the dual GL theory.

In 1981, 't Hooft showed that a partial gauge fixing for the non-Abelian part, which is called the *maximal Abelian* (MA) *gauge fixing*, in QCD yields topological degrees of freedom corresponding to color-magnetic monopoles [2]. In this gauge, off-diagonal gluons behave as charged matter fields with respect to the Abelian subgroup rotation, while diagonal gluons still behave as neutral gauge fields just like the electromagnetic fields. To derive the dual GL theory from QCD, it is also necessary to accept the *Abelian dominance* at a long-distance scale. The idea of Abelian dominance was first proposed by Ezawa and Iwazaki in 1982 as a hypothesis that, at a long-distance scale, only diagonal gluons dominate, while effects of off-diagonal gluons reduce in comparison with those of the diagonal gluons [3]. As a consequence, the off-diagonal gluons may either be neglected or be included into the theory as quantum effects [4] in accordance with the Wilsonian renormalization group. By virtue of the MA gauge fixing and the Abelian dominance, QCD reduces to an effective Abelian gauge theory (EAGT) containing monopoles. The dual GL theory is actually obtained by introducing monopole scalar fields and their suitable interaction terms into the EAGT so as to describe monopole condensation.

As was argued in Ref.[3], Abelian dominance may be achieved if off-diagonal gluons possess effective non-zero mass and so do not propagate at a long-distance scale. When the idea of Abelian dominance was introduced in QCD, it was only a hypothesis [3]; but recent Monte Carlo simulation performed by Amemiya and Suganuma shows that, in the MA gauge, off-diagonal gluons indeed behave as massive vector fields with the effective mass $m \simeq 1.2$ GeV in the region of $r \gtrsim 0,2$ fm [5]. This result strongly supports the Abelian dominance in this long-distance scale.

Once Abelian dominance is accepted, it seems natural to explicitly incorporate mass terms of off-diagonal gluon fields into the Yang-Mills (YM) Lagrangian in QCD at a long-distance scale. Accordingly, in the present research, we employ the non-Abelian Stückelberg formalism or the gauged non-linear sigma model with the YM Lagrangian to deal with massive gluon fields in a gauge-invariant manner. Consider now the SU(2) gauge symmetry

for simplicity. Then, with the YM fields ${A_\mu}^B$ ($B = 1, 2, 3$) and the Nambu-Goldstone scalar fields ϕ^i ($i = 1, 2$), the Lagrangian is given by

$$\mathcal{L}_{\rm MYM} = -\frac{1}{4g_c^2}{F_{\mu\nu}}^B F^{\mu\nu B} + \frac{m_0^2}{2g_c^2}\, g_{ij}(\phi) D_\mu \phi^i D^\mu \phi^j \,, \tag{1}$$

where ${F_{\mu\nu}}^B$ is the field strength of ${A_\mu}^B$, g_c is a (bare) coupling constant, m_0 a constant with dimensions of mass, and $g_{ij}(\phi)$ the metric tensor of the coset space $SU(2)/U(1)$. The D_μ denotes the covariant derivative for the non-linear gauge transformation of ϕ^i. The system defined by (1) includes the 't Hooft-Polyakov magnetic monopole (in the London limit). Hence, unlike the previous works, it is not necessary for this system to introduce magnetic monopoles by imposing the MA gauge "fixing". Denote now the YM fields in the unitary gauge by ${\tilde{A}_\mu}^B$. As is well known, taking the unitary gauge makes mass spectrum of the YM fields manifest. It is found that the off-diagonal gluon fields ${\tilde{A}_\mu}^b$ ($b = 1, 2$) behave as massive charged matter fields, while the diagonal gluon field ${\tilde{A}_\mu}^3$ behaves as a massless U(1) gauge field. From this, we see that the so-called MA gauge can be interpreted as the unitary gauge. In addition, the equation $(\delta^{ab}\partial^\mu + \epsilon^{ab3}\tilde{A}^{\mu 3}){\tilde{A}_\mu}^b = 0$, which has been put by hand in Ref.[4] as the MA gauge fixing condition, is now derived from (1) as the Euler-Lagrange equation for ϕ^i.

Consider now the generating functional based on (1), introducing the Faddeev-Popov (FP) ghost fields. Taking into account Abelian dominance at a long-distance scale, we carry out the integrations over ϕ^i, ${\tilde{A}_\mu}^b$ and the FP ghost fields after introducing an antisymmetric tensor field $\mathcal{B}_{\mu\nu}$ into the generating functional. Evaluating it at the one-loop level, we arrive at the following effective Lagrangian defining an AEGT:

$$\mathcal{L}_{\rm EAGT} = -\frac{1}{4g_c(\mu)^2}\mathcal{F}_{\mu\nu}\mathcal{F}^{\mu\nu} + z_1\epsilon^{\mu\nu\rho\sigma}\mathcal{B}_{\mu\nu}\mathcal{F}_{\rho\sigma} + z_2\mathcal{B}_{\mu\nu}\mathcal{B}^{\mu\nu} + \cdots \tag{2}$$

with $\mathcal{F}_{\mu\nu} \equiv \partial_\mu {\tilde{A}_\nu}^3 - \partial_\nu {\tilde{A}_\mu}^3 - \mathcal{S}_{\mu\nu}(\phi)$. Here z_1 and z_2 are certain constants and $g_c(\mu)$ is the renormalized coupling constant, which runs in a similar way to that of QCD. Thus the EAGT enjoys the property of asymptotic freedom, although this effective theory has Abelian structure. It should also be noted that degree of freedom of the magnetic monopole occurs in $f_{\mu\nu}$ in the form of the Dirac string tensor $\mathcal{S}_{\mu\nu}(\phi)$.

To derive the dual GL theory from the EAGT, we need to perform the dual transformation for ${\tilde{A}_\mu}^3$. In addition, it would be necessary to evaluate kinetic terms of the auxiliary fields that exist in the finite parts of the effective Lagrangian. These remaining works are now in progress and the results will be reported elsewhere.

References

1. Y. Nambu, Phys. Rev. D **10**, 4262 (1974).
2. G. 't Hooft, Nucl. Phys. **B190**[FS3], 455 (1981).
3. Z. F. Ezawa and A. Iwazaki, Phys. Rev. D **25**, 2681 (1982).
4. H. Reinhardt, "Confinement 95", proc., p.151 ; K.-I. Kondo, Phys. Rev. D **57**, 7467 (1998).
5. K. Amemiya and H. Suganuma, Phys. Rev. D **60**, 114509 (1999).

EDM Operator free from Schiff's Theorem

T. Asaga, T. Fujita and M. Hiramoto

We present generalized Schiff's transformation on electric dipole moments (EDM) in quantum field theory. By the unitary transformation, the time and parity violating interaction $ige\bar{\psi}\sigma_{\mu\nu}\gamma_5\psi F^{\mu\nu}$ is transformed into a new form, but its nonrelativistic reduction has a unique form, which is free from Schiff's theorem. The relativistic corrections to the new EDM operator turn out to be a small increase to the EDM as given by $b_2(\alpha Z)^2$ with $b_2 \simeq 2$. Therefore, the calculation of the EDM with nonrelativistic Hartree-Fock wave functions presents the most conservative but reliable estimation for the enhancement factor of the EDM in atoms.

Scaling of Bubble Motion in Sonoluminescence

F. Okiharu, T. Fujita and K. Yazaki

We study the scaling behavior of the bubble motion in the single bubble sonoluminescence. It is found that the bubble motion can be completely controlled by one scaling parameter. The bubble radius is obtained as the function of time with a simple analytic expression. This enables us to easily evaluate the energy of the gas deposited from the bubble boundary.

Bound states in Heisenberg xyz model

T.Kobayashi, M. Ishizuka and T . Fujita

We calculate the bound state spectrum in the Heisenberg xyz model. The diagonalization of the Heisenberg hamiltonian is done with the help of the sparse matrix method. The result is compared with the calculation with the Bethe ansatz method.

Analysis of Nucleon-Nucleon Interaction by Nonrelativistic Quark Two-Phase Model

M. Handa and M. Obu

Nucleon-nucleon interaction is analyzed by means of the nonrelativistic quark two-phase model formulated previously. The original aim was to provide with a model without the unphysical color van der Waals force between nucleons, which was achieved by introducing the link operator. Naive use of the link operator however does not allow natural cooperation with the one gluon exchange (OGE) interaction historically believed to be crucial for reproducing short-range repulsion in the nucleon-nucleon interaction. The two-phase model was proposed to remedy this situation in which the configuration space is smoothly divided into strong- and weak-coupling regions. The quarks are then bound to the link operator in the former region while they are free from the link in the latter region. The confinement force is shown to act only on linked quarks within a nucleon while the OGE interaction is found to be possible only between free quarks. Linked quarks are eventually distinguishable due to the link, so that in order for the Pauli principle between quarks to be effective all the quarks constituting the interacting nucleons must be unlinked, which is found to bring about very small exchange part of RGM kernels. This result enforces us to abandon the widely accepted understanding that the OGE interaction is a main source of the short-range repulsion in the nucleon-nucleon interaction. What is then a correct source of the short-range interaction? To get a clue for answering this question we make some numerical analysis of nucleon-nucleon scattering and find that the "delta part" in the inter-quark one pion exchange interaction yields a short-range repulsive interaction of sufficient strength. The figure below shows a fit to the experimental phase shift in $^1S_0$ channel.

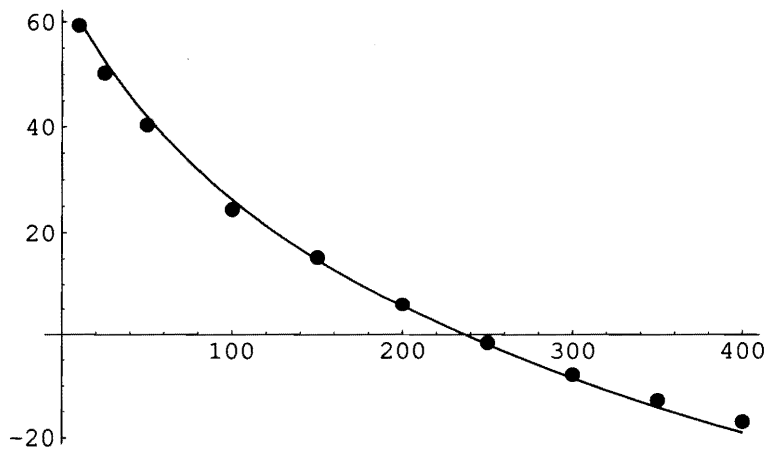

Hamiltonian-Model Analysis of $\pi\pi$ Scattering and Production

M. Obu

A simple hamiltonian model for $\pi\pi$ scattering and production is presented which incorporates both resonant and background interactions. The model assumes existence of bare resonance states, which are supposed to become physical resonances through coupling with scattering channels. We made some numerical analysis of isoscalar S wave $\pi\pi$ scattering below $\sim$ 1.2 GeV. The results shows that one-channel one-bare resonance treatment allows satisfactory fit in the energy region below 1 GeV where the σ resonance is considered to play a crucial role. Careful analysis of this energy range indicates that the background interaction plays only a minor role so that cancellation argument between the resonant and background phase shifts does not seem to work effectively. Actually, the σ resonance seems to appear as a result of interplay between two poles, one from the bare resonance and the other as a product of $\pi\pi$ dynamics. Figure 1 shows the trajectories of these S matrix poles in a complex energy plane as functions of the coupling constant. In reproducing the experimental phase shifts the dynamical pole is found to be more important.

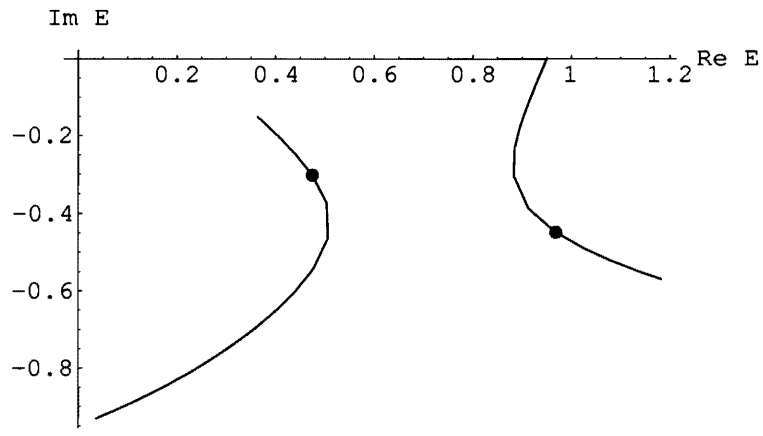

Figure 1: Pole trajectories as functions of coupling strength between the bare resonance and $\pi\pi$ continuum. The right-hand side trajectory represents resonance originated from the bare one, while the left-hand trajectory shows the dynamical resonance.

To get good fit upto 1.2 GeV, at least two bare resonances should be taken into account as well as some repulsive background interaction to stablize the fitting procedure. Before we can extract conclusive picture, however, we must make more extensive analyses of the scattering phase shifts and the FSI in production processes under multi-channel multi-bare resonance situation.

3C) History of Science

Personnel: Sigeko Nisio*, Eisui Uematsu*, Toru Yamashita**, Hidekazu Ezawa**, Takao Sakagami**, Daijiro Yamane‡, Kazuaki Seto‡

Introduction

The "History of Science" group has for its purpose the pursuit of this field as a scholarship in itself. The activities of the group are directed mainly to the history of physics. The history of physics aims at elucidating the historical structure of the development of the scientific cognition of physical world. In this field of research we attach importance to investigation what was the historical moment which brought about each progress of our physical knowledge and what a significance in historical context-not in the logical scheme of present-day physics each event in the history of physics had. For the time being the investigation is directed to the physics of the nineteenth and twentieth centuries. The subjects specifically investigated in 2000 were: a history of a fusion research in Japan, the formation of a magnetic theory in the nineteenth century, on the Islamic concept of a theory of motion, the formation of Euler's mechnics, a history of statistical mechanics, a history of quantum thories.

*concurrent member
**graduate student
‡research fellow

ISHIWARA JUN'S QUANTUM THEORY,1911-1915

NISIO, Sigeko

Ishiwara's frst paper dealing with quantum theory, the first in Japan to do so, appeared in 1911. It was based on Einstein's light quantum theory, then supported only by a minority. Ishiwara studied in Europe from 1912 to 1914 and continued to support the light quantum theory despite his studies in the summer term of 1912 under Sommerfeld who opposed this theory. He also submitted a theory on photochemical reactions based on the theory. After returning from Europe, however, he proposed a generallzed quantum conditlon, abandoning the light quantum theory in 1915.

I discussed how Ishiwara understood the studies on quantum theory that had been developed in Europe between 1 91 1 and 1915, and why he changed his mind.

EULER'S PRINCIPLES OF MECHNICS

EZAWA, Hidekazu

We discussed the role of Euler's work in the development of analytical mechanics.

Euler introduced the concept of mass-point into mechanics in his Mechanica of 1736. In Mechanica he criticized Newton's geometrical mechanics and tried to formulate differential equations of mass-point motion. In his 1744 book Euler introduced a principle of least action and obtained the trajectory of the projectile under the influence of gravity. He also proved that from the principle the motion of a body, its velocity depending on only its position, was derived. He described the equations of motion by rectangular Cartesian coordinates in his paper of 1747. He distinguished clearly the concept of force from inertia, momentum, the living force, in a manuscript " Anleitung zur Naturlehre", written between 1745 and 1750. In his 1750 memoir " Decouverte d'un nouveau principe de Mechanique", Euler proposed the equations of motion as the most fundamental principle of all the laws of mechanics. This principle became to be called

Newtonian equations.

4. Accelerator Science

4) Accelerator Science

Personnel: Isamu Sato, Kazuo Sato, Youichi Matsubara, Ken Hayakawa, Toshinari Tanaka, Yasushi Hayakawa, Hiroyuki Nakazawa**, Zhou Shuliang**, Kazue Yokoyama**, Koichi Kanno**, Takeshi Sakai**, Hiroyasu Inokawa**, Ken-ichiro Ishiwata**, Yoshihiro Nakamura**

Introduction

Main subjects of the accelerator science group are the R&D of the advanced science and technology of the electron linac, study of the free electron laser(FEL) and other lignt sources includeing those application, and the low temperature refregerator system.

The lineac was tuned up. The beam with pulse width of 20 μs has been achieved to the current of 140 mA with energy of 90 MeV after the energy analysis by the bending magnets.

The duties of klystron have been improved by the supplementary vacuum pumps installed on the wave-guide near the rf output window. It has been cleared the duties of 12.5Hz with pulse width of 20 μs and peak power of 22 MW.

In order to compensate the phase drift of rf in the pulse duration, function generators have been used for the fast pase control at the high speed phase shifter. As the result of the feed-forward method, the beam pulse width of 20 μs had been achieved.

The cathode of DC gun was replaced with EIMAC Y646E, wich has smaller diameter than the old one EIMAC Y646B, and the wehnelt electrode was modified to avoid the over-focus of the electron beam. The emittance of the beam from the new gun were measured using magnetic lenses and a wire scanner placed at the injector section. The obtained normalized emittance of horizontal and vertical directions were respectively 15.8πm̃m-mrad and 13.2π mm-mrad on the condition of the beam current of 400 mA.

A new undulator for IR has been operated and FEL at the wavelength of 1.5 μm has been attempted. The spontaneous radiatioins have been measured using a photodiode detector or a CCD camera and the accumulation of the fundamental radiation in the optical cavity has been observed. The decay time of the signal is consistent with the mirror loss. It indicates that the cavity should satisfy the condition of lasing except

**graduate student

the cavity length.

A new X-ray generator using Parametric X-ray Radiation (PXR) was designed and the characteristics of the system has been studied. Especially, the profiles and the energy dispersion of X-ray beam have been numerically estimated. A new beam line and the X-ray generator, which consists of 2 silicon single crystals mounted on goniometers in a vacuum chamber, has been constructed. The remote control system of the goniometers using TCP/IP protocol has been developed and tested.

The intensity of γ-rays generated at the beam dump was estimated from the numerical calculation using Monte Carlo Code EGS4 and the actual radiation level has been measured by a survey meter. In addition, the measurement of the neutron level has been done.

For the future application of the cryogenic system to the electron accelerator, the pulse tube cryocooler has been studied. It is noted that the use of the thermal compressor instead of the mechanical compressor is feasible for the pulse tube cooler of the cooling temperature below 4 K.

Activities of the group this year are as follows:

i) Study of the free electron laser.
ii) Improvement of the 125 MeV linac.
iii) Study and development of the X-ray generator using the linac.
iv) Design and construction of the beam transport system.
v) Design and construction of the optical beam line.
vi) Development of the superconducting magnet cooling system.
vii) The study of the pulse tube refrigerator.

Present Status of the LEBRA at Nihon University

Isamu SATO, Ichiro KAWAKAMI, Kazuo SATO, Yohichi MATSUBARA,Ken HAYAKAWA, Toshinari TANAKA, Yasushi HAYAKAWA,Hiroyuki NAKAZAWA[1],Kazue YOKOYAMA[1], Koichi KANNO[1], Takeshi SAKAI[1],Kenichiro ISHIWATA[1],Hiroyasu INOKAWA[1],Yoshihiro NAKAMURA[1]

Atomic Energy Research Institute,Nihon University
Narashinodai 7-24-1, Funabashi-shi, Chiba-ken, Japan
[1]College of Science and Technology, Nihon University
Narashinodai 7-24-1, Funabashi-shi, Chiba-ken, Japan

1. Introduction

The FEL project in Atomic Energy Research Institute (AERI) started in 1994. It is requested to promote accelerator technologies and to progress advanced researches in physics, chemistries, biologics, engineering, medical sciences and medical treatments. The FEL device consists a 125 MeV linac, a beam transport with three 45 degree bending magnets and five quadrupole magnet and a opitical mirror system. The linac also consists of a 100kV dc gun, a prebuncher, a buncher and three 4m acceleration structures. The FEL device was completed in 1997. The first commissioning of linac was at January of 1998. After that there were observed spontaneous emission, its spectrum in the FEL system, and were successively measured an emittance, an energy spread and a shape of bunched beam.

High quality beam for the FEL have been programed such a new projrct as for advanced research by using various radiations. These are based an electron of high energy and radiation proves as SE, FEL in a range of ultraviolet, parametric X-ray.

2. Research and Improvement

2-1 Klystron

The klystron with specifications of a short pulse had been tried to work on the duration pulse of 20 ì S. The rf window of klystrons were broken down one after another. Its trouble have been greatly improved by the enhancement of exhaust power in the vacuum system with the waveguide. Consequentrly, the klystron has been realized the duties of 12.5 Hz with pulse width of 20 ì s and peak power of 22 MW.

2-2 A new undulator

The permanent magnets of undulator suffered severe radiation damage. A new undulator was designed for infrared and was settled such a parameter as 50 periods and 48 mm period length. The new permanent magnets were delivered and the new one was fabricated. A beam duct along the undulator was decided on a dimension with the length of 3 m and the inside diameter of 25 mm.

2-3 Klyston modulator

The charging voltage in klystron modulator had been fluctuated each pulse to pulse. Its trouble was caused by fluctuations of discharge in the modulator, and was improved by keep the reservoir of thyratron under control.

2-4 Suppression of rf phase shift

Pulse duration of electron beam passed through the two 45 degree bending magnets was limited by the rf phase shift of microwave power supplied to accelerator structures. It was caused that amplifiers of two klystrons have warmed up in short time of several ì s. Inconsequence, the phase of rf power had been shifted 10 degrees after an interval of 20 ì s.

The phase shift suppression of amplifier was tried by method of a feed forward, and it was suppressed within a degree.

2-5 An optical cavity

An optical cavity was designed to accumulate infrared of 1.5 ì m. The mirror was coated its surface with multi-layer of a dielectric. A reflection ratio of mirror has been 99.5 %.

2-6 A new gun

A new gun was designed electron beam as keep parallel orbits. The old gun was exchanged the new one to achieve success low emittance. The normalized emittance by using of wire scan monitor was estimated about 15ð mm-mrad for the current of 200 mA with energy of 100 kV.

2-7 Others

Improvement for accelerator was performed a bunch monitor, focusing of injector section and waveguides. It was to be easy a beam handling.

3. Operation

A transmission efficiency of the electron beam in FEL system has been kept about 100 %.

The linac was continually tuned up, the beam dump in the FEL device was achieved current of 120 mA of 80 MeV.

An optical mirror system in FEL has been tuned at a wavelength of 1500 nm. In July of 2000, we have been observed frequently a accumulated light in the optical cavity of FEL. Accordingly, SE correspond to the bunched shape of electron beam was observed by using the Steak camera. Its shape was normal, but its pulses arrayed into macro pulse was irregular as come out a tooth of a comb. On the one hand, a spectrum of SE was carefully measured again by using the CCD camera in Jun of 2000.

Recently, the beam with pulse width of 20ì s has increased gradually and has achieved at the end of accelerator beam current of 240 mA with energy of 87 MeV.

The total time of the klystron operating has been 4969 hours since it's the conditioning was begun.

The table 1 shows separately the klystron operation of the physical year.

year	klystron operation			days with beam acceleration
	hours	days	hours/day	
1996	71	8	8.88	0
1997	559	61	9.16	13
1998	1617	159	10.16	40
1999	1257	127	9.89	39
2000	1465	109	13.44	45

4. Specification of Radiation Source Complex

The present project in LEBRA are to progress application program on researches using such four radiation sources as of the electron beam, the free electron laser, the spontaneous emission and the parametric X ray. Fabrication of a new undulator finished early in March of 2000. We are under testing for lasing of an infrared ray. A prametric Xray are under developement. Specifications for the five radiation sources give as shown in Table 2 to Table 5.

Table 2 Electron linac

Bean energy	125 MeV
Beam Intensity	200 mA
Beam pulse duration	25 ì s
Peak currents	20 A
Beam bunch width	3.5 ~ 10 ps
Beam energy spread	< 0.5 %
Repetition rate	12.5 pps
Maximum beam power	6.25 kW
Frequency	2856 Mhz
Accelerator structure	4 m×3
Dc gun	- 100 kV
Klystron power	30 MW×2

Table 2 FEL from near infrared to ultraviolet

Undulator structure	Halbach
Total length of undulator	2,400 mm
Gap space of magnet pole	13 ~ 25 mm
Periodicity	24 mm
Periodic numbers	100
Ordinary k-value	0.65 ~ 1.1
Length of optical cavity	6,718 mm
Mirror	multi-coated
Photon wave length	0.3 ~ 1.5ì m
Average power	0.3 ~ 3 W

Table 3 FEL from infrared to near infrared

Undulator structure	Halbach
Total length of undulator	2,400 mm
Gap space of magnet pole	28 ~ 40 mm
Periodicity	48 mm
Periodic numbers	50
Ordinary k-value	0.65 ~ 1.1
Length of optical cavity	6,718 mm
Mirror	multi-coated or metal
Photon wave length	0.8 ~ 5ì m
Average power	1 ~ 5 W

Table 4 Spontaneous Emission by the Undulator

Wave length of radiation	0.043 ~ 5 ì s
Photon energy	0.24 ~ 29 eV
Energy spread	1 %
Average photon flux	2.5×10^{11} photon/s

Table 5 Parametric X-ray

Energy of X-ray	3 ~ 30 keV
Energy spread	1 %
Average flux	1.2×10^{9} photon /s
Directional angle	~ 4 mrad

5. Application Program

The radiation source in LEBRA bases on photon from infrared ray to Xrays. These are radiation generator as a parametric X-rays, and it is superior to monochromatic, coherent and directive property. The generators are requested to promote accelerator technologies and to progress advanced researches in physics, chemistries, biologics, engineering, medical sciences and medical treatments. The generators in addition to high energy electrons are expanded the base of a research from nuclear physics to material science including biology and biomedicine. In order to advance application studies, seven study gropes were organized in Nihon-university at March of 2000. Those research item were chosen a biological reaction, a medical treatment and care, a macro-molecular structure spectroscopy, a photochemical catalysis reaction, a lithography and diffraction, a solid surface structure analysis and R&D as produce new material elements. The future plan in LEBRA were promoted a double proposal as science researches based on a material and a biology. Each proposal them have applied for the grant in aid for science research on priority area (B) and the enterprise for progressing advance research on private universities in order to progress them. The main title in the future project was named the development of monochromatic and brilliant light sources with variable wavelength and its advanced application.

The subtitle of project are the following items.

1) Studies of X ray radiation phenomena using of 125MeV linac and a development of monochromatic X ray source with variable wavelength.

2) Development of FEL and its higher harmonics radiation source.

3) A development of a rf amplifier with a super conductive cavity and its practical use.

4) A phase transition in cluster structure excited by a laser.

5) A study of XANES on high pressure using of parametric X ray.

6) A production of a super diamond using of FEL.

7) A research of photo chemical posses of contamination molecular in the atmosphere using of spectroscopy due to zero kinetic energy pulse field ionization.

8) Studies on high speed photo chemical reactions using of two color pump proves in picosecond.

Design of the rf-gun

K.Hayakawa

Introduction

A combination of an rf-gun with a photo-cathode and a magnetic buncher is one of the best choice for obtaining low emittance and long pulse electron beam. A photo cathode is driven by the strong and pulsed laser. Ordinary, the magnetic buncher is an alpha magnet that compresses longitudinally an electron beam with distribution of maximum energy at the beam head and gradually going down to the tail in an rf period. Another possibility is realized by a chicane, that compress an electron beam with reverse distribution of the case of an alpha magnet. A chicane consists of three or four simple dipole magnets. The electron orbits go back to the same beam axis after passing through the chicane. We investigated the latter configuration for the injector of LEBRA.

Cavity design

An electron beam with energy distribution mentioned above is realized by two or more cavity rf-gun. Making the first cavity shorter than a quarter of rf wavelength, and excite electric field along the axis comparable with the cavity bellow the second. We adopted the two cavities rf-gun. A resonant frequency and a field distribution are calculated by the numerical simulation code SUPERFISH. Electron trajectories are computed with space charge effect. To obtain the optimized electron beam distribution both transverse and longitudinal direction, these two processes have been iterated. Typical energy distribution along the beam axis is

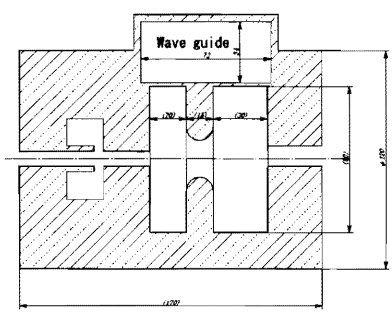

Fig.1 Conceptual diagram of an rf-gun.

shown in fig. 1. Electron energy is minimized at the beam head and gradually up to the tail. Conceptual diagram of an rf-gun is shown in fig. 1. Typical longitudinal energy distribution emitted from an rf-gun is shown in fig.2.

RF coupling

Field distribution and rf coupling between the cavities are depending on the operating mode. At the π-mode operation, the excite field distribution is the most efficient for acceleration. However, group velocity of rf is zero. Then, field distribution is very sensitive for the cavity detuning and the beam loading. For inserting a small coupling cavity, π/2-mode operation and field stabilization is performed. We adopted another solution. Attach the H-wall of the wave-guide to the rf-gun, and make coupling irises in each cavity. The transmission mode of TE_{01} excites antisymmetric magnetic field with respect to the center plane, then the π-mode like field distribution is excited.

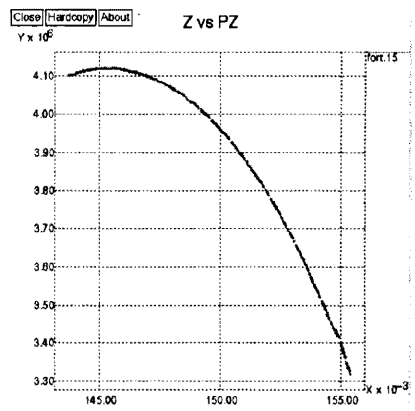

Fig.2 Longitudinal energy distribution of electrons.

Drive laser

A drive laser is an amplified third harmonics (355nm) of a Nd:YAG laser. The laser system consists of a diode pumped mode-locked oscillator .The oscillator produces an output with repetition rate 89.25 MHz and power greater than 80 mW. The mode-locked pulse train is sliced to 20μs by Pockels cell pulse slicer operating at 12.5Hz repetition rate. Following the pulse slicer the beam will make a total of eight passes through three amplifiers prior to frequency doubling in an LBO crystal. Specifications are shown as bellow.

Table 1. Specifications of the drive laser

Wavelength	355	nm
Micro pulse duration	50	ps
Micro pulse energy	40	μJ
Micro pulse repetition rate	89.25	MHz
Macro pulse duration	20	μs
Macro pulse energy	72	mJ
Macro pulse repetition rate	12.5	Hz

IMPROVEMENT OF FEEDBACK SYSTEM IN LOW POWER RF PHASE STABILIZER

T.Tanaka, K.Hayakawa, Y.Hayakawa, K.Yokoyama, H.Nakazawa, K.Sato, Y.Matsubara, I.Kawakami and I.Sato

1. Introduction

The energy of the electrons accelerated in the rf linac is quite sensitive to fluctuation of the rf phase when the accelerating tubes are fed separately with 2 or more klystrons. Fluctuation of the rf phase also leads fluctuation of the separation between successive beam bunches, which affects the build up process and oscillation of the free electron laser (FEL).

Fig.1 shows the observed drift of the phase between the output of the cw synthesizer and the output of 800W rf amplifier. The output power of the amplifier was about 600W. In order to test the possibility of fast phase control and improvement of the phase drift in the rf pulse duration, a phase stabilizer circuit based on a digital feedback system has been developed for the low power stage of the rf system.

Results of primary test and improvement of the feedback system are reported in the following sections.

2. Performance of the feedback system

As a result of primary test of the feedback system, the phase drift has been found suppressed within 0.5° except for initial 5~6μs of total 20μs rf pulse duration. Fig.2 shows a typical waveform of the phase when compensated with the feedback system. The difference of output phases between the cw synthesizer and the 800W rf amplifier was detected with a double-balanced mixer (DBM), then the amplifier output phase was corrected by means of a digital phase shifter in the feedback system so that the IF output voltage of the DBM was adjusted to zero.

The phase shift at each end of the rf pulse, given by the feedback system as a result of compensation for the phase drift, was kept until beginning of the next pulse. Thus the feedback in the next pulse was started always with a large phase displacement. The waveform in Fig.2 shows that the maximum phase shift rate of 0.9°/μs in the digital feedback system was not sufficiently fast to correct and lock the large phase difference in less than 1~2μs.

3. Improvement of the system

As seen in Fig.1 the phase drift is monotonic with drift rate of 0.5~1.5°/μs, which means that the phase shift rate of 0.9°/μs in the feedback system is not necessarily enough for complete compensation of the phase drift. However, the phase drift rate, which depends strongly on the output power of the rf amplifier, was less than 0.8°/μs when the amplifier was operated at the output less than 400W i.e. at nominal operating power. It implied that if the initial phase can be adjusted to an optimum value, the time required to lock the phase is reduced and no improvement is required to raise the phase shift rate.

The phase offset at the beginning of the rf pulse, required for optimization of initial phase, has been realized by placing a slow 12bits up/down counter as a feedforward circuit. The counter has been used to estimate the phase difference between the beginning and the end of the rf pulse when no feedback has been applied. Principle of operation of this circuit is very simple as follows.

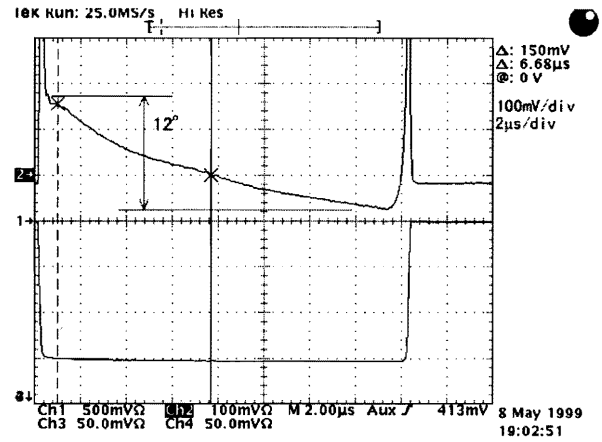

Fig.1. Observed phase drift between source and the output of the rf amplifier (upper). The lower signal shows the amplitude of the amplifier output.

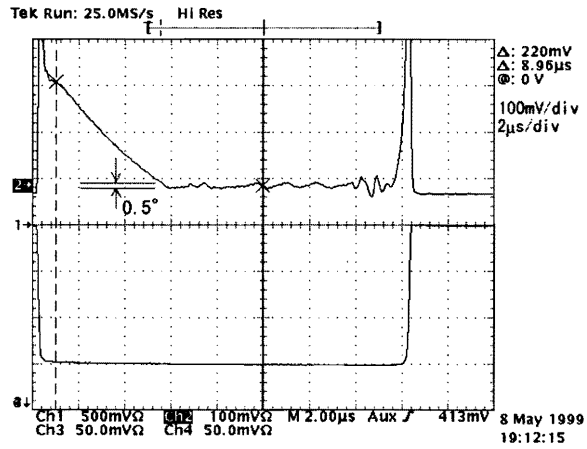

Fig. 2. Typical waveform of the phase drift between the synthesizer output and the rf amplifier output when the phase stabilizer circuit is inserted (upper). The lower signal is the waveform of the power observed simultaneously (not regulated).

The DBM IF output voltage representing the phase of the rf amplifier output is compared with 0V. If the IF voltage at the beginning of the rf pulse is greater than 0V the count is decreased by 1 digit, otherwise increased by 1 digit. The count is added to the feedback counter output after the end of the rf pulse, or before the beginning of the next rf pulse. Then the initial phase is shifted by 1 digit. Iteration of this process in successive rf pulses gives an optimum initial phase offset. By this iteration the phase offset is optimized at every rf pulse.

The effect of the feedforward circuit is show in Fig.3. The timing of phase comparison for feedforward has been adjusted to 1μs after the beginning of the rf pulse. In Fig.3 a clear effect is found that the time spent for phase locking, as seen in Fig.1, has been suppressed considerably and the phase stability of almost within 1° has been obtained for pulse duration of about 20μs.

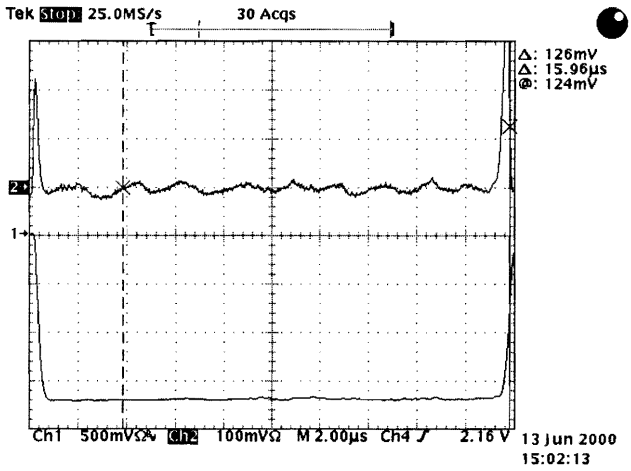

Fig. 3. Typical waveform of the phase difference between the synthesizer output and the rf amplifier output when the feedback circuit and also the feedforward offset circuit are applied (ch2 upper, 23mV/°). The lower signal is the waveform of the amplifier output power regulated simultaneously.

Other improvements on the stabilizer circuit are the reduction of counting error occurred both in the phase and the amplitude stabilizer feedback circuits, speedup of feedback cycle from 5MHz to 10MHz and change of phase shift step from 0.18°/digit to 0.09°/digit. The phase shift rate has been still the same.

The previous feedback circuit allowed both counting up and down in the same feedback cycle, which led to counting error and correspondingly led to jump of phase and amplitude very frequently. Therefore, in order to test only stabilization of phase drift and to avoid difficulty of analysis of feedback operation, the regulation of the amplitude was not applied in the preliminary test.

In the present circuit only one counting action, i.e. either counting up or down is allowed in one feedback cycle. Since this change no counting error has been found. On the other hand this change has slowed down the feedback response, which caused less stable rf phase than in the case of previous circuit.

4. Summary

The phase drift of the rf amplifier output compared with the source rf from the cw synthesizer has been suppressed by the phase stabilizer system within 1° for a long pulse duration of 20μs. But the stability achieved here is not necessarily enough for driving rf of klystrons when the accelerated electron beam is assumed to be used for FEL oscillation. Further improvement of the digital feedback circuit is desired to achieve phase stability within 0.2° and amplitude stability within 0.1% for sufficiently reliable use in the linac rf system.

DEVELOPMENT OF THE PARAMETRIC X-RAY GENERATOR AT LEBRA

Y. Hayakawa, I. Sato, K. Sato, K. Hayakawa, T. Tanaka, H. Nakazawa, K. Yokoyama, K. Kanno, T. Sakai, K. Ishiwata, H. Inokawa and Y. Nakamura

1 Introduction

At Laboratory for Electron Beam Research and Application (LEBRA), an X-ray generator using Parametric X-ray Radiation (PXR) has been developed. PXR is a kind of the coherent X-ray radiations from a crystal medium irradiated with relativistic charged particles. It is expected as a X-ray source using 100 MeV class linac because of its monochromaticity and directivity.

2 Performance of the PXR generator

The PXR generator consists of two goniometers in the vacuum chamber that is placed on the beam line. Figure 1 is a plan of the new beam line. To make the PXR source practicable, a new beam line from the linac and a chamber for PXR were designed and have been constructed. It should be a excellent pulse X-ray source which has monochromatic and variable wavelengths.

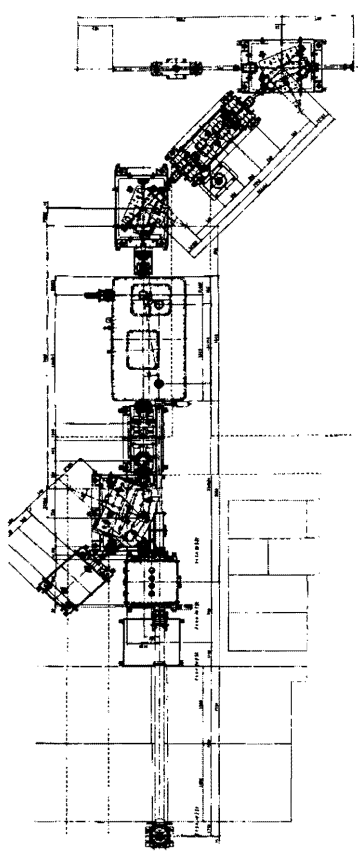

Figure 1: New beam line for PXR.

Table 1: Performance of the goniometers for PXR.

axis	driving range	resolution	motor type
1st			
X	+5 ~ -65 mm	4 μm	air
θ_x	±10°	52.4 μrad	vacuum
θ_y	±10°	35 μrad	vacuum
θ_z	0 ~ 35°	11.6 μrad	vacuum
2nd			
X	±5 mm	1 mm/rev	manual
Y	-10 ~ +1030 mm	5 μm	vacuum
θ_x	±10°	52.4 μrad	vacuum
θ_y	±10°	35 μrad	vacuum
θ_z	0 ~ 35°	11.6 μrad	vacuum

One of the goniometers has 4 axes and another has 5 axes. The first goniometer is used to control a target crystal that is irradiated with electron beams and generates PXR. The second one, which is a kind of the crystal monochrometer, has a role of a mirror for X-rays. The second crystal should reflect PXR toward a same direction in all range of wavelength. The performance of the goniometers is shown in Table 1 and Fig. 2 shows those photographs. The system is driven with sevral stepping motors which could be operated by remote control through the Local Area Network. As the targets wafers of silicon single crystal should be used because of its quality and cost.

3 Expected characteristics of PXR

The energy (wavelength) of PXR is selected by the crystal plane and its Bragg angle. Table 2 shows the energy range of X-rays that could be obtained with the PXR generator using a few kinds of Si crystal planes. Actually the energy range from 5 keV to 30 keV is practical with regard to the radiation yield.

Since PXR from the target crystal has the angular divergence and the wavelength gradation, the beam profiles of X-rays obtained by the system are sensitive to the arrangement of the 2nd crystal. The calculations of the PXR spatial distributions are shown in Fig 3, where a) is a raw distribution of PXR emitted from the target in the case of 5.4 keV, b) and c) are ones after reflection with the 2nd crys-

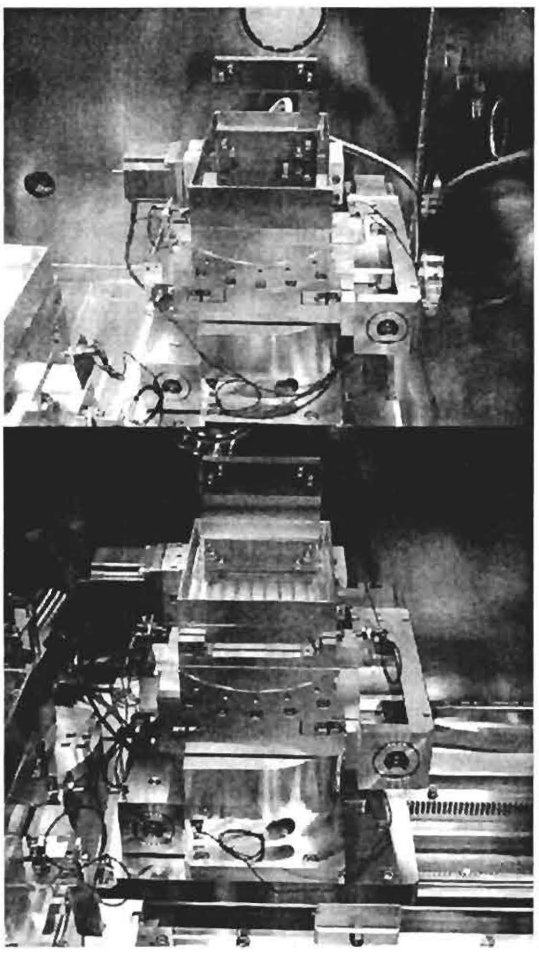

Figure 2: Upper is a photograph of the first goniometer and lower is one of the second goniometer. Those are mounted in the vacuum chamber.

tal. b) is the case that has the largest yield and c) is the case that has the smallest energy dispersion, respectively. The dependence on the 2nd crystal angle is significant to use this X-ray beams, particularly in the case of using concentrating mirrors. In addition, the 2nd crystal has a role as a filter for higher harmonics due to the width of Bragg reflection.

4 Final remarks

The new monochromatic X-ray source using PXR should be experimentally studied to estimate its practical performance. In particular it is important to investigate the characteristic of PXR such as the linearity of the yield to the electron beam current and the wavelength selection.

Table 2: Energy range of PXR generated by the system.

plane of the target crystal	X-ray energy (Bragg angle: 5 ~ 30°)
Si (111)	3.95 ~ 22.6 keV
Si (220)	6.46 ~37.0 keV
Si (333)	11.9 ~67.9 keV

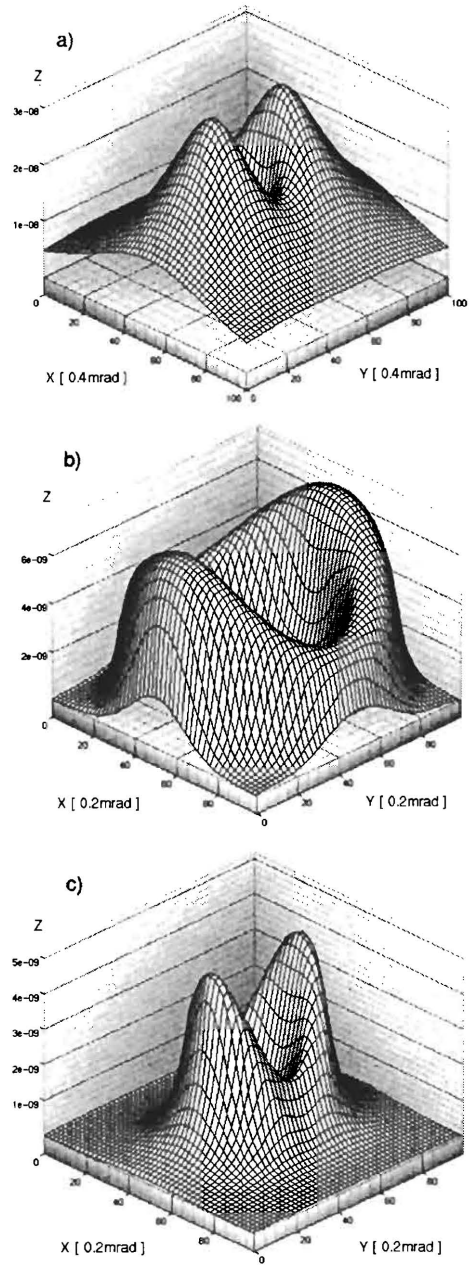

Figure 3: Typical PXR beam profiles in the case of 5.4 keV. a) Spatial distribution of PXR emitted from the target crystal. b),c) Distributions after reflection with the 2nd crystal for monochronization. The 2nd crystal angles of those are different.

References

[1] Y. Hayakawa et al., Proc. of the 12th Symposium on Accelerator Science and Technology, p. 391-393 (1999)

[2] Y. Hayakawa et al., Journal of the Physical Society of Japan Vol. 67, p. 1044-1049 (1998)

RF PHASE DRIFT COMPENSATION OF FEL LINAC

K.Yokoyama*, I.Sato, K.Hayakawa, T.Tanaka, K.Sato, Y.Matsubara, Y.Hayakawa, H.Nakazawa*, K.Kanno*, T,Sakai*, H.Inokawa, Y.Nakamura and K.Ishiwata

1 Introduction

The performance of the linac has been improved for the application to the FEL experiment in LEBRA (Laboratory for Electron Beam Research and Application). It has been observed that there is the fluctuation of the accelerated electron beam energy of the linac supplied to the FEL system. The rf power amplified by two klystrons is used for the acceleration of the electronic beam. The rf amplifier for klystron to drive consists of semiconductors, and then a phase fluctuation in the pulse duration isn't avoided. This phase fluctuation is different with each klystron. These lead to change the energy of the bunched beam in the pulse duration. Beam current changes significantly when such a beam is transported through the analyzer with momentum acceptance of about 1%. Uncompensated phase fluctuation of about 8° was observed over the rf pulse duration of 20μs. Less than 1° of phase stability has been achieved by introducing a phase compensation circuit that consist of a function generator and a fast ϕ/A controller. According to phase stabilization, constant beam current in the pulse duration can be supplied to an FEL system. The phase and the room temperature were observed. A correlation between them of 10°/ °C is appeared. An additional stabilization system for slow phase drift is required.

2 Linac RF Systems

2.1 The RF Drive System

The Linac of our facilities accelerates the electron beam emitted from the DC electron gun up to 125MeV with rf. Operating conditions of rf under now are frequency of 2856 MHz, pulse duration of 20μs and repetition rate of 2 Hz. Accelerating rf is supplied to accelerating tubes by two klystrons as shown in Fig 1. Rf amplifiers drive klystrons independently. The 2856MHz oscillator is locked in to 28.56MHz of the master oscillator, followed by the rf amplifier through the low-speed phase shifter. To regulate a phase and amplitude, a fast ϕ/A is inserted before the rf amplifier. The low-speed phase shifter adjusts the phase of the rf output from each klystron relatively. A fast ϕ/A input signal to the klystron is modulated to rf output a pulse by a fast ϕ/A. This rf signal is amplified up to 800W by the rf amplifier, and up to 20MW by klystron. It is supplied to the electronic acceleration.

2.2 RF Phase Compensation

A DBM (double balanced mixer) is used as phase detector. The application of two identical frequency, constant amplitude signals to mixer results in a dc output which is proportional to the phase difference between the two signals. The function for the phase drift compensation in the pulse duration is made from the wave shape which is the phase difference between the rf reference signal and the klystron output detected by the DBM [1]. This function generated by the function generator is applied to a fast ϕ/A, and phase modulation is occurred. At this time, the output amplitude of the function and transmission timing is adjusted so that a detection signal from DBM becomes flat. Outputs for a phase detector before and after applying the phase control signal, and the phase control signal are shown in the figure 2. The phase drift of about 8.5° is reduce to within 1° by this method.

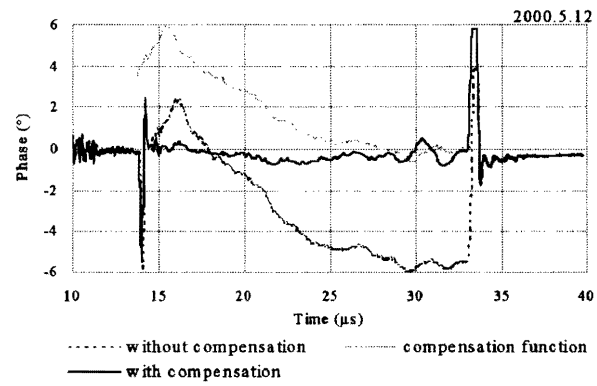

Fig. 2 Phase drifts of the rf klystron output relative to the rf reference signal.

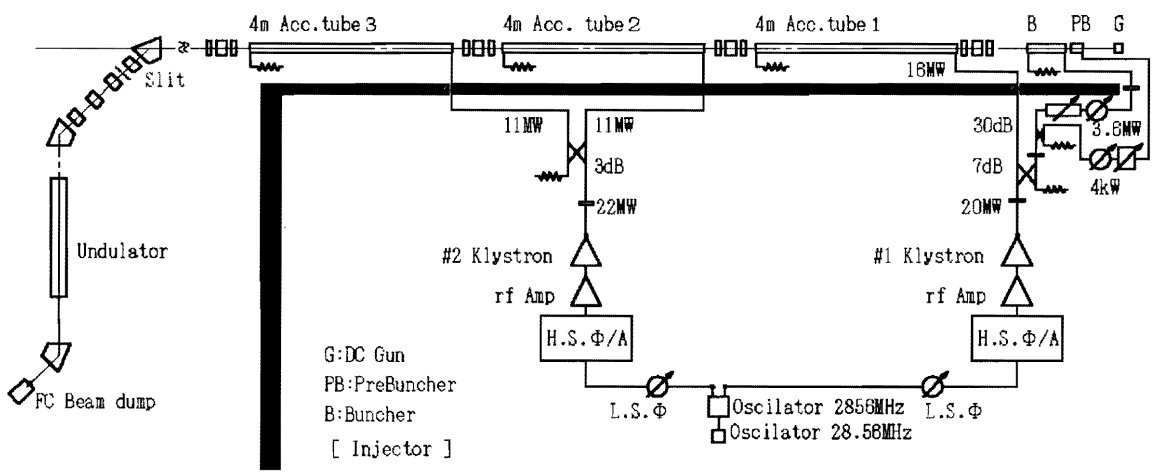

Fig. 1 RF drive system.

*College of Science and Technology, Nihon University

3 Results and Discussion

3.1 Results of RF Phase Drift Compensation with a Function Generator

The phase compensation has been performed by applying the phase control signal generated by a function generator to a fast ϕ/A controller. Figure 3 is shown the electron beam current transported through the momentum analyzer with and without compensation. These were detected by the Faraday cup which is a insulated beamdump placed at downstream of the undulator. At this time, the beam energy spread is 1% of full width, the mean energy is 98MeV and current is 88mA at the accelerator exit. A dotted line is the electron beam current without compensation. It is hard to adjust parameters at the injector of the linac as to keep the analyzed electron beam current constant over the rf pulse duration of 20μs. A solid line shows one with phase drift compensation. This result indicates that the energy fluctuation is improved.

3.2 RF Phase stability depend on a Temperature

The phase, the room temperature and the fluctuation of a line voltage with time are measured. The results are shown in figure 4. It is clear that the slow phase drift is depended on the temperature significantly. To compensate temperature dependence, there is a simple method of using a thermostatic bath that keeps the temperature of the amplifier constant, but it isn't reasonable in cost. Therefore, it has also been tried to compensate this change by the fast ϕ/A controller. A digital feedback circuit has been developed and introduced for compensation of the fluctuation with time. This result is shown in the figure 4-(b). This slow drift is improved in less than 0.5°. It will be investigated effects on the electron beam.

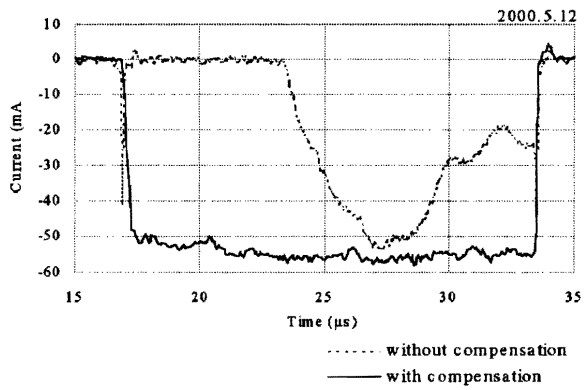

Fig. 3 Beam current through the FEL system.

4 Conclusion

The phase stability was achieved to within ±0.5° by the method of compensation with a function generator. Also the fluctuation of the electron beam energy was improved considerably over the rf pulse duration of 20μs. As the result of this compensation optical yield of spontaneous radiation that it could get from undulator was improved significantly [2]. However, it is not enough for application to FEL. Actually, stability in desired region is not achieved because the relative phase between two klystrons is often adjusted according to get a flat beam current over the rf pulse duration. Any drifts or changes in the phase of rf drive affect the phase stability of the rf accelerating fields. And it is a serious problem that these systems can't prevent from in electrically noisy environments.

References

[1] K.Yokoyama et al., Proc. of 25th Linear Accelerator Meeting in Japan, (2000) 108.

[2] Y.Hayakawa et al., Proc. of 25th Linear Accelerator Meeting in Japan, (2000) 358.

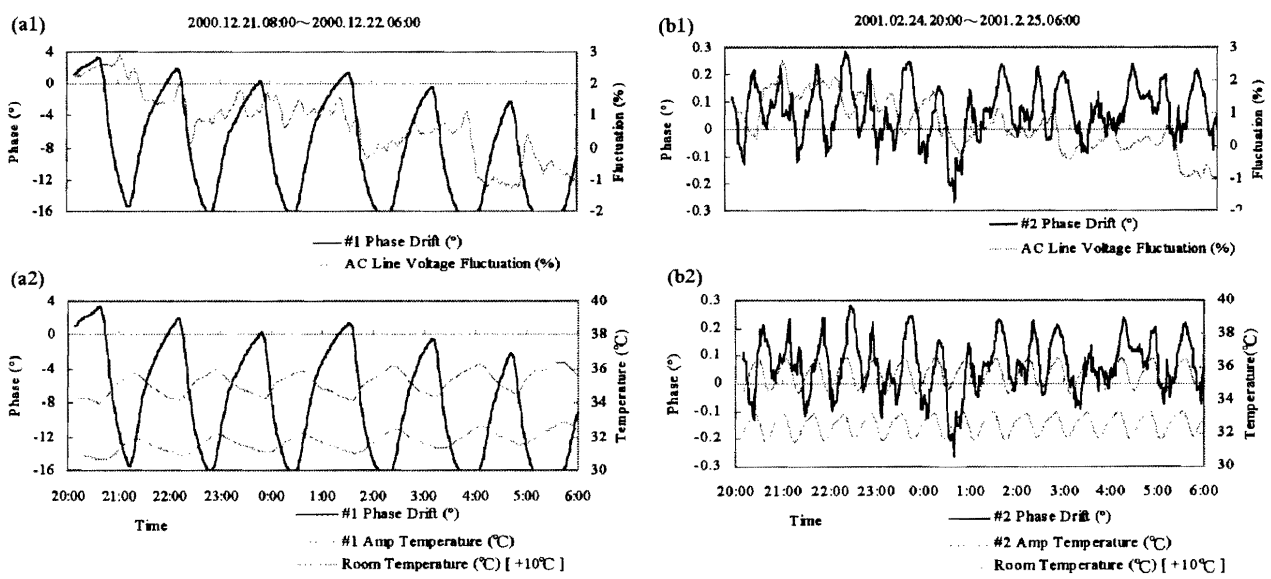

Fig. 4 The phase variation. (a1) and (a2) are without a digital feedback. (b1) and (b2) are with a digital feedback.

5. Quantum Optics

5) Quantum Optics

Personnel: Shuichiro Inoue, Takahisa Ymazoe**, Hiroyuki Watanabe**

Introduction

We have been investigating quantum nature of light and developing new technologies controlling or utilizing it in the field of optical measurements, imaging and communications.

The main research subjects are as follows:

i) High efficient interaction-free measurements using a Fabry-Perot resonator
ii) Quantum imaging using interaction-free measurements
iii) Development of a 1550 nm single photon detector
iv) Long-distance quantum cryptography
v) Development of an ultrabright source of polarization-entangled photons at 1550 nm

**graduate student

SELF-HOMODYNE TOMOGRAPHY

H. Watanabe, T. Yamazoe and S. Inoue

The state of a quantum mechanical system is completely described by density matrices or a phase-space distribution such as the Wigner function. For the light field, the Wigner function has been reconstructed from a large number of measurements by the balanced homodyne detection, so-called optical homodyne tomography[1]. Here, we present self-homodyne tomography using a Fabry-Perot cavity, where the local oscillator is generated in the same process as the signal field[2].

Figure 1 shows a schematic picture of our set-up. The light from the laser diode, which is supposed to be a quasi-monochromatic field, is fed into a Fabry-Perot cavity. Each Fourier components of the reflected field undergoes a different phase rotation depending on the detuning between the cavity resonant frequency and the incoming field frequencies. If the analyzing frequency of the fluctuations was set out of the cavity linewidth, the phase of the fluctuation doesn't rotate. Therefore, using the monochromatic field component as a local oscillator, the relative angle between the fluctuation ellipse and the mean value can be rotated arbitrarily. The homodyne detection allows one to transform the fluctuations in a quadrature of the field into amplitude fluctuations that permit a direct detection. Figure 2 shows the amplitude fluctuations of the reflected field while cavity length was sweeped. The solid line is the noise power at $8MHz$ and the dotted line is the best theoretical fitting. The phase fluctuation was 30.4dB above the shot-noise level and the relative phase rotation was approximately 5.2 degrees. Figure 3 shows the noise current from the homodyne detector while the relative phase was rotated.

In conclusion, we have demonstrated the principle of self-homodyne tomography. In this measurement, the rotation of the fluctuation ellipse in the quadrature was only 5.2 degrees. Therefore, if the phase is rotated $\pi/2$ using a single end Fabry-Perot cavity, we will be able to obtain the Wigner function of any quantum states of light without a local oscillator.

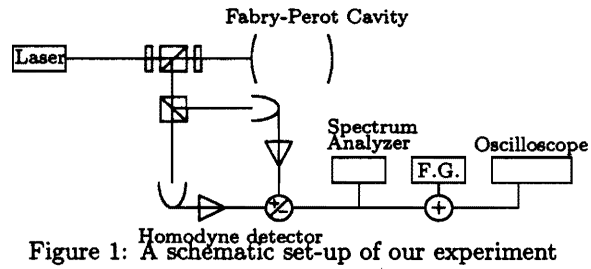

Figure 1: A schematic set-up of our experiment

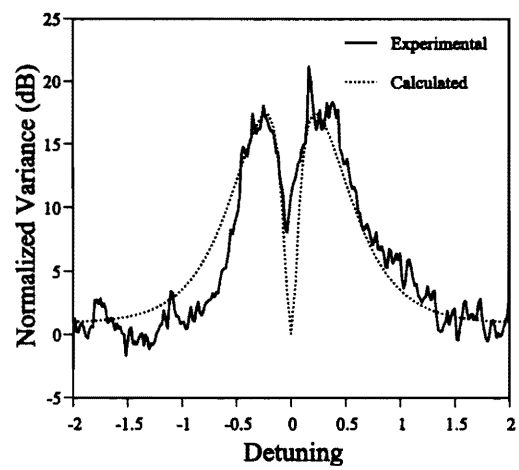

Figure 2: Plot of the normalized variance of amplitude fluctuations of reflected field versus cavity detuning.

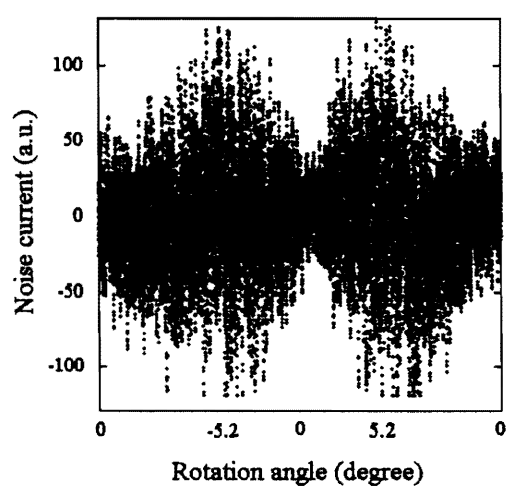

Figure 3: Noise current from the homodyne detector

[1] K. Vogel and H. Risken, Phys.Rev A **40**, 2847 (1989)
[2] P. Galatola et al., Opt. Commun. **85**, 95 (1991) .

A 1550nm SINGLE-PHOTON DETECTOR FOR LONG-DISTANCE QUANTUM CRYPTOGRAPHY

N.Namekata, Y.Makino, H.Watanabe and S.Inoue

In order to apply quantum cryptography (QC) to practical optical comunications, the wavelength of a single photon must be around 1550nm, because at the wavelength the transmission losses in an optical fiber are minimum. The most difficult problem to realize long-distance QC is that a commercial high efficient single photon detector for 1550nm does not exist. Therefore, it is indispensable to develop a single photon detector to realize long-distance practical QC.

We used $InGaAs$ avalanche photodiodes (APD) to detect a single photon at 1550nm. APDs were operated in Geiger mode. The cause of decreasing APD's efficiency is the dark counting due to carriers trapped in the depletion layer during an avalanche (afterpulsing) and thermal carriers. To restrain afterpulsing, we operated the APD with a gated quenching circuit ($GPQC$) by which Geiger mode is switched on and off cyclically. Here, Geiger mode-off time was longer than the lifetime of trapped carriers. Moreover, to restrain thermal carriers, APDs were cooled down to $110K$.

The performance of a single photon detector must be characterized by both of the quantum efficiency and the dark count rate, because in QC not only the poor quantum efficiency but also the dark count rate reduces Quantum Bit Error Rate ($QBER$). The quantum efficiency η is approximately expressed as

$$\eta = \sqrt[N]{\frac{1-P_l}{1-P_d}}, \qquad (1)$$

where P_l is the avalanche probability, P_d is the dark count probability. In the Geiger mode, APD is biased above the breakdown voltage by V_E which is called an excess voltage. Increasing V_E, both of the dark count rate and the quantum efficiency are increased.

In order to characterize the performance of the single photon detector, both of them must be evaluated. We adoptted noise equivalent power (NEP) to characterize the performance. The NEP is defined as the signal power required to attain an unity signal-to-noise ratio within 1 second integration time,

$$NEP = \frac{h\nu}{\eta}\sqrt{2R_d}, \qquad (2)$$

where h is Planck's constant, ν is the frequency of light, η is the quantum efficiency and R_d is the dark count rate.

In our $GPQC$, the Geiger mode-on time was $4ns$ and the Geiger mode-off time was $5\mu s$. Therefore, the repetition rate of the gated pulse was $200kHz$. The NEP is plotted as a function of V_E in Figure 1. The APD has optimal V_E at which NEP is minimum. The minimum NEP was obtained at $V_E = 2V$. Here, the temperature was $110K$, $P_l = 0.038$, and $P_d = 2.8 \times 10^{-5}$.

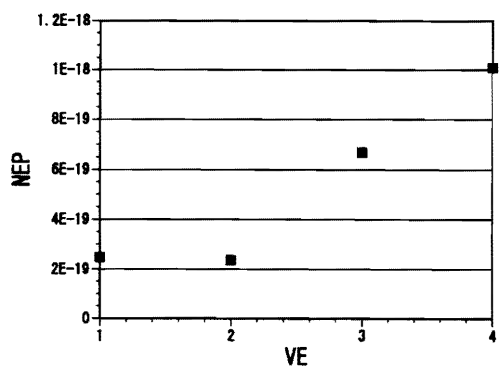

Figure 1: Dependence of NEP on V_E.

In QC, $QBER < 15\%$ is required for security. Using our single photon detector, $QBER$ exceeds 15% for transmission length $L = 68km$. Thus, we would be able to realize the secure QC over $60km$.

[1] A. Muller, et al., Appl. Phys. Lett. 70, 634 (1997)
[2] S. Cova, et al., Appl. Opt. 35, 1956 (1996)

CRYPTOGRAPHY USING LONGITUDINAL-MODE-PARTITION NOISE OF SEMICONDUCTOR LASERS

T. Yamazoe and S.Inoue

The sidemode intensities of a typical semiconductor laser are only 20-30 dB below the main mode intensity. These relatively large sidemodes compete with the main mode for depletion of carriers, and this process introduces huge fluctuations of the each mode intensities. These fluctuations are called longitudinal-mode-partition noise. When the gain medium of a semiconductor laser is homogeneously broadened, negative intensity noise correlation is formed between the main mode and the sidemodes. By this negative intensity noise correlation the longitudinal-mode-partition noise can be suppressed [1]. When the each longitudinal mode is separated in time or space, the performance of the optical communication is degraded by the huge longitudinal-mode-partition noise. In this paper, we propose and demonstrate a new cryptosystem using the longitudinal-mode-partition noise. Here, we regard the longitudinal-mode-partition noise as a cryptographic key.

The longitudinal-mode-partition noise can be generated using a non-symmetric Mach-Zehnder interferometer [2]. When two arm-lengths are equal, all modes are output into the bright fringe. When the even-numbered modes interfere constructively and the odd-numbered modes interfere destructively, the even-numbered modes are output into the bright fringe, and the odd-numbered modes are output into the dark fringe. In this case, the longitudinal-mode-partition noise is maximum.

The experimental setup to realize the cryptosystem is shown in Figure 1. The arm-length difference is set at which the longitudinal-mode-partition noise is maximum. A sender generates a signal by modulating the amplitude of an output from the bright fringe. By detecting both of the outputs from the bright and the dark fringes, receiver can read the signal. Even if an eavesdropper detects the output of the bright fringe, she can't read the signal because of the huge longitudinal-mode-partition noise.

Figure 2 shows the intensity noise detected by the receiver. The modulation frequency was 5 MHz. Line (a) shows the intensity noise of the bright fringe. Line (b) shows the sum of the intensity noise of the bright and the dark fringes.

In conclusion, we proposed cryptography using longitudinal-mode-partition noise of a semiconductor laser and demonstrated the principle. If a dual-wavelength semiconductor laser is developed in the future, this cryptosystem can be used for the long distance optical communications.

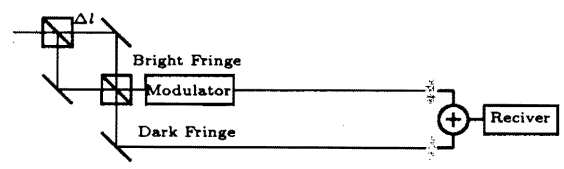

Figure 1: Experimental setup. Δl is the arm-length difference of Interferometer.

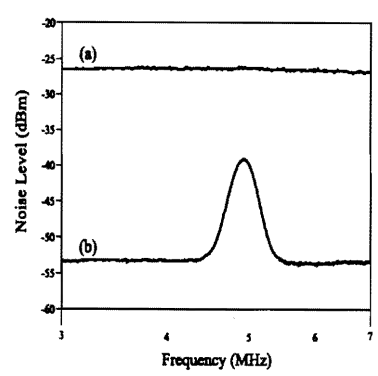

Figure 2: Intensity noise detected by the reciver. (a):Intensity noise of the bright fringe. (b):The sum of the intensity noise of bright and the dark fringes.

[1] S. Inoue, H. Ohzu, S. Machida and Y.Yamamoto, Phys. Rev. A **46**, 2757 (1992)
[2] S. Inoue and Y. Yamamoto, Opt. Lett. **22**, 5 (1997)

AMPLITUDE SQUEEZED STATE GENERATION IN LOW-FREQUENCY REGION FROM TJS LASERS

T. Yamazoe and S. Inoue

Since it is theoretically predicted that a pump-noise-suppressed laser can produce amplitude squeezed states [1], amplitude squeezed states have been generated from a pump-noise-suprressed semiconductor laser [2].

According to the pump-noise-suppression theory, the amplitude squeezed states should be observed from dc to the frequency at which the intensity noise starts increasing due to the relaxation oscillation. However, in the low frequency region, the amplitude squeezed states have not been observed. This is because the $1/f$ noise which is approximately inversely proportional to the frequency destroys amplitude squeezed states. In order to apply the amplitude squeezed states to some low-frequency measurements, the $1/f$ noise must be suppressed.

Although the $1/f$ noise of semiconductor devices has been investigated for a long time, the physical origin of the $1/f$ noise is not yet quite clear. One possible generation mechanism of the $1/f$ noise in a semiconductor laser is as follows. A semiconductor laser is driven by a constant-current source, but the carrier number around the surface of the semiconductor laser can fluctuate due to random trapping and detrapping by the surface states of oxide which is located between the surface of the device and the dielectric film.

In order to suppress the $1/f$ noise, we performed argon plasma spattering before coating the dielectric film. It takes oxide off the surface of the semiconductor laser by irradiating argon plasma. We fabricated five types of lasers to find an optimal spattering condition. The plasma spattering power was 20 W. The front facets were irradiated for 0, 40, 60, 120, 300 seconds, respectively. The rear facets of all samples were irradiated for 20 seconds. The plasma spattering power was the same.

Figner 1 shows the intensity noise of the five types of lasers at 70 K which was normalized by the corresponding shot-noise level. We calibrated the shot-noise level using a white light source. The pumping rate was 10 times the threshold current and the external quantum efficiency was about 0.60. With the increase of spattering time, the $1/f$ noise was suppressed. The minimum $1/f$ noise was observed when the front facets were irradiated for 120 seconds. With the further increase of spattering time, the $1/f$ noise was increased. This is due to the defects which were caused by the damage in removing oxide.

In conclusion, we have demonstrated that $1/f$ noise can be significantly suppressed by removing oxide. We observed the amplitude squeezed states down to 30 kHz when the spattering time was 120 seconds. If we can find an optimal spattering condition of rear facets, we might produce the amplitude squeezed states at much lower frequency.

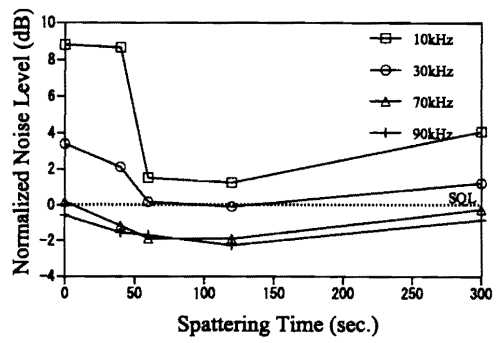

Figure 1: Normalized intensity noise vs spattaring time at 70K. SQL : Standard Quantum Limit

[1] Y. Yamamoto, S. Machida and O. Nilsson, Phys. Rev. A **34**, 4025 (1996)
[2] S. Lathi, K. Tanaka, T. Morita, S. Inoue, H. Kan and Y. Yamamoto, IEEE J. Quantum Electron. **35**, 387 (1999)

EXPERIMENTAL DEMONSTRATION OF TWO-DIMENSIONAL INTERACTION-FREE IMAGING

H. Watanabe and S. Inoue

The complementary wavelike and particle-like natures of photons allow one to ascertain the presence or absence of an object without any photons being absorbed[1]. This counter-intuitive measurement is called an *interaction-free measurements* (*IFM*). The measurement can be realized using a Fabry-Perot (FP) resonator as a measurement apparatus [2]. Here, we present experimental results of classical two-dimensional *interaction-free imaging* (*IFI*) of a photographic film using a high-finesse FP resonator[3].

Figure 1 shows a schematic picture of our set-up. If the object is absent in the resonator when the resonator is on resonance, the incident light will be transmitted with a high probability. If the object is present in the resonator, the incident light will be reflected by the resonator front mirror since the object destroys the interference. We used photographic film O (Kodak High Speed Infrared Black & White Film) as an observed object to monitor the absorption of the object directly. In the first experiment, another film M with the same photosensitivity was used as a photodetector. Scanning both films inside and outside the FP resonator through the optical axis, a negative of film O's piece was imaged on film M without exposing film O as shown in figure 2. In the second experiment, by measuring the optical intensity of the transmitted and the reflected light with photodiodes D_t and D_r, a positive and a negative images of film O was obtained simultaneously. The signals from the detectors were saved on the digital oscilloscope and analyzed by the PC while scanning film O. The result of the measurement is shown in Figure 3.

In conclusion, we have demonstrated that a negative and a positive images of a two-dimensional non-transparent object can be simultaneously imaged without having the object absorb a single photon. In our laboratory, we have measured the probability of success in *IFM* using single photon counting modules and realized 82 % of success rate. If the resonator is actively stabilized, we would be able to make two-dimensional *IFI* with 82 % of success rate.

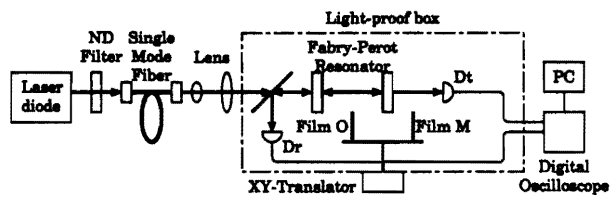

Figure 1: A schematic set-up of our experiment

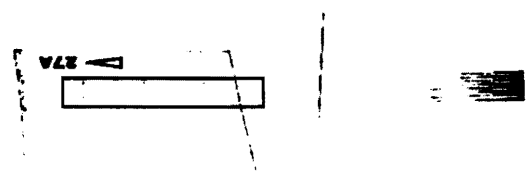

Figure 2: Left: a developed O film. The framed rectangle was imaged. No trace of exposure can be seen. Right: a negative image of the framed rectangle to the left. The film O's edge and rectangular holes to the left are shown.

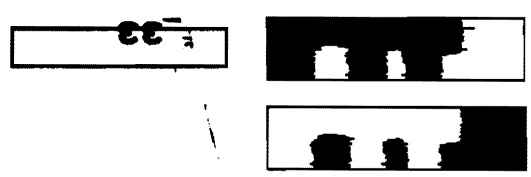

Figure 3: Left: a developed O film. Right: a negative and a positive computer images of the framed rectangle to the left.

[1] A. Elizur and L. Vaidman, Found. Phys. **23**, 987 (1993)

[2] T. Tsegaye et al., Phys. Rev. A **57**, 3987 (1998)

[3] H. Watanabe and S. Inoue, proceedings of the Asia Pacific Physics Conference (2000)

6. Other Researches

DOSIMETRY FOR LINAC-BASED STEREOTACTIC IRRADIATION

S.Urahashi,Y.Tanaka,K.Ishikawa and F.Shishikura

Linac-based stereotactic irradiation is a high precision irradiation technique, in which narrow photon beams are directed at a small target lesion, combined in the patient couch angles and accelerator gantry rotations. Stereotactic irradiation at *Nihon Univ. Itabashi Hospital* are performed with 4MV photon beams (*MEVATRON* M2/6740) using the treatment planning program X Knife4 (*RADIONICS Inc.*). In stereotactic irradiation, check of the irradiation accuracy and verification of the dose delivery are required.

The purpose of this study is to evaluate the usefulness of a imaging plate (IP) dosimetry and to investigate the accuracy of the dose distribution planned using the X Knife4 program for stereotactic irradiation.

Measurements were made with IP placed in a spherical head phantom 16cm in diameter. This phantom is made of tissue equivalent material (*Tough Water Phantom, KYOTO KAGAKU Co. LTD.*). In stereotactic irradiation experiments, target dose in head phantom was given about 20~30Gy undergoing the same dose as a patient treatment. Photon beams are defined using circular focused collimators (field diameters of 5,10 and 12.5mm at the isocentre). IP detector is high sensitive to radiations and their dose reduction procedure of the irradiated IP was performed. This procedures were carried out by mean of exposing red light before reading IP detectors.

IP readings were made with BAS-2000 imaging analyzer system (*Fujifilm Co. LTD.*). This system can be converted IP image data into isodose distribution and described color display.

The results of this study indicated that IP dosimetry is a convenient and useful tool for evaluation of dose distribution calculated by the stereotactic irradiation X Knife4 program.

SYNTHESIS OF ULTRATHIN FULLERENE POLYMER FILMS BY RADIATION LIGHT

Personnel: Hiroshi Yamamoto, Nobuyuki Iwata

The purposes of this work are to synthesize three dimensional Fullerene polymers under high pressure and/or very strong irradiation of ultra-violet ray, and to clarify characteristic properties of the novel polymers of C60. We expect the obtained polymers will have more hardness than a diamond and they may be named as a "superdiamond".

In this work polymerization reactions of C60 by ultra-violet ray are very important processes. Then we have prepared ultrathin C60 films and/or ultrafine fibers of C60 as the specimens for experiments of the polymerization in this year. Obtained results are following.

1) A self-assembly monolayer (SAM) of C60 derivatives with alkanethiol has been prepared on the substrates of Au. The adsorbing reactions of C60 derivatives saturated for about 15h in a 1mM benzen solution of C60 derivatives at room temperature. The microstructures observed by AFM or TEM revealed that ultrathin films exactly covered on Au substrates.

2) Macroscopic needle-like structures with few millimeters length were also assembled by an extraction from nonelectrolysis supersaturated toluene solution. A huge needle-like C60 was obtained by a very slow extraction. In the sample, ultrafine fibers with a diameter of about 50nm were observed.

Small-angle X-ray scattering from poly(*N*-isopropylacrylamide) in aqueous solution of acetonitrile

K. Kurita and S. Shimizu

Segment-segment interaction parameters of poly(*N*-isopropylacrylamide) in acetonitrile-water mixed solvent were determined by using small-angle X-ray scattering. Small-angle X-ray scattering measurements were carried out in conditions of the semidilute poor solvent regime and just below the lower critical solution temperature. From concentration dependence of the correlation length, the binary and ternary cluster integrals, B_1 and B_2, were determined.

The values of B_1 and B_2 for each system decreased with increasing the temperature. The Θ temperatures defined as the temperature at which $B_1 = 0$ decreased with increasing AcN content. These decreases correspond to the results of the cloud point measurements same as the results of the aqueous propanol(PrOH) mixed solvent systems[1]. The contribution of the segment-segment interactions to the entropy S_{int} and the enthalpy H_{int} has been calculated from the temperature dependence of these cluster integrals. It has been found that both values are positive. On addition of a small amount of acetonitrile into aqueous solution of poly(*N*-isopropylacrylamide), S_{int} and H_{int} increase. Further addition of acetonitrile, these values reached maximum and then decreased. These behaviors may be explained as due to the strong interaction between AcN and water molecules. That is, the increases of S_{int} and H_{int} are due to disruption the structure between AcN and water by the segment-segment contacts of PNIPAM.

1) S.Shimizu, M.Kimura, T.Maruyama and K.Kurita, *J. Appl.Cryst.*, (1997)**30**, 712–716.

PROPAGATION CHARACTERISTICS OF SINGLE-POLARIZATION OPTICAL FIBER WITH THE CROSS SECTION OF ARBITRARY SHAPE

Takashi HINATA , Tsuneki YAMASAKI and Hiroyuki HOSONO

In this paper, propagation characteristics of a single polarization optical fiber with the cross section of arbitrary shape are analytically studied by applying the circular Fourier expansion method. Firstly, for a single elliptical core fiber, an accuracy of the circular Fourier expansion method (CFEM) is discussed by comparing to a rigorous analysis method using Mathieu functions. Secondly, as an application of the circular Fourier expansion method, a single polarization optical fiber composed of an elliptic core with round shoulder and fluctuations in the pit of circular periphery (non-ideal SPF, see Fig.1(b)) is designed so as to satisfy the zero total dispersion and is discussed for the single polarization bandwidth and the wavelength sensitivity of the total dispersion. These results are compared with the case of the single polarization optical fiber without round shoulder and fluctuations (ideal SPF, see Fig.1 (a)).

Fig.2 shows the single-polarization bandwidth $\delta\lambda$ versus b/a, which is computed by the relative index difference Δ and the semimajor core radius a satisfying the zero total dispersion. $\delta\lambda$ of non-ideal SPF becomes fairly smaller by influence of round shoulder and fluctuations than that of ideal SPF.

Fig.3 shows the total dispersion S_e versus the wavelength λ at b/a=0.5. For a start, ideal SPF is assumed to design so as to satisfy the zero total dispersion (see ① in Fig.3). However, if this ideal SPF is caused round shoulder and fluctuations in production process, the zero total dispersion cannot be satisfied (see ② in Fig.3). Then, the zero total dispersion can be realized by beforehand estimating Δ, a, and b/a for non-ideal SPF (see ③ in Fig.3). The wavelength sensitivity $dS_e/d\lambda$ of the total dispersion for non-ideal SPF(③) becomes slightly larger than that for ideal SPF (①).

So far, CFEM was not fully confirmed for an accuracy of propagation constants that were the most fundamental data for various propagation characteristic analyses of waveguides. For single elliptical core fiber, we compared propagation constants computed by CFEM with those computed by the rigorous analysis method using Mathieu function. A good agreement of both results was found.

REFERENCE

[1]S. Furukawa , M. Saitou, and T. Hinata: " Propagation Characteristics of Single-Polarization Optical Fiber with the Cross Section of Arbitrary Shape ", Proc. of Japan-China Joint Meeting on Optical Fiber Science and Electromagnetic Theory ,P.223-226,Dec., Osaka, Japan(2000).

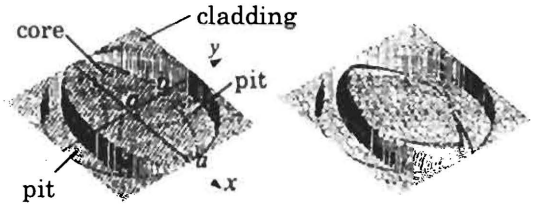

(a) ideal SPF (b) non-ideal SPF

Fig.1 Refractive index profiles of ideal SPF and non-ideal SPF

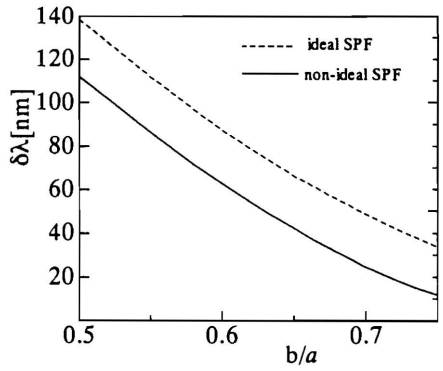

Fig.2 The single polarization bandwidth λ versus b/a

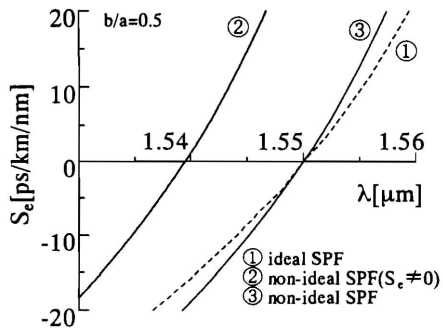

Fig.3 The total dispersion S_e versus wavelength λ

RADIATION EFFECT ON SEMICONDUCTOR DEVICES

Kazunori Ohnishi and Yoshihiro Takahashi

The radiation-induced trapped charge in the insulation layer of Metal-Nitride-Oxide-Semiconductor (MNOS) structure has been investigated. The charge trapping mechanism under irradiation is discussed by analyzing the radiation-induced mid-gap voltage shift (ΔV_{mg}). The irradiation tests were carried out using Co-60 gamma ray source up to 1 Mrad(Si) with the gate voltage of +6 or −6 V. Points in fig. 1 show the measured ΔV_{mg} of MNOS structure with various insulator thicknesses. A simple charge trap model fit to the experimental data is constructed, in which the hole traps are located at silicon-oxide interface and the hole and electron traps are located at oxide-nitride interface. The lines in Fig. 1 show the calculated results using the proposed model. The results can be fit successfully to the experimental data. From these results, it is confirmed that this calculation model is very useful to estimate the radiation-induced trapped charge in insulators of MNOS structure, and that the densities and the capture cross sections of traps can be obtained by fitting analysis using the model.

The ΔV_{mg} of MNOS structures with varying insulator thicknesses are simulated using the calculation model. As the results of simulation, it was found that $\Delta V_{mg} = 0$ can be obtained using MNOS structure with specific oxide and nitride thicknesses when the gate voltage during irradiation (V_g) is positive. The thicknesses are considered to be the optimum thicknesses for radiation hardened MNOS structure because the net radiation-induced trapped charges in the insulator is zero when $\Delta V_{mg} = 0$. The optimum insulator thicknesses with different radiation conditions are also calculated. Figure 2 shows the obtained optimum thicknesses with different radiation conditions. In this figure, the equivalent oxide thickness is same on the each dashed line. It is found that the optimum thicknesses do not depend much on the total dose and on the gate voltage during irradiation when the equivalent oxide thickness is less than about 100 nm. It was also confirmed that ΔV_{mg} of MNOS structure is almost same as that of MOS structure which has same equivalent oxide thickness when $V_g < 0$. From these results, it is expected that the radiation hardened device can be achieved using MNOS structure in terms of radiation-induced trapped charge.

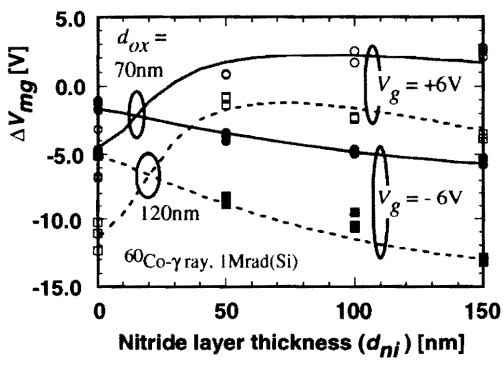

Fig. 1 ΔV_{mg} of MNOS structures in which the oxide layer thicknesses are 70 and 120nm. Points show the experimental results. Lines show the calculated results.

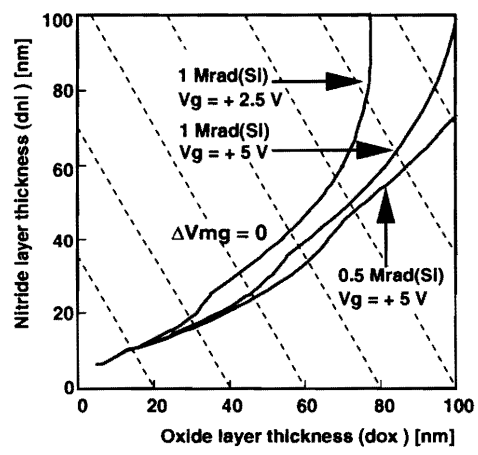

Fig. 2 The optimum insulator thicknesses of MNOS structures with different radiation conditions when $V_g > 0$. The equivalent oxide thickness is the same on each dashed line.

Single crystal growth of $CaGa_2S_4$:Ce^{3+} and its photoluminescence properties

C. Hidaka and T. Takizawa

Ce^{3+} doped $CaGa_2S_4$ compounds have attracted much attention as suitable materials for blue emitting devices. Since laser oscillation was observed in a Eu^{2+} doped $CaGa_2S_4$ single crystal, a crystal doped with Ce^{3+} is expected as a host material for blue light lasers. [1] A crystal for a laser host material is required to have no cracks and no voids along with homogeneous refractive index. Based on the phase diagram, crystals have been grown at a speed of 0.5cm/h from temperature 20°C above the melting point (1132°C) by the Bridgman method. However, the grown crystals had many cracks and voids, and the crystallinity should still be improved.

To improve the crystallinity, we have tried to find a proper condition by preparing the single crystals under various conditions. A carbon boat was adopted instead of a quartz boat coated with carbon film, as the carbon prevents the crystal from sticking to the boat. Here, the growth speed was set at 0.25cm/h, and crystals were grown from the temperature at 1130, 1132 and 1134°C, respectively. Single domains became larger as maximum temperature increased.

Figure 1 shows photoluminescence spectra of various Ce^{3+} concentration. The intensity of the emission varies almost linearly with the Ce^{3+} concentration between 0.1 and 0.5wt%. The emission intensity seems to be saturated in the Ce^{3+} concentration above 0.5wt%. In the Ce^{3+} doped $CaGa_2S_4$, photoluminescence spectra were measured in temperature range from 10 to 300K. Integrated intensities of the two peaks are the same amount at low temperature. The integrated intensity of the B band having a peak at 515nm is twice as large as that of the A band at 465nm independent of Ce^{3+} concentration near 300K.(Fig. 2) The detailed study of these photoluminescence is now in progress. We will also measure the electron spin resonance.

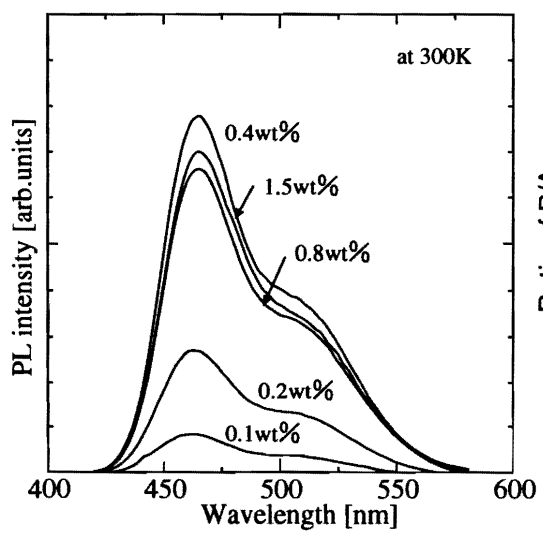

Fig. 1. Photoluminescence spectra of various Ce^{3+} concentration.

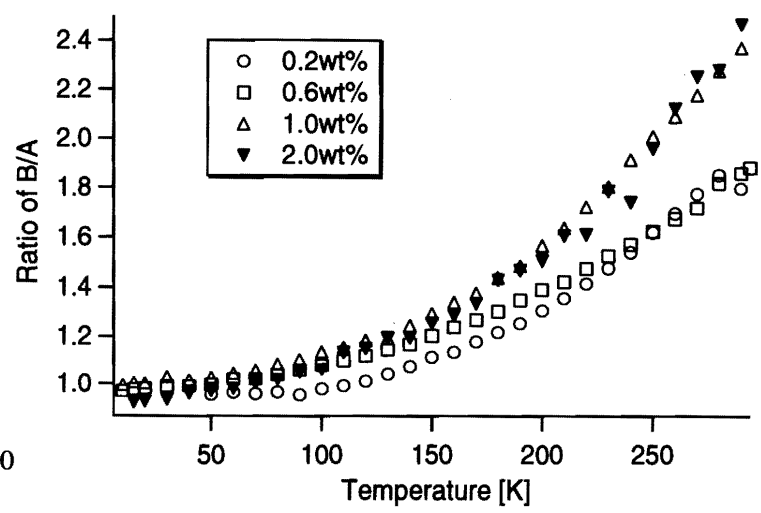

Fig. 2. Ratio of integrated intensities of the B band to the A band.

References

[1] S. Iida, T. Matsumoto, N.T. Mamedov, Y. Maruyama, A.I. Bairamov, B.G. Tagiev, O.B. Tagiev and R.B. Dzhabbarov: Jpn. J. Appl. Phys. **36** (1997) Lett.857.

Phase diagrams and crystal structures of the $CdS-In_2S_3-Ga_2S_3$ system

K. Asaka*, C. Hidaka, T. Takizawa and H. Matsushita[1]
Department of Physics, College of Humanities and Sciences, Nihon University,
3-25-40 Sakurajosui, Setagaya-ku, Tokyo 156-8550, Japan

Several different kinds of crystal structures have been found in the $CdS-In_2S_3-Ga_2S_3$ system, such as tetrahedral, layer and spinel structures. Recently, the layer compounds of the pseudo-ternary $AX-B_2X_3-B'_2X_3$ (A=Mg, Mn, Fe, Co, Ni, Zn, Cd, Hg: B, B'=Al, Ga, In, Sc, V, Cr: X=S, Se) system have attracted much attention because of the polytypic form, superstructure, and anisotropic physical properties [1]. We have investigated the phase equilibrium, crystal structures and optical properties in the following three regions of the $CdS-In_2S_3-Ga_2S_3$ system.

(i) $(1-x)CdGa_2S_4-xCdIn_2S_4$ (x=0~1), (ii) $(1-x)CdGa_2S_4-2xGaInS_3$ (x=0~1),
(iii) $(1-x)CdS-xGaInS_3$ (x=0~1)

First, we have investigated the pseudo-binary phase diagram of the (i) system, where the $ZnIn_2S_4$ (III) type of the layer phase exists in the intermediate region between the end compounds [2]. We found that the layer phase becomes single in between x=0.58 and 0.68. This result was confirmed by an actual crystal growth for $CdIn_{1.2}Ga_{0.8}S_4$ compound.

Second, we have searched for a new layer phase and polytypic form in the (ii) and (iii) systems. We have succeeded in finding a new layer phase in this ternary system. The new phase crystallizes in the structure shown in Table I.

Last, we have performed the optical absorption measurement for the new layer and already known $ZnIn_2S_4$ (III) phase compounds (see Fig. 1) and determined the optical band gaps of both phases from this results as the following.

$CdIn_{1.2}Ga_{0.8}S_4$	2.49eV(indirect)	2.65eV(direct)
$Cd_{0.2}In_{1.6}Ga_{0.8}S_{5.6}$	2.58eV(indirect)	2.76eV(direct)

Table I: The structure of $Cd_{0.2}In_{1.6}Ga_2S_{5.6}$ phase.
Space group; $P\bar{3}m1$ (164), Z=1
Hexagonal cell; a=3.80, c=18.3 Å

Atom	x	y	Z	Occupation
Cd/Ga	1/3	2/3	0.301	0.1/0.6
Ga/In	1/3	2/3	0.877	0.5/0.4
In	0	0	0.500	1.0
S1	1/3	2/3	0.425	1.0
S2	1/3	2/3	0.748	1.0
S3	1/3	2/3	0.085	1.0

Interatomic distance:
Cd/Ga-S; 2.32 Å, Ga/In-S; 2. 33 Å, In-S; 2.59 Å

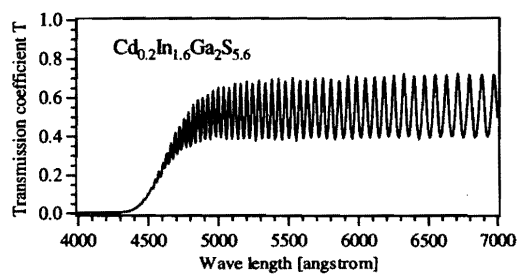

Fig. 1 The transmission coefficient for $Cd_{0.2}In_{1.6}Ga_2S_{5.6}$ (thickness 15 μ m).

Refferences [1] H. Haeuseler and S. K. Srivastava; Z. Kristallogr. **215**, 205-221 (2000)
[2] K. Asaka, C. Hidaka, T. Takizawa and H. Matsushita; Jpn. J. Appl. Phys. (in printing)
[3] C. Razzetti, P. P. Lottici, L. Tarricone and L.Zanotti; Prog. Cryst. Growth and Charact. **10** 353-360 (1984)

CRYSTAL GROWTH AND CHARACTERIZATION OF Cu_2-II-IV-S_4 COMPOUND SEMICONDUCTORS

H.MATSUSHITA and T.TAKIZAWA

Department of Physics, College of Humanities and Sciences, Nihon University, 3-25-40 Sakura-josui, Setagaya-ku, Tokyo 156-8550

Tetrahedrally coordinated ternary and quaternary semiconductors which belong to the crystal systems such as chalcopyrite, defect chalcopyrite, spinel, stannite and famatinite, are derived by various combinations of the elements in the vicinity of the IV group. To examine the possibility of such compound semiconductors to be used in practical devices is important to develop the new material applications. We have studied the basic structural and optical properties of Cu_2-II-IV-Se_4 compound semiconductors (II = Zn, Cd; IV = Ge, Sn). As a result, $Cu_2ZnSnSe_4$ and $Cu_2CdGeSe_4$ compounds are found to have band gaps suitable for optimum conversion efficiency for solar cells (1.2-1.5 eV).

In this work, the method of the synthesis of Cu_2-II-IV-S_4 compounds (II = Zn, Cd; IV = Ge, Sn), where VI group atoms are substituted by S atoms, has been investigated. The single phases of Cu_2-II-IV-S_4 are synthesized from melts. The melting points, crystal systems and lattice constants are determined using the differential thermal analysis and X-ray diffraction, which are summarized as shown in Table I. The structural investigation is also performed as compared to the calculated model structures by means of Rietveld method. It is found that the Cu_2-II-Sn-S_4 compound has a stannite structure, while Cu_2-II-Ge-S_4 has an orthorhombic one. Among these compounds, bulk single crystals of Cu_2ZnSnS_4 and Cu_2CdSnS_4 are grown by the horizontal gradient freezing method. Optical band gaps of Cu_2ZnSnS_4 and Cu_2CdSnS_4 are determined using the grown single crystals by optical absorption to be 1.39 and 1.37eV, respectively.

Table 1: Melting point, crystal structure, lattice constants and band gaps of Cu_2-II-IV-S_4 compounds.

Compounds	Melting point(℃)	Crystal system	Lattice constants			Cond. type	Band gap (eV)
			a(Å)	b(Å)	c(Å)		
Cu_2ZnGeS_4	1120	Orthorhombic	7.57	6.47	6.13	p	–
Cu_2ZnSnS_4	990	Tetragonal	5.43	–	10.81	p	1.39
Cu_2CdGeS_4	1020	Orthorhombic	7.70	6.55	6.28	p	–
Cu_2CdSnS_4	926	Tetragonal	5.59	–	10.84	p	1.37

HIGH-PRESSURE EFFECT ON TRANSPORT PROPERTIES OF SPIN-LADDER COMPOUND $Na_{1-x}Ca_xV_2O_5$ and $Ca_{0.7}Li_{0.3}V_2O_5$

H. Takahashi, H. Takahashi, T. Nakanishi, *T. Arima, *M. Noguchi, *M. Oyanagi, **N. Takeshita, **N. Môri

Electrical resistivity of layered vanadium oxides $Na_{1-x}Ca_xV_2O_5$ and $Ca_{0.7}Li_{0.3}V_2O_5$ has been measured under high pressure up to 10 GPa. These compound has V-O network forming two-leg spin-ladder layer in some composition range. In the spin-ladder compound $Na_{1-x}Ca_xV_2O_5$, the electrical resistivity measurements show semiconducting behavior. However, the electrical resistivity has been significantly reduced under high pressure as shown in Fig. 1, although it remains semiconducting up to 8GPa. On the other hand, the electrical resistivity of $Ca_{0.7}Li_{0.3}V_2O_5$ which has also two-leg spin-ladder layer is lower than $Na_{1-x}Ca_xV_2O_5$ system in several order. The electrical resistivity of $Ca_{0.7}Li_{0.3}V_2O_5$ was reduced largely even at low temperature range with applying pressure, as shown in Fig.2.

In the spin-ladder materials it is thought that the conduction of carriers occurs through the ladder layer. All these experiments make it clear that the pressure plays an important role to delocalize carriers in the ladder layer, which is similar to the pressure effect observed in $Sr_{14-x}Ca_xCu_{24}O_{41}$ system. From Fig.1 the lowest resistivity for $Ca_{0.7}Li_{0.3}V_2O_5$ is 4×10^{-1} Ωcm at 300 K and 10 GPa. In superconducting $Sr_{2.5}Ca_{11.5}Cu_{24}O_{41}$ spin-ladder system, the electrical resistivity is about 4×10^{-4} Ωcm at 300 K and 3 GPa. The electrical resistivity in usual high-T_C superconductor shows less than 1×10^{-3} Ωcm at 300 K. Thus further carrier doping and/or applying higher pressure are thought to be necessary to give rise to the insulator-metal transition in this system. Superconductivity is also expected in such a metallic phase.

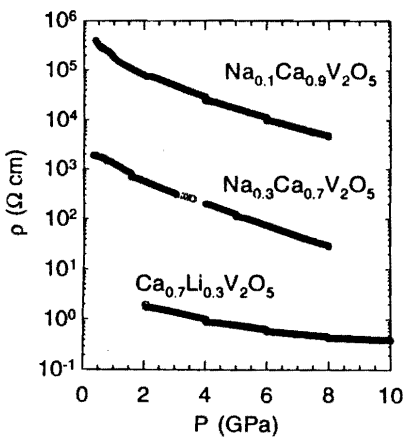

Fig.1 Pressure dependence of electrical resistivity for Spin-ladder vanadium oxides.

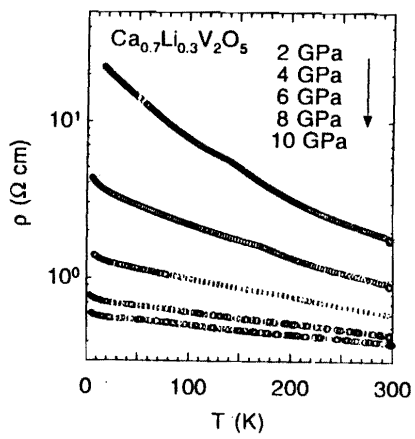

Fig.2 Temperature dependence of electrical resistivity for $Ca_{0.7}Li_{0.3}V_2O_5$

*Institute of Materials Science, University of Tsukuba, **Institute for Solid State of Physics, The University of Tokyo

Photoinduced spectral change in Eu_2O_3

Shosuke Mochizuki*, Yuya Suzuki and Tauto Nakanishi
Department of Physics, College of Humanities and Sciences, Nihon University, Tokyo 156-8550 Japan

Kimihiro Ishi
Research Institute for Scientific Measurements, Tohoku University, Sendai 980-8577, Japan

Corresponding author: motizuki@physics.chs.nihon-u.ac.jp

Recently, considerable attention has been devoted to research for new materials to be used for erasable optical storage and for laser media for tunable wide-band lasers. The interest in photoluminescent materials showing photo-induced reversible spectral change at room temperature has significantly grown, because a combination of such reversible phenomenon and the near-field optical microscope[1] is very promising when applied to high-density optical storage with nanometer resolution. It is a hope that we can find white PL material, which is useful for the wide-band tunable-laser medium. Hitherto, X ray- and photo-induced spectral change of rare-earth ions has been observed mainly on Eu- and Tm-doped ionic crystals.[2] However, there is a limitation to dopant concentration. The storage density of such doped crystals cannot, in principle, prevail against that of rare-earth metal compounds (for example, Eu_2O_3 and Sm_2O_3). We have observed recently for the first time reversible photo-induced phenomenon and white PL state in Eu_2O_3 powder compact and film.

When Eu_2O_3 powder compact and film are irradiated with an UV laser light in vacuum, their photoluminescence (PL) spectra change from a red sharp-line structure to a white broad one, which can be clearly seen with the naked eye. After stopping the UV laser light, the white PL state lasts for more than several months at room temperature, in spite of any changes of atmosphere. By irradiating with the same UV laser light at room temperature under O_2 gas atmosphere, the original red PL state re-appears. Such reversible phenomenon as observed for the first time by the present study, may well yield materials for white-light-emitting devices and erasable optical storage.

REDUCTION OF SPECIMEN ETCHING DAMAGE BY ION ABSORPTION IN WET CELL ELECTRON MICROSCOPY

A. Ishikawa and E. Kanda

The environmental cell (EC) method is very useful for observation of wet specimens in the electron microscope. By circulating the gas saturated with water vapor in the film-sealed type EC, the specimen can be held wet. But under the observation in the gas atmosphere, etching damage of the specimen occurs more severely compared with in vacuum of the ordinary microscope.This damage rate depends on the gas environment, such as the gas components, humidity, pressure and so on, and is especially high when organic materials are observed. We confirmed that the damage is caused by the ions produced by the electron irradiation to gas molecules, and can be reduced by absorption of ions with a small electrode unit [1]. We try to improve the ion absorption efficiency to reduce the damage much more.

A new electrode unit was made and was assembled in the EC (3.5 mm in diameter and 1 mm in height). The electrode is embedded in a glass ceramic matrix and the resistance between the electrode and the specimen is high enough for the measurement of the ion current of the order of nA. The new electrode is cylinder type and has larger area ($2mm^2$) for ion absorption and lager ion-absorption efficiency compared with the electrode used previously. Fig.1 shows the comparison of the ion current absorbed by the both electrodes. The gas circulation in the EC and the voltage supply to the electrodes are controlled from the outside of the microscope column through the 4 stainless pipes. Using the polystyrene latex spheres of 314 nm in diameter as the specimen and dry CO_2 gas as the carrier gas, the damage or the size change was measured for the electron dose. The experimental condition was set at the gas pressure of 40 Torr, the accelerating voltage 100 kV, the electron density 1.0×10^{-2} A/cm^2.

The electric field, positive or negative, was applied between the specimen and the electrode. To make clear the effect of the electric field for absorbing the ions, the damage rate was measured on the same specimen in both the case of the field was on and off during the electron irradiation.The comparison of the efficiency of damage reduction obtained with the new electrode (Column electrode) and previous one (Bar Electrode) are shown in Fig.2 and Fig.3. Fig.2 shows the specimen size change due to the electron irradiation, at first the positive field was applied to absorb the negative ions and then the field was turned off after 15 minutes. Fig.3 shows the case at first the field was off and then negative field was applied, to absorb the positive ions. The results suggest the positive ions cause the etching damage and the absorption of the ions can reduce the damage rate.

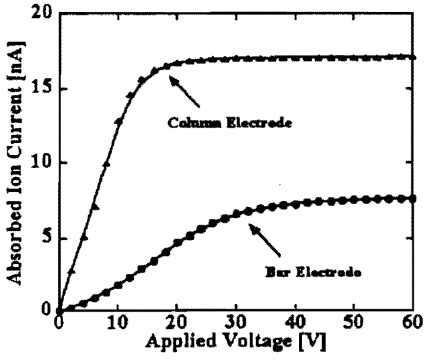

Fig.1 Ion current absorbed with new and previous electrode.

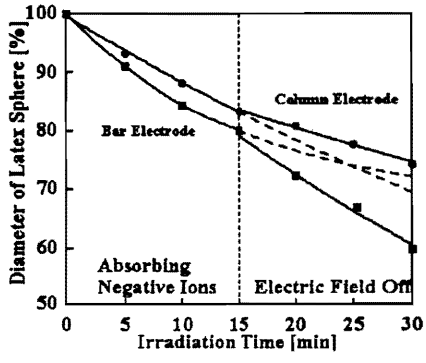

Fig.2 Size change of the specimen. Electric field was off at 15 min after absorbing negative ions.

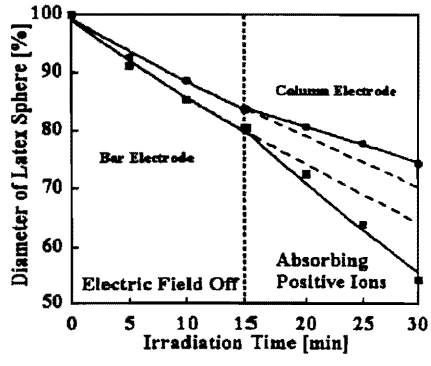

Fig.3 Size change of the specimen. At first electric field was off and turned on after 15 min iraddiation.

[1] A.Ishikawa and H.Sasaki : Proc. 14th Intern. Congr. Electron Microsc., Vol.3, 519-520 (Cancun,1998)

TRIAL MANUFACTURE OF CLOSED TYPE ENVIRONMENTAL CELL FOR ELECTRON MICROSCOPE

A. Ishikawa and H. Miyata

For observation of hydrated specimens in the electron microscope, we have used the environmental cell (E.C.) of film-sealed type. A fairly technical skill is required for assembling this type of the E.C. and for controlling the gas environment surrounding the specimen. We try to make a simple closed type E.C., because this type is satisfactory only for the observation of the specimen in wet environment. It is designed to fit to the specimen stage used for observation in scanning microscopy mode in the JEM2000EX microscope. The E.C. is assembled in a specimen holder with the components, two special *grid-meshes*, one *O-ring* and one *screwed cap*, as shown in Fig.1 schematically. The grid-mesh (diameter 3.5mm, thikness 0.2mm) has 7holes (diameter 0.15mm) or 13holes (diameter 0.1mm) at the center part. A special *sealing film* is pasted on the center part of the grid-mesh to seal the gas molecules in the E.C. The sealing film should have many properties such as the resistance to the gas pressure, the enough transmittance for the electrons, the resistance to the electron irradiation, and so on. We find that the flat carbon film of about 20 nm thick, deposited by vacuum evaporation method, is the best satisfying above requirement.

The E.C. is assembled and sealed at one atmospheric pressure and the thickness of the gas layer is determined by the thickness of the O-ring. The gas pressure in the E.C. increases slightly by tightening with the screwed cap. Therefore the pressure resistance of above 1.5 atm is required for the sealing film. In order to prevent the tear of the sealing film when the surrounding of the E.C. holder is pre-evacuated for inserting it into the microscope column, a set of gas pressure meter and flow controlling valve was attached to the pumping system for controlling the pumping speed. The sealing ability of the E.C. was confirmed by observing micro water droplets sealed in the E.C. at one atmospheric pressure. Fig.2 shows an example of the electron micrograph of water droplets sealed in 1 atm air of about 0.2mm thick, observed at the accelerating voltage of 200 kV.

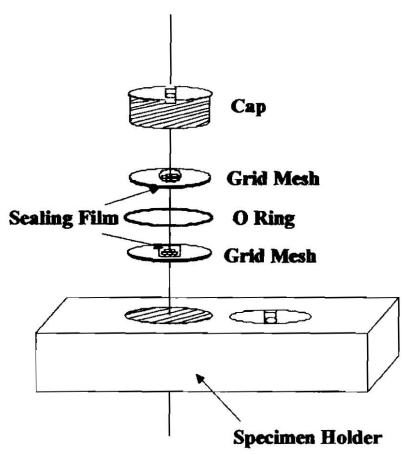

Fig.1 Schematic diagram of Closed type E.C.

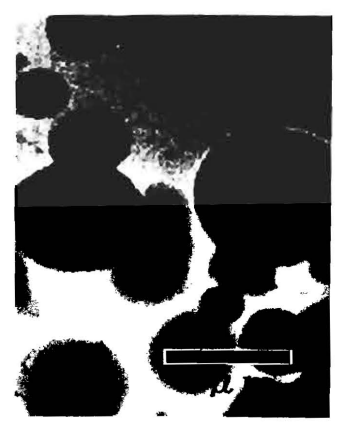

Fig.2 Water droplets observed at 1atm.

7. International Exchange Activities

7A) Visitors from Abroad

1) Dr. Donald J. Rej (Deputy Director of Physics Division LosAlamos National Laboratory) July 1 2000.
2) Prof. M. Ghoranneviss (Director of Plasma Research Center, Azad University, Iran) visited at December 8, 2000, and consulted about future cooperation.
3) Prof. Nils A. Törnqvist (University of Helsinki, Finland) June 4 - June 18, 2000.
4) Prof. Evgeny Shabalin (Institute of Theoretical and Experimental Physics, Moscow) June 8 - 22, 2000.
5) Prof. Michael D. Scadron (University of Arizona, USA) May 29 - June 30, 2000.
6) Dr. S. Arunagiri (University of Madras, India) May 24, 2000.
7) Dr. Lewis. H. Ryder (University of Kent at Canterbury) October 11, 2000.
8) Dr. Tilo Wettig (Yale University, USA) November 24, 2000.
9) Dr. Valery V. Burov (Dubna, Russia) January 26, 2001.
10) Dr. Edmond Orignac (Ecole Normale Supeŕieure, France) February 22 - 23, 2001.
11) Dr. Stephen Benson (Jefferson Lab, USA), March 8 - 15, 2001.
12) Prof. Anders Karlsson (Royal Institute of Technology, Sweden), January 17 - 28, 2000.

7B) Visitors to Abroad and International Conferences

Nuclear Fusion

1) S.Shiina attended IEA/RFP workshop held in Wisconsin, U.S.A., 28 February to 1 March 2000 and presented a paper entitled "Bootstrap Current in Low Aspect Ratio Reversed Field Pinch".
2) S.Shiina attended 27th European Physical Society Conference on Controlled Fusion and Plasma Physics held in Budapest, Hungary, 12-16 June 2000 and presented papers entitled "Neoclassical Transport in Helical Magnetic Axis System Controlled by Effective Toroidal Curvature", "Bootstrap Current in Low Aspect Ratio Reversed Field Pinch" and "Plasma Confinement and Relaxation on ATRAS-RFP Experiment".
3) S.Shiina attended ICPP/APS-DPP 2000 held in Quebec, Canada, 23-27 October 2000 and presented a paper entiled "Cocept Development of Steady State Reversed Field Pinch Reactor" and "Stability Beta Limits of Partially Relaxed State Model Reversed Field Pinch".
4) K.Saito attended 27th European Physical Society Conference on Controlled Fusion and Plasma Physics held in Budapest, Hungary, 12-16 June 2000 and presented papers entitled "Plasma Confinement and Relaxation on ATRAS-RFP Experiment" and "Bootstrap Current in Low Aspect Ratio Reversed Field Pinch".
5) T. Takahashi attended the 42nd Annual Meeting of the Division of Plasma Physics and the 10th International Congress on Plasma Physics on 23-27 October, 2000, at Que'bec City , Que'bec, Canada and presented a paper entitled "Global Motion of Highly Elongated Low Aspect Ratio Tokamak produced by Negative Bias Theta Pinch".

Plasma Sience

1) T. Miyamoto, K. Takasugi and M. Kashani attended the 13th International Conference on High-power Particle Beams (BEAMS 2000) held at Nagaoka, Japan. T. Miyamoto presented a paper entitled "Effects of Thermal Conduction to Steady State of Dense Z-pinches". M. Kashani and T. Miyamoto presented a paper "Optical Observations of Dense Sheet Z-pinch". K. Takasugi and T. Miyamoto pre-

sented papers "Control of X-ray Emission from The SHOTGUN Z-pinch Plasma" and "X-ray Spectra of Argon and iron Ions in a Gas-puff Z-pinch".

2) M. Kashani attended "The 8th Asia Pacific Physics Conference" held at Institute of Physics, Academia Sinica, Taipai from August 7 to 10, and presented the paper entitled "Effects of Cathode Electrode in Plasma Focus".
3) M. Kashani attended "International Symposium on Pulsed Power and Plasma Applications" held at Korean Institute of Electrical Engineers, and presented the paper entitled "Cathode Effects in Plasma Focus Discharge".

Superconductivity

1) K.Yasohama attended International Cryogenic Material Conference held in Rio de Janeiro, Brazil on June 11-15 2000, and presented two papers entitled
   i) "Hysteresis Loss and Critical Current Density of Maltifilamentary (NbW)3Sn Composite Conductor";
   ii) "Critical Current and Magnetization of Proximity Effect Induced Superconducting Cu in Maltifilamentary NbTi/Cu Composite Conductor"

Plasma, Astronomy and Statistical Physics

1) M. Aizawa attended the 27th European Physical Society Conference on Controlled Fusion and Plasma Physics held in Budapest, Hungary, 12-16 June 2000 and presented a paper entitled "Neo-classical Transport in Helical Magnetic Axis System Controlled by Effective Toroidal Curvature".
2) K. Konno was an international editorial board of "Chaos, Solitons & Fractals".
3) K.Konno attened the Workshop on RCP264: Inverse Problems and Nonlinearity held at Montpellier, France, June 20-24 2000, and reported a paper entitled "Recursion Formula for Integrable Equations Derived from IKK System".

High and Low Energy Physics

1) S. Ishida attended the Workshop, Possible Existence of the σ-Meson and its Implications to Hadron Physics, held at Yukawa Institute for Theoretical Physics (Kyoto) June 12-14 2000, and presented the following two talks :
   "S-matrix Bases and Relation between $\pi\pi$-Scattering and Production Amplitudes".

"Covariant Level-Classification Scheme and Chiral Symmetry".

2) T. Komada attended the Workshop, Possible Existence of the σ-Meson and its Implications to Hadron Physics, held at Yukawa Institute for Theoretical Physics (Kyoto) June 12-14 2000, and presented the talk :
"Light σ-Meson Production in Excited Υ Decay Processes I — Analyses — "

3) Visiting Resarchers of AERI attended the Workshop, Possible Existence of the σ-Meson and its Implications to Hadron Physics, held at Yukawa Institute for Theoretical Physics (Kyoto) June 12-14 2000, and presented the following talks, respectively :
Nils A. Törnqvist, "How to Understand the Lightest Scalars".,
"Summary Talk of the Conference on the Sigma Resonance".
Evgeny Shabalin, "On the Role of Sigma-Particle and Other Resonances in Low-Energy Mesonic Processes".
Michael D. Scadron, "Quark Level Linear σ Model (LσM) via Loop Graphs".

4) Tetsuo Sawada attended the Workshop, Possible Existence of the σ-Meson and its Implications to Hadron Physics, held at Yukawa Institute for Theoretical Physics (Kyoto) June 12-14 2000, and presented the talk :
"On the Consistency Check of the Resonances of the π-π System".

5) S.Ishida visited the Institute of High Energy Physics (IHEP) at Beijin, October 11 to 17 2000, to make a plan of Collaboration between the σ group in Japan and the J/ψ group in China, and presented the following two talks at the Workshop held in this occasion:
"Existence of $\sigma(600)$ Meson and Right S-matrix Bases".
"Covariant Quark Representation New Meson Multiplets, Chiralons".

6) Tsai was invited to present his paper entitled "CP, T and/or CPT Violations in the Neutral Kaon System - Implications of the KTeV, NA48 and CPLEAR Results -" at the Third Joint Meeting of Chinese Physicists Worldwide held at Chinese University of Hong Kong on July 31- August 4, 2000.

7) S. Deguchi, E. Umezawa and Y. Kokubo attended the International Workshop on Color Confinement in Quantum Chromodynamics "Confinement 2000" held at Research Center for Nuclear Physics in Osaka University, March 7-10, 2000.

8) H. Maiwa attended the International Workshop on Low Energy Solar Neutrinos

held at University of Tokyo, December 4-5, 2000.

9) M. Obu attended the Workshop, Possible Existence of the σ-Meson and its Implications to Hadron Physics, held at Yukawa Institute for Theoretical Physics (Kyoto) June 12-14 2000, and presented the talk :
"Hamiltonian Model Analysis of $\pi\pi$ Scattering and Production"

Accelerator Science

1) Y. Matsubara invited from Indian Institute of Technology (Bombay) on February 21 2001 to attend the Day Course on Pulse TubeCryocoolers and he presented a lecture of "Pulse Tube Mechanism and Thermodynamic Analysis".
2) Y. Matsubara attend the 18th International Cryogenic Engineering Conference (Bombay) on February 22-25 2001 and he served as a member of Advisory Board and the chair of a technical session. He presented a paper entitled "Feasibility Study of Applying Thermal Compressor to 4 K Pulse Tube Cooler".
3) Y. Matsubara invited from University of Giessen (Germany) on April 26-28 2000 to attend the workshop of Challenges of Applied Cryoelectrics" and he presented an invited talk of "Design Criteria of Thermally Driven Pulse Tube Coolers".
4) Y. Matsubara attend the 11th International Cryocooler Conference held at Keystone Colorado on June 18-24 2000 and he presented 3 papers:
   (1) "Thermally Actuated ^{3}He Pulse Tube Cooler";
   (2) "Development of a long life Stirling Pulse Tube Cryocooler for Superconducting FilterSubsystems";
   (3) "Experimental Study of a 4 K Pulse Tube Cryocooler";
5) Y. Matsubara attend the 6th Joint Seminar on Japan and Sino held at Lanzhou (China) on August 20-24 2000 and he presented a paper entitled "Thermally Driven 4 K Pulse Tube Cryocooler". He served as chairman of Japanese organizing committee.

Quantum Optics

1) S. Inoue attended the 8th Asian Pacific Physics Conference held in Taipei, Taiwan, 7-10 August 2000 and presented a paper entitled "Experimental Demomstration of Two-Dimensional Interaction-Free Imaging"

Other Researches

1) K. Ohnishi attended to the 2000 Annual International Nuclear and Space Radiation Effects Conference, Reno, U.S.A., Jun. 24-28, 2000.
2) K. Ohnishi presented a paper entitled "Characterization of Anodic Oxide Films in Pure Water" at the 3rd International Symposium on Advanced Science and Technology of Silicon Materials, Hawaii, U.S.A., Nov. 20-24, 2000.
3) Prof. H. Yamamoto attended to International Conference on Electronic Materials & European Materials Research Society Spring Meeting held at Strasbourg Congress Center, France on May 27-June 4, 2000. During the conference he attended the meeting of the executive committee of IUMRS on May 28 and 29. He presented the following paper in the session of O on July 1. "LOW VOLTAGE ELECTRON BEAM EXCITEMENT LUMINESCENCE OF OXIDE THIN FILMS WITH MULTILAYERED STRUCTURE"
4) Prof. H. Yamamoto attended to International Union of Materials Research Societies(IUMRS)-International Conference on Asia(ICA) held at Hong Kong, China on July 23-26, 2000. During the conference he attended the meeting of the executive committee of IUMRS on July 24.
5) Prof. H. Yamamoto attended to Fall Meeting of Materials Research Society held at Boston, United States on November 26-December 2, 2000. During the meeting he attended the meeting of the editorial committee of Journal of Materials Research on November 27, and the meeting of the executive committee of IUMRS on November 28.

8. List of Publications

8A) Publications in Periodical Journals and Conference Reports

Nuclear Fusion

1) M.Aizawa and S.Shiina; New Approach to Transport Improvement in a Helical Magnetic Axis System by Introduction of Effective Toroidal Curvature: Phys. Rev. Lett. 84 (No.12) 2638 (2000).
2) Y.Nagamine, Y.Osanai, Y.kondoh, K.Kusano, E.Uchimoto, S.Shimamura, K.N.Saito, K.H.Saito, S.Shiina; Bootstrap Current in Low Aspect Ratio Reversed Field Pinch: in the 27th EPS on Contr. Fusion and Plasma Physics P4.033
3) M.Aizawa, K.H.Saito, I.Kawakami, S.Shiina; Neoclassical Transport in Helical Magnetic Axis System Controlled by Effective Toroidal Curvature: ibid. P4. 032.
4) T.Namba, Y,Osanai, S.Shiina, K.N.Saito; Plasma Confinement and Relaxation on ATRAS-RFP Experiment: ibid. P4. 034.
5) S.Shiina, Y.Nagamine, Y.Osanai, K.N.Saito, K.H.Saito, Y.Kondoh, T.Takahashi, A.Smirnov, R.Harvey, E.Uchimoto; Concept Development of Steady State Reversed Field Pinch Reactor: 10th ICPP and 42nd Annual Meeting of DPP, DP1 116 (ICPP 4423).
6) R.Ukai, Y.Nagamine, T.Namba, Y.Osanai, K.N.Saito, K.H.Saito, K.Kusano, E.Uchimoto, S.Shiina; Stability Beta Limits of Partially Relaxed State Model Reversed Field Pinch: ibid. DP1 117 (ICPP 4417).
7) Y. Narushima, T. Takahashi, Y. Nogi, 'Global Motions of Highly Elongated Low Aspect Ratio Tokamak', Journal of Plasma and Fusion Research Series, Vol.3 (Proceedings of 10th Toki Conference on Plasma Physics and Controlled Nuclear Fusion (ITC-10) Physics and Technology for Steady State Plasma), p125
8) T. Takahshi , K. Iwata, Y, Nogi, 'Source Plasma Formation of Field Reversed Configuration for a Long Pulse Operation', Journal of Plasma and Fusion Research Series, Vol.3 (Proceedings of 10th Toki Conference on Plasma Physics and Controlled Nuclear Fusion (ITC-10) Physics and Technology for Steady State Plasma), p498
9) T. Takahashi, H. Gota, Y. Narushima, Y. Nogi, 'Global Motion of Highly Elongated Low Aspect Ratio Tokamak produced by Negative Bias Theta Pinch', (VP1-91) ,Bull. American Physical Society Vol45(7), p346

Plasma Sience

1) A. Muravich, T. Miyamoto and K. Takasugi ; Numerical Simulations of Dynamic Dense Sheet Z-pinch : NIFS-PROC-45, pp. 64 - 77 (2000).
2) K. Takasugi, T. Yoshida and T. Miyamoto ; X-ray Imaging Using a Concave X-ray Mirror : NIFS-PROC-45, pp. 78 - 83 (2000).
3) E.O. Baronova, M.M. Stepanenko, N. Pereira, A. Muravich, K. Takasugi and T. Miyamoto ; X-ray Device for 0.7 – 200 keV Based on Johansson Quartz Crystals on Optical Contact and Cauchois Crystal : NIFS-PROC-45, pp. 84 - 90 (2000).
4) A. Muravich, T. Miyamoto and V. Vikhrev, "Steady State of Dense Sheet Z-Pinches with Thermal Conduction", To be published in JJAP (2001).
5) M.A.M. Kashani, K. Sato, T. Miyamoto, A. Baba, A. Horiuchi, K. Takasugi, S. Sasaki, M. Lu and V. Vikhrev, "Cathode Effects in Plasma Focus Discharge", "Int. Symp. on Pulsed Power and Plasma Applications", (Oct. 26 - 27, 2000, Korea), to be published in J of Korean Electric Soc.
6) M.A.M. Kashani, A. Baba and T. Miyamoto, "Observations of Dense Sheet Z-Pinches", To be published in Proc. of 13th Int. Conf. on High-Power Particle Beams (June 25 - 30, 2000, Nagaoka).
7) E.O. Baronova, K. Takasugi, V.V. Vikhrev and T. Miyamoto, "X-Ray Spectra of Argon and Iron Ions in a Gas-Puff Z-Pinch", To be Published in Proc. of 13th Int. Conf. on High-Power Particle Beams (June 25 - 30, 2000, Nagaoka).
8) K. Takasugi, T. Igusa, K. Tatsumi, and T. Miyamoto, "Control of X-Ray Spectra of Argon and Iron Ions in a Gas-puff Z-Pinch", To be Published in Proc. of 13th Int. Conf. on High-Power Particle Beams (June 25 - 30, 2000, Nagaoka).
9) M.A.M. Kashani, K. Sato, T. Miyamoto, A. Baba, A. Horiuchi, K. Takasugi, S. Sasaki, M. Lu and V. Vikhrev, "Effects of Cathode Electrode in Plasma Focus Discharges", Proc. of "The 8th. Asia Pacific Phys. Conf.", (Aug. 7 - 10, 2000, Taipei) pp. 243 - 246.
10) S. Yamada, M. Kashani, A. Baba, T. Miyamoto, V. Vikhrev, "Cathode Effects on Plasma Focus", Proc. of "Research Meeting on Pulsed Power and Plasma", PPT-00-61 (2000) pp. 37 - 40.

Superconductivity

1) T. Okamura, M. Takahashi, H. Kobayashi ; Configuration effect of superfluid helium channel on t he λ - transition heat flux : Cryogenic 40 (2000) p.403-406
2) R. Akasaka, K. Fukuda, H. Kobayashi, et al. ; Numerical Analysis for Two-dimensional Heat Transfer of Hett with Phase Transition : Cryogenic Engineering 36 (2000) p.16-22
3) K.Yasohama, Y. Kubota, H. Kobayasi, T. Ogasawara, H. Kasahara, S. Torii, and S. Akita ; Hysterisis Loss and Critical Current Density of Multifilamentary (NbW)3Sn Composite Conductor : Physica C, to be published.
4) Y. Kubota, T. Moriya, and K. Yasohama ; Critical Current and Magnetization of Proximity Effect Induced Superconducting Cu in Multifilamentary NbTi/Cu Composite Conductor : Physica C, to be published.
5) Y. Fukuoka, S. Ikeda, K. Kumagai, K. Mori, Y. Takano, and K . Sekizawa ; Metal-Insulator Transition in oxysulfides ($La_{1-x}Ca_xO$)$Cu_{1-x}Ni_xS$ studied by NMR : Phys. Rev. B, 62 (2000) p.15598-15603.
6) K. Takase, K. Kubota, Y. Takano, H. Negishi, M. Sasaki, M inoue and K. Sekizawa ; Anisotropic Magnetic Properties of Intercalation Compound $Mn_{1/4}TiS_2$: Physica B, 284-288 (2000) p.1513-1514 .

Plasma, Astronomy and Statistical Physics

1) M. Aizawa and S. Shiina; New Approach to Transport Improvement in a Helical Magnetic Axis System by Introduction of Effective Toroidal Curvature; Phys. Rev. Lett. **84**, 2638 (2000)
2) M. Aizawa, K.H. Saito, I.Kawakami and S. Shiina; Neo-classical Transport in Helical Magnetic Axis System Controlled by Effective Toroidal Curvature; *Proceedings of the 27th European Physical Society Conference on Controlled Fusion and Plasma Physics* (Budapest, Hungary, 12-16 June 2000) 480 (2000)
3) S. Misawa; Proposal for Detecting the Susceptibility Maximum of Liquid ^{3}He with Respect to Field: Physica B 284-288(2000)196.
4) J. Xue, Q. zhou, H. Suzuki and S. Misawa; Susceptibility Maximum of Niobium Metal: J. Low Temp. Phys. 121(2000)127.
5) M. Morishita and S. Misawa; Temperature-Squared Terms in the Heat Capacities

of ^{3}He Fluid Films: J. Low Temp. Phys. 121 (2000) 483.

6) S. Misawa; Temperature and Field Dependence of the Spin Susceptibility and Specific Heat in 1, 2 and 3-Dimensional Fermi Liquids: Physica B, in press.

7) K.Konno and H.Kakuhata; Relationship between the dispersionless equation and the localized induction hierarchy through the Pohlmeyer-Lund-Regge equation J. Physic A33 (2000) 7821

8) K.Konno and H.Kakuhata; An integrable system with two hierarchies and related topics in "Nonlinearty, Integrability and all that: Twenty years after NEEDS '79" (World Scientific) (2000) P.160-167.

High and Low Energy Physics

1) K. Yamada, S. Ishida, R. Oda, M. Sekiguchi and H. Wada; Mass Spectra and Wave Functions of Meson Systems and the Covariant Oscillator Quark Model as an Expansion Basis: Prog. Theor. Phys. **102** (1999) pp.297-312.

2) M. Oda, K. Nishimura, M. Ishida and S. Ishida; Semi-Leptonic B Meson Decays to Excited D Mesons in the Covariant Oscillator Quark Model: Prog. Theor. Phys. **103** (2000) pp.1213-1225.

3) M. Ishida, T. Komada, S. Ishida, T. Ishida, K. Takamatsu and T. Tsuru; Effect of Light σ Meson Production in $p\bar{p} \to 3\pi^0$ at Rest: Prog. Theor. Phys. **104** (2000) pp.203-210.

4) S. Ishida, M. Ishida and T. Maeda; Covariant Quark Representation of Composite Meson Systems and Chiral Symmetry: Prog. Theor. Phys. **104** (2000) pp.785-807.

5) Rukmani Mohanta, Anjan K. Giri, Mohinder P. Khanna, Muneyuki Ishida and Shin Ishida; Weak Radiative Decay Width $B^{\pm} \to K^{*\pm}\gamma$ in COQM Including Long-Range Contributions: Prog. Theor. Phys. **104** (2000) pp.1109-1114.

6) Y. Takeuchi and S. Y. Tsai; Direct CP, T and/or CPT Violations in the Neutral Kaon System - Implications of the Recent KTeV Results on 2-Pion Decays - : Phys. Rev. D61 (2000) 077302.

7) Y. Kouchi, Y. Takeuchi and S. Y. Tsai; CP, T and/or CPT Violations in the Neutral Kaon System - Implications of the KTeV, NA48 and CPLEAR Results - : Eur. Phys. J. C17 (2000) 269-277.

8) S. Naka, S. Abe, E. Umezawa and T. Matsufuji; Bi-Local Higgs-Lke Fields Based

on Non-Commutative Geometry: Prog. Theor. Phys. 103(2000), 411.

9) Y. Sato and S. Naka; Bi-Local Field Equation Out of Bethe-Salpeter Equation: Prog. theor. Phys. 103 (2000) 847.

10) S. Deguchi and B. P. Mandal; A Superspace Formulation of Abelian Antisymmetric Tensor Gauge Theory: Mod. Phys. Lett. A 15 (2000) 965-978.

11) T. Fujita, T. Kake and H. Takahashi; Strong coupling limit of Bethe ansatz solutions in massive Thirring model: Annals of Physics 282 (2000) 100-114.

Accelerator Science

1) Hiratsuka, Y., Kang,Y.M., Fujiyama, N., Sotojima,T. and Matsubara Y. ; Development of a 5 W at 80 K Stirling Pulse Tube Cryocooler: Advances in Cryogenic Engineering, Vol.45., Plenum Press. (2000) p57-63.

2) Zhou, S. L., Thummes, G. and Matsubara Y. ; Experimental Investigation of Loss Mechanisms in a 4 K Pulse Tube: Advances in Cryogenic Engineering, Vol.45., Plenum Press. (2000) p81-88.

3) Fujiyama, N., Oodo, T., Kang,Y.M., Kanyama, T. and Matsubara Y. ; Experimental Investigation of Some Phase Shifting Types on Two-stage GM Pulse Tube Cryocooler: Advances in Cryogenic Engineering, Vol.45., Plenum Press. (2000) p127-133.

4) Zhu, S. W. and Matsubara Y. ; Replacement of Regenerator with a Stack in a Stirling Refrigerator: Advances in Cryogenic Engineering, Vol.45., Plenum Press. (2000) p357-364.

5) Matsubara, Y. and Zhou, S. L. ; Feasibility Study of Applying Thermal Compressor to 4 K Pulse Tube Cooler : Proceedings of the Eighteenth International Cryogenic Engineering Conference, Mumbai, India (2000) p535-538.

6) Kang,Y.M., Fujimoto, S., Hiratsuka, Y. and Matsubara Y. ; Pulse Tube Cryocoolers for Cryoelectronics Applications : Proceedings of the Sixth Joint Sino-Japanese Seminar on Cryocooler and its Applications, Lanzhou, China. (2000) p7-12.

7) Zhou, S.L. and Matsubara Y. ; Thermally Driven 4 K Pulse Tube Cryocooler : Proceedings of the Sixth Joint Sino-Japanese Seminar on Cryocooler and its Applications, Lanzhou, China. (2000) p38-43.

8) Ohtani, Y., Kuriyama, T., Kasamatsu, S., Okamura, T., Matsubara Y., Murakami, H. and Iida, T. ; Development of a Pre-cooled Pulse Tube Cryocooler : Proceedings

of the Sixth Joint Sino-Japanese Seminar on Cryocooler and its Applications, Lanzhou, China. (2000) p44-49.

9) I. Sato, I. Kawakami, K. Sato, Y. Matsubara, K. Hayakawa, T. Tanaka, Y. Hayakawa, et al. ; ADVACED STATUS AT LEBRA IN NIHON UNIVERSITY: Proc. of the 25th Linear Accelerator Meeting in Japan p.24-28 (2000)

10) .T. Tanaka, K. Hayakawa, I. Sato, Y. Hatakawa, K. Sato, Y. Matsubara, I. Kawakami, H. Nakazawa, K. Yokoyama, K. Kanno, T. Sakai ; IMPROVEMENT OF THE LOW POWER RF PHASE STABILIZER TEST CIRCUIT : Proc. of the 25th Linear Accelerator Meeting in Japan p.105-107 (2000)

11) K. Hayakawa, T. Tanaka, Y. Hayakawa, Y. Matsubara, K. Sato, I.Sato, H. Nakazawa, K. Yokoyama, T. Sakai, K. Kanno, K. Ishiwata, H.Inokawa, Y. Nakamura ; CONSTRUCTION OF THE INFRARED UNDULATOR AT LEBRA : Proc. of the 25th Linear Accelerator Meeting in Japan p.56-58 (2000)

12) K. Kanno, I. Sato, K. Sato, K. Hayakawa, T. Tanaka, Y. Hayakawa, H. Nakazawa, K. Yokoyama, T. Sakai, K. Ishiwata, H.Inokawa, Y. Nakamura, S. Michizono, S. Ohsawa, S. Fukuda; ANALYSIS OF THERMIONIC DC ELECTRON GUN FOR 125MeV LINAC : Proc. of the 25th Linear Accelerator Meeting in Japan p.168-170 (2000)

13) T. Sakai, I. Sato, K. Hayakawa, T. Tanaka, Y. Hayakawa, K. Sato, H. Nakazawa, K. Yokoyama, K. Kanno, K. Ishiwata, H.Inokawa and Y. Nakamura ; IMPROVEMENT OF THE LONG PULSE OPERATION OF THE S-BAND KLYSTRON : Proc. of the 25th Linear Accelerator Meeting in Japan p.228-230 (2000)

14) K. Yokoyama, I. Sato, K. Hayakawa, T. Tanaka, K. Sato, Y. Hayakawa, Y. Matsubara, H. Nakazawa, T. Sakai, K. Kanno, K. Ishiwata, H.Inokawa, Y. Nakamura ; RF PHASE DRIFT COMPENSATION WITH A FUNCTION GENERATOR : Proc. of the 25th Linear Accelerator Meeting in Japan p.108-110 (2000)

15) Y. Hayakawa, I. Sato, K. Sato, K. Hayakawa, T. Tanaka, Y. Matsubara, H.Nakazawa, K. Yokoyama, K. Kanno, T. Sakai, K. Ishiwata, H.Inokawa, Y. Nakamura ; OBSERVATION OF IR SPONTANEOUS RADIATION AT LEBRA : Proc. of the 25th Linear Accelerator Meeting in Japan p.358-360 (2000)

16) K. Ishiwata, H.Inokawa, Y. Nakamura, K. Sato, I. Sato, K. Hayakawa, T. Tanaka, Y. Hayakawa, H. Kobayashi, H. Nakazawa, K. Yokoyama, K. Kanno, T. Sakai, K.

Shinohara, N. Matsunaga, S. Anami, S. Fukuda and H. Homma ; BREAKDOWN OF THE BACK-DIODE OF THE PULSE MODULATOR FOR FEL LINAC AT NIHON UNIVERSITY : Proc. of the 25th Linear Accelerator Meeting in Japan p.222-224 (2000)

Quantum Optics

1) S. Inoue and G. Björk; Experimental Demonstration of Exposure-Free Imaging and Contrast Amplification: J. Opt. B:Quantum Semiclassical Opt. 2 (3), 338-345 (2000).
2) G. Björk, S. Inoue and J. Söderholm; Visibility is not a good measure of a well-defined relative phase: Phys. Rev. A 62, 023817-1-023817-8 (2000).
3) H. Watanabe and S. Inoue; Experimental Demonstration of Two-Dimensional Interaction-Free Imaging: Proceedings of the 8th Asian Pacific Physics Conference (2000).

Other Researches

1) Y. Takahashi and K. Ohnishi; Total Dose Effect of Metal-Nitride-Oxide-Semiconductor Structure: Proc. of the 4th International Workshop on Radiation Effects on Semiconductor Devices for Space Application, p.9 (2000).
2) K. Ohnishi and A. Ito; Characterization of Anodic Oxide Films in Pure Water: Proc. of the 3rd International Symposium on Advanced Science and Technology of Silicon Materials, p.543 (2000).
3) M. Hirai, H. Iwase, T. Hayakawa, T. Takizawa, K. Hayashi, S. Shimizu and M. Furusaka; Specificity of Interaction of Glycosphinogolipid Micelles with Proteins through Sugar Chains, *KENS REPORT-XII*, **1997/98**, 223–225(2000).
4) H. Iwase, M. Hirai, S. Arai, S. Mitsuya, S. Shimizu, T. Otomo and M. Furusaka; Study of denaturation of globular protain, *KENS REPORT-XII*, **1997/98**, 226–228(2000).
5) Y. Watanabe, T. Otomo, S. Shimizu, T. Adachi, Y. Sano and M. Furusaka; Neutron scattering studies on a water-soluble protein complexed with sodium dodecyl sulfate, *KENS REPORT-XII*, **1997/98**, 230–232(2000).
6) S. Shimizu, R. Sekine and K. Kurita; Small-angle X-ray scattering study of poly(N-isopropyl-acrylamide) in aqueous acetonitrile solutions, *J. Appl. Cryst.*, **33**, 731–

734(2000).

7) H. Ikake, W. Hashimoto, T. Obara, K. Kurita and S. Yano; Photochromic Properties and Microstructure of Poly(tetramethylene oxide)/Tungsten Trioxide Hybrid Materials, *Kobunshi Ronbunshu*, **57**, 376–382(2000).(in Japanese)

8) S. Yano, K. Iwata, K. Kurita and T. Swawaguchi; Structure and Physical Properties of Sol-Gel Derived Polypropyleneglycol/Silica Hybrid, *Kobunshi Ronbunshu*, **57**, 383–388(2000).(in Japanese)

9) T. Saito, S. Yano, T. Sawaguchi, W. Hashimoto and K. Kurita; Preperation of Copoly(ethylacrylate/3-methacryloxpropyltriethoxysilane) Hybrids by Sol-Gel Process, *Kobunshi Ronbunshu*, **57**, 389–395(2000).(in Japanese)

10) S. Ogawa, H. Furusawa, T. Watanabe, and H. Yamamoto ; Observation of condensed structure of C_{60} assembled from solution : J. Phys. Chem. of Solids, 61 (2000) pp.1047-1050.

11) H. Furusawa, K. Sakaguchi, T. Shimizu, T. Watanabe, H. Yamamoto, M. Chikamatsu, and T. Kikuchi ; Preparation of Self-Assembly Monolayer by C_{60} Derivatives : Trans. of the MRS-J, Vol. 25, No. 2 (2000) pp.413-416.

12) H. Yamamoto, H. Isogai, and Y. Yoshida ; Low-voltge electron beam excitement luminescence of oxide thin films with multilayered structure : Thin Solid Films, (2001) (to be published)

13) N. Iwata, Y. Ishii, H. Yamamoto, H. Zama, T. Morishita, and K. Kohn ; Ferromagnetic Insulator EuO Thin Film : Proc. of The 8th International Conference on Ferrites(ICF 8), (2001) (to be published)

14) N. Iwata, N. Hashimoto, and H. Yamamoto ; Preparation of Continuous C_{60} Thin Films with Flat Surfaces : Trans. of the MRS-J, Vol. 26, (2001) (to be published)

15) K. Suzuki, T. Kato, Y. Nakamura, N. Iwata, and H. Yamamoto ; Preparation of Phthalocyanine Derivative Ultrathin Films by Langmuir-Blodgett Method : Trans. of the MRS-J, Vol. 26, (2001) (to be published)

16) N. Iwata, T. Morishita, and K. Kohn ; Development of ferromagnetic insulator EuO thin films for the insulator barrier of high-Tc Josephson junction : Technical Report of IEICE, Vol. 100, SCE2000-2 (2000-4) pp.7-12. (in Japanese)

17) K. Ooshita, N. Iwata, and H. Yamamoto ; Preparation of C_{60} Ultrathin Film by Vacuum Evaporation : Technical Report of IEICE, Vol. 100, CPM2000-87

(2000-08) pp.19-24. (in Japanese)

18) Y. Ishii, H. Zama, T. Morishita, and H. Yamamoto ; Surface Treatment of MgO Single-Crystal Substrate : Technical Report of IEICE, Vol. 100, SCE2000-11 (2000-08) pp.1-5. (in Japanese)

19) T. Kaneda, T. Yamada, H. Sato, H. Yamamoto, and Hiroshi Akoh ; Fabrication of c-axis Oriented YBaCuO Trilayer Junction with Ar Plasma Treatment : Technical Report of IEICE, Vol. 100, SCE2001-2 (2001-01) pp.6-11. (in Japanese)

8B) Nihon University Preprints

NUP-A Series

NUP–A–2000–1 Annual Report (1999年)

NUP–A–2000–2 Bi-Local Field Equation Out of Bethe-Salpeter Equation

Yoshitaka SATŌ and Shigefumi NAKA

NUP–A–2000–3 CP, T and/or CPT Violations in the $K^0 - \overline{K^0}$ System
- Implications of the KTeV, NA48 and CPLEAR Results -

Yutaka Kouchi, Yoshihiro Takeuchi and S. Y. Tsai

NUP–A–2000–4 Comment on Instability of the replica action for the Random Field Ising Model

Hisamitsu Mukaida and Yoshinori Sakamoto

NUP–A–2000–5 Covariant Description of Composite Meson Systems and Chiral Symmetry

Shin Ishida, Muneyuki Ishida and Tomohito Maeda

NUP–A–2000–6 Space-Time Quantization and Nonlocal Field Theory
- Relativistic Second Quantization of Matrix Model -

SHO TANAKA

NUP–A–2000–7 Proposal to observe the strong Van der Waals force in the low energy neutron-Pb scattering

Tetsuo Sawada

NUP–A–2000–8 Effect of light σ-meson Production in $p\overline{p} \to 3\pi^0$ at rest

Muneyuki ISHIDA, Toshihiko KOMADA, Shin ISHIDA

NUP–A–2000–9 How do Neutrinos Propagate?

- Wave-Packet Treatment of Neutrino Oscillation -

Yoshihiro TAKEUCHI, Yuichi TAZAKI, S. Y. TSAI

NUP–A–2000–10 Present Status of the Long Range Component of the Nuclear Force

Tetsuo Sawada

NUP–A–2000–11 Semi-Leptonic B Meson Decays to Excited D Mesons in the Covariant Oscillator Quark Model

Masuho ODA, Kazunori NISHIMURA, Muneyuki ISHIDA and Shin ISHIDA

NUP–A–2000–12 Covariant Quark-Representation of Composite Meson Systems and Chiral Symmetry

Shin ISHIDA, Muneyuki ISHIDA and Tomohito MAEDA

NUP–A–2000–13 Interference pattern of the Coulomb and the strong Van der Waals forces in p-p scattering

Tetsuo Sawada

NUP–A–2000–14 Compositeness Condition and Vacuum Stability

Eizou UMEZAWA

NUP–A–2000–15 Random field $O(N)$ spin model near four dimensions

Chigak Itoi, Hisamitsu Mukaida and Yoshinori Sakamoto

NUP–A–2000–16 Phase diagram of a one-dimensional spin-orbital model

Chigak Itoi, Shaojin Qin, Ian Affleck

NUP–A–2000–17 Strongly reduced gap in the zigzag spin chain with a ferromagnetic interchain coupling

Chigak Itoi and Shaojin Qin

NUP-B Series

NUP–B–2000–1 Possible Existence of the σ-meson and Its Implications to Hadron Physics

S. Ishida, M. Y. Ishida, T. Kunihiro, T. Hatsuda, M. Oka, H. Shimizu, K. Takamatsu, T. Tsuru, C. S. Lim

8C) Books and Proceedings

1) S. Ishida and M. Ishida; "S-matrix Bases and Relation between $\pi\pi$-Scattering and Production Amplitudes": In proc. of Possible Existence of the σ-Meson and its Implications to Hadron Physics, YITP, Kyoto, June 12-14, 2000(σ-workshop) Soryushiron Kenkyu (Kyoto) **102** No.5 (2001) E26-E31, KEK-Proceedings 2000-4 p.26-31, HEP-PH/0012323.

2) M. Kobayashi, T. Tsuru, K. Takamatsu, S. Ishida, T. Komada, A. Wakabayashi and M. Ishida; "Production of $3\pi^0$ and $\eta 2\pi^0$ from $\pi^- p$ Collision in GAMS Experiment": In proc. of Possible Existence of the σ-Meson and its Implications to Hadron Physics, YITP, Kyoto, June 12-14, 2000(σ-workshop) Soryushiron Kenkyu (Kyoto) **102** No.5 (2001) E92-E97, KEK-Proceedings 2000-4 p.92-97, HEP-PH/0012326.

3) T. Komada, S. Ishida and M. Ishida; "Light σ-Meson Production in Excited Υ Decay Processes I — Analyses —": In proc. of Possible Existence of the σ-Meson and its Implications to Hadron Physics, YITP, Kyoto, June 12-14, 2000(σ-workshop) Soryushiron Kenkyu (Kyoto) **102** No.5 (2001) E98-E102, KEK-Proceedings 2000-4 p.98-102, HEP-PH/0012327.

4) M. Ishida, S. Ishida and T. Komada; "Light σ-Meson Production in Excited Υ Decay Processes II — Theoretical Investigation —": In proc. of Possible Existence of the σ-Meson and its Implications to Hadron Physics, YITP, Kyoto, June 12-14, 2000(σ-workshop) Soryushiron Kenkyu (Kyoto) **102** No.5 (2001) E103-E107; KEK-Proceedings 2000-4 p.103-107, HEP-PH/0012328.

5) S. Ishida, M. Ishida and T. Maeda; "Covariant Level-Classification Scheme and Chiral Symmetry": In proc. of Possible Existence of the σ-Meson and its Implications to Hadron Physics, YITP, Kyoto, June 12-14, 2000(σ-workshop) Soryushiron Kenkyu (Kyoto) **102** No.5 (2001) E139-E144; KEK-Proceedings 2000-4 p.139-144, HEP-PH/0012329.

6) S. Ishida and M. Ishida; "Covariant Classification of $q\bar{q}$ Meson Systems and Existence of New Scalar and Axial-Vector Mesons": Proceedings of the International Workshop on e^+e^- Collisions from ϕ to J/ψ, Budker Institute of Nuclear Physics, Novosibirsk, Russia (1999) pp.156-158, HEP-PH/9905258.

7) Nils A. Törnqvist; "How to Understand the Lightest Scalars": In proc. of Possible

Existence of the σ-Meson and its Implications to Hadron Physics, YITP, Kyoto, June 12-14, 2000(σ-workshop) Soryushiron Kenkyu (Kyoto) **102** No.5 (2001) E133-E138; KEK-Proceedings 2000-4 p.133-138.

8) Nils A. Törnqvist; "Summary Talk of the Conference on the Sigma Resonance": In proc. of Possible Existence of the σ-Meson and its Implications to Hadron Physics, YITP, Kyoto, June 12-14, 2000(σ-workshop) Soryushiron Kenkyu (Kyoto) **102** No.5 (2001) E224-E231; KEK-Proceedings 2000-4 p.224-231.

9) Evgeny Shabalin; "On the Role of Sigma-Particle and Other Resonances in Low-Energy Mesonic Processes": In proc. of Possible Existence of the σ-Meson and its Implications to Hadron Physics, YITP, Kyoto, June 12-14, 2000(σ-workshop) Soryushiron Kenkyu (Kyoto) **102** No.5 (2001) E63-E66; KEK-Proceedings 2000-4 p.63-66.

10) Michael D. Scadron; "Quark Level Linear σ Model (LσM) via Loop Graphs": In proc. of Possible Existence of the σ-Meson and its Implications to Hadron Physics, YITP, Kyoto, June 12-14, 2000(σ-workshop) Soryushiron Kenkyu (Kyoto) **102** No.5 (2001) E146-E153; KEK-Proceedings 2000-4 p.146-153.

11) Tetsuo Sawada; "On the Consistency Check of the Resonances of the π-π System": In proc. of Possible Existence of the σ-Meson and its Implications to Hadron Physics, YITP, Kyoto, June 12-14, 2000(σ-workshop) Soryushiron Kenkyu (Kyoto) **102** No.5 (2001) E67-E72; KEK-Proceedings 2000-4 p.67-72.

12) Tetsuo Sawada; "Pion Form Factor and the Anomaly of the Pi-Pi Phase Shift": Proceedings of the International Workshop on e^+e^- Collisions from ϕ to J/ψ, Budker Institute of Nuclear Physics, Novosibirsk, Russia (1999) pp.171-173.

13) Mitsuaki Obu; "Hamiltonian Model Analysis of $\pi\pi$ Scattering and Production": In proc. of Possible Existence of the σ-Meson and its Implications to Hadron Physics, YITP, Kyoto, June 12-14, 2000(σ-workshop) Soryushiron Kenkyu (Kyoto) **102** No.5 (2001) E73-E78; KEK-Proceedings 2000-4 p.73-78.

14) Proceedings of Workshop at Yukawa Institute; Possible Existence of the σ-Meson and its Implications to Hadron Physics, June 12-14 2000,
Soryushiron Kenkyu (Kyoto) **102** No.5 (2001); NUP-B-2000-1; KEK-Proceedings 2000-4.
Editers : S. Ishida, M. Y. Ishida, T. Kunihiro, T. Hatsuda, M. Oka, H. Shimizu,

K. Takamatsu, T. Tsuru, C. S. Lim

(S. Ishida was one of the organizers and editers of the workshop)